Integration of PDGF and Adhesive Signaling in *Xenopus* Mesendoderm Migration

Crystal Monique Richardson

B.S., University of Richmond, 2010

A Dissertation presented to the Graduate Faculty
of the University of Virginia in Candidacy for the Degree of
Doctor of Philosophy

Department of Cell Biology

University of Virginia
December 2017

Abstract

Embryonic development requires precise regulation of large-scale tissue movements. During morphogenesis, many cell movements occur in response to chemokines, morphogens, and soluble growth factors that guide directional movement. Platelet-derived growth factor (PDGF) signaling is required for directional *Xenopus* mesendoderm migration on the fibrillar fibronectin (FN) matrix of the blastocoel roof. Gradients of PDGF ligand can direct cell migration *ex vivo*, but in the context of the developing embryo it remains unclear whether PDGF gradients are present. The PDGF ligand can attach to FN and act as a short-range signal. However, signaling via the PDGF receptor (PDGFr) can be upregulated without direct interaction with PDGF ligand but rather by cooperation with integrin receptors. Because the developing embryo is dynamic and gradients of soluble cues are difficult to regulate, the spatial-temporal regulation of PDGFr may be necessary for mesendoderm migration. The purpose of this dissertation is to evaluate the roles of integrin-dependent adhesive signaling and growth factor signaling during mesendoderm migration. I established a role for the PDGFr functioning independent of a PDGF ligand gradient in directional mesendoderm migration on FN. The PDGFr functions to modulate adhesion to FN by regulating the actin cytoskeleton and the size of focal adhesions in a manner that depends on signals from focal adhesion kinase (FAK) and Pi3k-Akt.

Integrin adhesion initiates the assembly of the extracellular matrix (ECM), and integrin activation requires talins and kindlins. During neurulation, several ECM proteins are assembled and remodeled at the somitic mesoderm and notochord boundary. This

boundary forming ECM has essential roles in morphogenesis and is necessary for adhesion and orientation of tractive protrusions of mesoderm cells that undergo mediolateral intercalation behaviors during convergence and extension (CE). It has been demonstrated that perturbing FN results in severe defects in CE. I established a function for kindlin in the assembly of FN and fibrillin (FB) at the notochord somite boundary. This is the first demonstration of the role for kindlin functions in matrix assembly around the notochord. My dissertation describes how integrin-dependent adhesive signals can cooperate with growth factor signals for directional mesendoderm migration and how integrin activation by kindlin can regulate the assembly of the FN and FB matrix.

Acknowledgements

I am grateful for the support and guidance of so many people. First, I thank my advisor Doug DeSimone. The opportunity to train under his guidance has profoundly shaped the way I approach research. He taught me to be fearless and persistent in chasing down answers. Thank you for developing my ability to create, to teach, to write, to think, and to imagine! This work would not have been possible without Doug's support and support from my committee members: Ann Sutherland, Adrian Halme, and Ray Keller. Thank you for your time, your questions, your edits, and your suggestions.

From the moment I entered Doug's lab I found myself surrounded by people dedicated to understanding the problem of morphogenesis. Among those, I thank Bette Dzamba for her guidance in experimental design and data interpretation. Next, I thank Kära. Her care for the frog colony was fundamental to our research. Special thanks to Bette for the cake and Kära for the candy! Thank you to Pooja and Glen, the grad students I've spent the most time with in the lab. Thank you for cutting explants and discussing my project with me. Together, we've filled the hallway white boards with our ideas! I also thank the former and current lab members: Tania, Maureen, Chong, Greg, Fred, Claire, Shuo, Guo, Dave, and Wiktor. You all have made my time in the lab memorable.

I thank my incoming classmates Tim, Jake, and Katherine. My graduate experience would not have been the same without your help and advice. I also thank LaToya. She is an exceptional training buddy, scientist, and friend! Thank you for challenging my ideas and pushing me to be better. Special thanks to the Primal family!

With your support I am an award-winning Strongwoman competitor— a remarkable part of my graduate experience.

Thank you to my undergraduate advisor April Hill at the University of Richmond for teaching me the fundamentals. She taught me how to pipette, how to make solutions, and how to read scientific literature. April Hill pushed me to share my ideas and to think outside the box. Her passion and dedication to giving minority students access and educational opportunities changed my life!

I am grateful for my incredible family. Throughout my life I watched my Mom work hard to provide for us. She has always made my education a priority. My mother is an exceptional problem solver and critical thinker. Her influence has made me into the scientist I am today! I can't thank her enough for the sacrifices she made so my sister and I could have so many opportunities. I thank my sister Tiffany. It has been my pleasure to watch her grow into an intelligent and kind young woman. I'm so proud of her! I'm thrilled you decided to go to grad school to become a research scientist! The road is tough. Keep going! Never give up! I love you, Tiff!

Last but not least, I would like to thank God, *in Him all things are possible*. My graduate school experience began with a conversion to the Catholic faith and it is that faith that has guided me. My strength comes from God, and I am eternally grateful for the gift of perseverance. Through the struggles of life, my faith has created the path necessary for me to walk on.

Table of Contents

List of Figures

FIGURES **PAGE**

List of Abbreviations

AFM	Atomic Force Microscopy
BCR	Blastocoel Roof
cAMP	cyclic Adenosine Monophosphate
CE	Convergence and Extension
DMZ	Dorsal Marginal Zone
DSHB	Developmental Studies Hybridoma Bank
Dsp	Desmoplakin
ECM	Extracellular Matrix
FA	Focal Adhesion
FAK	Focal Adhesion Kinase
FB	Fibrillin
FGF	Fibroblast Growth Factor
FGFr	Fibroblast Growth Factor receptor
FN	Fibronectin
GFP	Green Fluorescent Protein
IgG	Immunoglobulin G

IF	Intermediate filament
LN	Laminin
MBS	Modified Barth's Saline
MO	Morpholino
p120	p120 catenin; $p120^{ctn}$
PDGF	Platelet-derived Growth Factor
PDGFr	Platelet-derived Growth Factor Receptor
Pi3k	Phosphatidylinositol 3-kinase
PLC	Phospholipase C
PLL	Poly-L-Lysine
PPSRN	Pro-Pro-Ser-Arg-Asn
RGD	Arginine–Glycine–Aspartic acid
RTK	Receptor Tyrosine Kinase
TEM	Transmission Electron Microscopy
TIRF	Total internal Reflection Fluorescence
VEGF	Vascular Endothelial Growth Factor
VEGFr	Vascular Endothelial Growth Factor receptor
WIP	WASP-interacting Protein

Chapter 1

Introduction

1.1 Understanding Collective Cell Migration

1.1.1 Why study collective cell migration?

The study of collective cell migration, defined by cells moving as a cohesive group, is critical to the understanding of multiple biological processes. Collective cell migration mediates morphogenesis (Caussinus, Colombelli, & Affolter, 2008; Ewald, Brenot, Duong, Chan, & Werb, 2008; Friedl & Gilmour, 2009), embryonic development (Haas & Gilmour, 2006; Montell, 2001; Weijer, 2009), cancer metastasis (Friedl, Locker, Sahai, & Segall, 2012; Gaggioli et al., 2007; Wolf et al., 2007), wound healing (Matsubayashi, Ebisuya, Honjoh, & Nishida, 2004), and angiogenesis (Hellström et al., 2007). In recent years, it has become clear that cohesive cell movements are essential for proper spatial and temporal patterning of developing tissues and organs (Lecaudey & Gilmour, 2006). In many instances, cells migrate with more persistence as a cohesive group of cells (Kolega, 1981; Winklbauer, Nagel, Selchow, & Wacker, 1996). This finding suggests that collective cell migration is a more efficient way for cells to travel and may provide some insight into why cells migrate collectively *in vivo*.

Studying collective cell migration also has clinically relevant applications. A greater emphasis should be placed on understanding collective cell migration when developing therapeutics designed to slow the progression of cell movements during disease states (Alexander, Koehl, Hirschberg, Geissler, & Friedl, 2008). Most therapeutic drugs targeting metastasis are initially evaluated using single-cell migration assays with cells in tissue culture (Friedl & Wolf, 2003). Although *in vitro* studies can inform *in vivo* treatment, often cell migratory behavior is vastly different *in vivo* where cells can undergo collective cell migration. Single cell and collective cell migration use many of

the same subcellular proteins, but the ways in which these proteins are regulated can be vastly different (Friedl, 2004). Thus, the differences between single-cell and collective-cell migration are worth investigating.

Most migration research has focused on studying cells migrating along tissue culture plastic (Lauffenburger & Horwitz, 1996; Ridley et al., 2003). For single cell migration to proceed, a breaking of symmetry must occur to establish a front and rear cell polarity. At the front of the cell, actin polymerization causes the formation of cell protrusions, which can be in the form of filopodia or lamellipodia that extend in the direction of travel (Fig. 1.1 A). The filopodia or lamellipodia form cell-extracellular matrix (ECM) adhesions mediated by integrin receptors embedded within the cell membrane (Fig. 1.1 A). Integrin engagement triggers the assembly of focal adhesion complexes that anchor the cell to the surrounding ECM (Fig. 1.1 A). The focal adhesions allow the cell to generate traction stresses necessary for cell movement. The rear of the cell undergoes an actomyosin-driven cellular contraction that separates the cell from the ECM following the disassembly of adhesions causing the forward cell translocation.

Cells undergoing collective cell migration share many of the same features as single cell migration. There is a breaking of symmetry, actin polymerization to form protrusions, and adhesions break because of actomyosin-driven cellular contraction resulting in cell movement (Mayor & Etienne-Manneville, 2016; Sheetz, Felsenfeld, Galbraith, & Choquet, 1999; Fig. 1.1 B). Although the sequence of events is the same as single cell migration, during collective cell migration, the cells remain cohesive. For this process to occur properly, signals must be transmitted across the group of cells to coordinate cellular behaviors. Cells organize at a supracellular level to join actomyosin

networks to coordinate cell protrusion dynamics, regulate cell–ECM attachment and detachment, allow for myosin-driven contraction at the rear of the cell group, and ultimately undergo a unified global movement.

1.1.2 Directional collective cell migration

Cells receive directional cues from the surrounding microenvironment. Cells can undergo chemotaxis following chemical cues (Swaney et al., 2010), cells can undergo haptotaxis migrating toward more adhesive surroundings (Carter et al., 1967), cells can undergo durotaxis migrating toward increased stiffness (Lo et al., 2000), and cells can follow aligned ECM which is known as contact guidance (Dunn & Heath, 1976). Recent studies in our lab described how collective cell migration can occur by cohesotaxis, whereby mechanical tension at cell-cell junctions enhances directional migration (Weber, Bjerke, & DeSimone, 2012). The interpretation and integration of multiple cues at the same time allows for directed migration. During collective cell migration the cells must remain attached making the integration of these cues more complex. Groups of cells migrate over and modify ECM exposing chemotactic cues and altering haptotactic and durotactic cues. If the cells align the ECM during migration, contact guidance allows follower cells to follow the tracks. Thus follower cells are exposed to different cues then leader cells. Because cell remain attached to one another, cohesotaxis is important for collective migration because tension at cell-cell junctions can act as a guidance cue as the cells exert tractions on the ECM.

1.1.3 Influences of directional mesendoderm migration

Xenopus mesendoderm migrates directionally along a fibrillar FN matrix and disrupting the fibrillar state of the FN matrix enhances mesendoderm migration (Rozario, T. & DeSimone, D.W., 2010). This suggests that the fibrillar network provides haptotactic and durotactic imputs that slow down migration of mesendoderm. There is no evidence that FN is aligned on the BCR and thus it remains unlikely that contact guidance governs directional mesendoderm migration. However, it is clear the cohesotaxis governs collective migration of *Xenopus* mesendoderm and applying mechanical force specifically to cell-cell junctions directs polarized protrusive activity of mesendoderm (Weber, Bjerke, & DeSimone, 2012). It also remains unclear whether chemotaxis influences directional migratory behaviors of mesendoderm. It has been suggested that mesendoderm follows the chemoattractant PDGF-A ligand (Nagel et al., 2004). However, mesendoderm that has been explanted away from the source of ligand can still undergo directional migration (Davidson et al., 2002). Is cohesotaxis alone sufficient to guide directional mesendoderm migration? Do non-ligand dependent PDGFr signals influence directed migration? And if so, how? This dissertation sought out to uncover answers to these questions.

1.2 Leader Cells and Follower Cells

Unlike single cell migration, in collective cell migration, the breaking of symmetry establishes leader cells and follower cells. Leader cells characteristically have active cellular protrusions, whereas follower cells maintain more stable cell–cell junctions and have less dynamic protrusive behaviors. Cell–ECM adhesion and

detachment must be carefully orchestrated so that leader cells are able to make adhesions to the ECM while follower cells break ECM adhesions, causing the group to migrate forward in unison. Although it is clear that differences between single and collective cell migration allow groups of cells to migrate with greater directionality, how cells interpret and integrate signals to coordinate cellular behaviors remains unknown.

Leader cells may be a singular cell or multiple cells that are localized to the front of a migrating sheet. Highly dynamic protrusive behaviors are characteristic of leader cells. For example, sprouting angiogenesis is directed by a singular leader cell at the branching tip that extends an elongated protrusion to orient the cell group in the direction of migration (Weavers & Skaer, 2014). During mesendoderm migration, multiple leader cells are found along the leading edge of the sheet of cells (Davidson, Hoffstrom, Keller, & DeSimone, 2002). Each mesendoderm leader cell has a monopolar lamellipodial protrusion oriented in the direction of migration. In both examples, the maintenance of polarized protrusive behavior is required for directional cell migration.

Leader cells are on the front edge of the migrating group and are the first to come into contact with guidance cues. Therefore, leader cells are essential in interpreting guidance cues (Mayor & Etienne-Manneville, 2016). Often leader cells internalize chemical guidance cues and respond to signals before the following cells can access the cue (Mayor & Etienne-Manneville, 2016). This internalization and response occurs with the collectively migrating cells of the *Dictyostelium discoideum* that respond to the secretion and internalization of cyclic adenosine monophosphate (cAMP; Kimmel & Parent, 2003). The leader cells secrete cAMP, creating a wave of signaling that is highest within leader cells; then the signal is propagated to follower cells. Leader cells also have

important roles in propagating cell signaling. In Madin-Darby canine kidney (MDCK) cells, active Rac and β1 integrin are found localized to leader cells. These leader cells are essential for the up-regulation of Pi3k-Akt signaling (Yamaguchi, Mizutani, Kawabata, & Haga, 2015). When a cohesive group of cells migrate, each cell remodels ECM by locally degrading with proteases or locally depositing basement membrane (Sternlicht, M. D. & Werb, Z., 2001). When leader cells do this, a track forms for the following cells to collectively migrate along.

Leaders can be determined in several ways. During mesoderm migration in *Drosophila* embryos, leader cells are spatially constrained and maintain position after invagination (McMahon, Supatto, Fraser, & Stathopoulos, 2008). However, endothelial cells respond to vascular endothelial growth factor (VEGF) and platelet-derived growth factor (PDGF) signals to induce the formation of leader cells, whereas follower cells respond to Notch/Dll4 signals (Khalil & Friedl, 2010; Quillien et al., 2014). Fibroblast growth factor signaling causes the formation of leader cells in tracheal outgrowth and the cells with the highest activation of fibroblast growth factor receptor to become leader cells (Ghabrial & Krasnow, 2006; Sato & Kornberg, 2002; Sutherland, Samakovlis, & Krasnow, 1996). During wound healing, leader cells activate Rho-A, and a constitutively active version of Rho-A is sufficient to induce follower cells to become leader cells (Omelchenko, Vasiliev, Gelfand, Feder, & Bonder, 2003). Because Rho-A signaling can induce the formation of leader cells, the number and position of leader cells can be highly dynamic. During border cell migration, the leader cell is defined as having the highest level of receptor tyrosine kinase signaling required for active cell protrusive behaviors and cell motility (Janssens, K., Sung, H.-H. & Rørth, P, 2010). As the border cell cluster

migrates, the cells change position in response to guidance cues and compete to become the leader cell (Prasad & Montell, 2007). Eventually the leader cell emerges, and the other cells in the border cell cluster become followers (Prasad & Montell, 2007).

Follower cells are found attached to and behind leader cells. Follower cells often have less dynamic protrusive behaviors and maintain stable cell–cell junctions with neighboring cells. During dorsal closure (Jacinto et al., 2000) and border cell migration (Prasad & Montell, 2007), follower cells are pulled along by leader cells. Follower cells do not extend actin-rich filopodial or lamellipodial protrusions like leader cells. Although there are many examples of leader cells pulling along follower cells, the follower cells do not always have a passive role in migration. During mammary gland branching morphogenesis, the highly proliferative cells of the stalk push leader cells from the rear (Ewald et al., 2008). Follower cells do not always remain as follower cells. During border cell migration, the follower cells can become leader cells based on signaling. Therefore, each cell within the group must interpret chemical and physical cues according to the location within the group. The interpretation of these signals in a spatially dependent manner is essential for efficient and directional collective cell migration.

1.3 Geometric Organization of Cohesive Groups of Cells

Cells migrate as sheets, clusters, or cords during collective cell migration (Fig. 1.2). Each geometric cellular organization helps to promote directional collective cell migration during a specific physiological or disease processes. In many instances, the tissue geometry influences the number of leader and follower cells within the group. The

configuration and number of the cells in the group influences the cell polarity, directionality, and speed of migration. Collective cell migration is more efficient when cells are organized to navigate the surrounding microenvironment.

Epithelial cells migrate as a two-dimensional sheet (Fig. 1. 2 A, 1. 2 D sheet). This geometry is necessary for wound healing along a planar surface. The collective cellular movement of epithelial cells in a sheet is driven largely by cell crawling and actomyosin-driven "purse-string" contractions at wound edges (Anon et al., 2012). The physical geometry of the wound dictates how the closure happens. When polydimethylsiloxane stencils were used to create wounds of varying shapes within a sheet of MDCK cells, the closure of concave edges protruding into the gap was driven by cell crawling, whereas convex or flat edges were closed by actomyosin-based cell contractions at the front of cells (Ravasio et al., 2015). Thus, the physical geometry of the wound edges dictates the mode of cell migration.

As wound healing progresses, the front edge of the cells contract forming a rosette-like geometry to enhance gap closure. Laser ablation of the actomyosin cable in the front of the cells causes the cell migration to become driven by cell crawling (Ravasio et al., 2015). The formation of an actin cable at the front of cells is regulated by the presence of ECM. If ECM is localized at the edge of the wound, cell crawling is predominant; if there is no ECM, then there is enhanced formation of an actin cable (Grasso, Hernandez, & Chifflet, 2007). During epithelial wound healing, the two-dimensional sheet allows leader cells to form along the edge of the sheet, and the geometry of the wound determines the mode of migration. The geometry also influences the speed of migration, because cell crawling is slower than the actomyosin contraction

of the actin purse string.

In *Xenopus* gastrula, mesendoderm tissue has a free leading edge, and the rear of the cell group is attached to mesoderm tissue, creating an intrinsic tissue polarity. The cells along the leading edge exert the highest traction stresses on the fibronectin (FN) substratum, pulling along the follower cells that are connected by C-cadherin-rich cell-cell adhesions (Sonavane et al., 2017). Asymmetric tissue tension within mesendoderm directs cell protrusion polarity. Mesendoderm cell protrusions become directionally oriented after the application of mechanical force on C-cadherin adhesions, causing cells to migrate in a directional manner (Weber, Bjerke, & DeSimone, 2012). Mesendoderm explants migrate at twice the speed when placed in a round configuration (Davidson et al., 2002). Thus, the geometry of the mesendoderm cells within the tissue governs the speed and directionality of migration.

Cells can collectively migrate in clusters; the shape of the cluster defines the direction of migration, and the size of the cluster determines the migration speed (Kumar, Chen, Co, & Ho, 2011). When groups of fibroblasts were geometrically confined in varying shapes using micropatterned substrates, clusters migrated preferentially along the major axis of a rectangle or ellipse, whereas circular clusters had randomized migratory movements (Kumar, Chen, Co, & Ho, 2011). During border cell migration, the cluster forms an ellipse shape once the leader cells are determined, migrating along the major axis of the ellipse (Fig. 1.2 B, elliptical cluster). Groups of cells are better able to respond to chemical cues necessary for directional migration. A theoretical model was used to determine that the larger the border cell clusters were, the faster the migration speed was, up to a certain size (Kumar et al., 2011). If the border cell cluster becomes too large,

there is increased viscous drag. Thus, there is an optimal cell cluster size at which border cell migration occurs.

Schwann cells migrate as cords (Fig. 1.2 C) along "tracks" of blood vessels to guide axons during regeneration (Cattin et al., 2015). The cord-like geometry is regulated by ephrin/Eph signaling; if ephrin-B2 protein is microprinted into stripes on coverslips, the Schwann cells will organize into parallel cords (Cattin et al., 2015). Because the Schwann cell cord leads the outgrowth of the axon, the geometry of the Schwann cells is essential. Disrupting ephrin/Eph signaling results in a loss of directionality and causes the cords to cross (Cattin et al., 2015). Taken together, these data suggest that the physical geometry of the tissue (e.g., a sheet, cluster, or cord, Fig. 1.2) dictates the directionality and speed of migration. The data also suggest that in some instances, the efficiency of cell migration is dependent on the maintenance of a particular geometry.

1.4 PDGF Signaling in Collective Cell Migration

1.4.1 Structure and Function of PDGFr and PDGF Ligand

PDGF ligand was first described in the 1970s as a serum growth factor released from platelets during blood clotting and wound healing (Andrae, Gallini, & Betsholtz, 2008; Kaplan, Chao, Stiles, Antoniades, & Scher, 1979; Scher, Shepard, Antoniades, & Stiles, 1979). PDGF acts as a mitogen and proliferative factor for several cell types, including fibroblasts (Seppä, Grotendorst, Seppä, Schiffmann, & Martin, 1982), glial cells (Assanah et al., 2009), and vascular smooth muscle cells (Grotendorst, Chang, Seppä, Kleinman, & Martin, 1982). Although PDGF has been well established as a

chemoattractant for directed cell migration (Deuel, Senior, Huang, & Griffin, 1982), PDGF has been identified as a regulator of collective cell movements only in the past 20 years (McDonald, Pinheiro, & Montell,, 2003).

Both the platelet-derived growth factor receptor (PDGFr) and the PDGF ligand are dimers of disulfide-linked polypeptide chains (Fig. 1.3). The PDGFr has five extracellular immunoglobulin G (IgG) domains, a transmembrane domain, and an intracellular tyrosine kinase domain (Fig. 1.3; Heldin & Westermark, 1999). PDGF ligand binds to the extracellular IgG domains, resulting in the dimerization of the PDGFr, which causes autophosphorylation at conserved residues, specifically Tyr-849 in the α-receptor and Tyr-857 in the β-receptor (Fig. 1.3). This phosphorylation causes activation of the PDGFr, which creates docking sites for SH2 domain containing signaling molecules such as Pi3k, Fak, phospholipase C, and the Src family of tyrosine kinases (Heldin & Westermark, 1999; Fig. 1.3).

1.4.2 PDGF Signaling in Protrusion Formation

PDGF signaling leads to enhanced actin crosslinking, which is essential for lamellipodia protrusion formation (Herman & Pledger, 1985; Nagano et al., 2006). Addition of PDGF ligand to fibroblasts results in increased actin polymerization, which causes the formation of circular membrane ruffles (Anton, 2003; Veracini et al., 2006). The membrane ruffle is a result of PDGF signaling causing activation of the Rho-GTPase family member, GTP-Rac, and causing the recruitment of WASP-interacting protein (WIP), which binds actin filaments for crosslinking (Anton, 2003). PDGF signals are also

important for migration *in vivo*. PDGF signaling activates Rac in the leader cell to orient protrusions in the forward direction during border cell migration (Poukkula, Cliffe, Changede, & Rørth, 2011), *Xenopus* mesoderm cell migration (Nagel, Tahinci, Symes, & Winklbauer, 2004), and zebrafish mesendoderm migration (Montero, Kilian, Chan, Bayliss, & Heisenberg, 2003). Thus, PDGF ligand causes increased actin polymerization to direct protrusions during collective cell migration. However, it remains unclear if active PDGFr is localized to leader cells in a ligand independent manner.

1.5 Cell–Cell Junctions in Collective Cell Migration

Cell–cell junctions not only provide a physical connection between cells but also anchor cells to the intracellular cytoskeleton. These mechanical linkages allow groups of cells to move together at the roughly the same speed. The maintenance of cell–cell junctions is a defining feature of collective cell migration. Cadherin-rich cell–cell junctions mediate adhesions in several cell types during collective migration. Cadherins are a family of calcium-dependent cell adhesion molecules that mediate cell–cell adhesions. During morphogenesis, cadherins regulate cell sorting behaviors (Gumbiner, 2005). Cadherins are part of desmosomes and adherens junctions. Desmosomes contain cadherins associated with keratin intermediate filaments are formed and resist mechanical forces. Cadherins interact with catenins to bind to actin filaments and microtubules in adherens junctions.

1.5.1 PDGF in the regulation of cell-cell junctions

Several types of cells require cell–cell contacts to migrate directionally or to respond to chemotactic cues. *Xenopus* mesendoderm migrates directionally in response to PDGF, but only if the cells have intact C-cadherin cell–cell junctions (Nagel et al., 2004; Winklbauer et al., 1996). If C-cadherin cell–cell junctions are disrupted, the cells disperse and migrate randomly because the cells are unable to respond to chemotactic cues embedded in the BCR (Winklbauer et al., 1996). Similarly, during border cell migration, if E-cadherin is knocked down, the cells disperse and can no longer migrate directionally in response to PDGF (Cai et al., 2014). During gastrulation in chick embryos, PDGF signals enhance expression of N-cadherin in mesoderm cells to allow for directional migration (Yang, Chrisman, & Weijer, 2008). During neural crest cell migration, PDGF signaling modulates the expression of N-cadherin and inhibiting PDGF-A ligand or PDGFrα results in decreased levels of N-cadherin (Carmona-Fontaine et al., 2008). Thus, regulating cadherins at cell–cell junctions is a conserved mechanism to enhance directional collective cell migration during chemotaxis, and mechanisms of chemotaxis have evolved to maintain cell–cell junctions for more efficient directional migration.

1.6 Integrin Signaling in Collective Cell Migration

Integrins are heterodimeric glycoproteins with noncovalently bound α and β subunits that function as adhesion receptors important for signal transduction (Luo, Carman, & Springer, 2007). Integrins have an extracellular head domain, a transmembrane domain, and a short cytoplasmic tail (Moser, Legate, Zent, & Fässler, 2009). The globular head domain binds to ECM, and the short cytoplasmic tail binds to intracellular adaptor proteins that link to the actin cytoskeleton. Integrins provide a direct

link between the extracellular and intracellular environment. Integrins are key mediators of cell adhesion and cell migration (Hynes, 2002). During collective cell migration, integrins can be more highly expressed in leader cells to mediate adhesion in the front of the tissue (Hegerfeldt, Tusch, Bröcker, & Friedl, 2002). For example, integrin β1 is localized to the front of leader cells in a sheet of MDCK epithelial cells (Yamaguchi et al., 2015). The localization of integrins creates hubs for cell signaling of Rho-GTPases, such as Rac, Fak, and Pi3K. These signaling molecules allow for the formation of protrusions, focal adhesion complexes, and actomyosin contractile machinery necessary for collective cell migration.

1.6.1 Integrin Activation

Integrin activation is defined as a rapid and reversible conformational change that occurs in the extracellular head domain of integrins (Hynes, 2002). This conformational change causes the integrin to convert from a bent "low-affinity" state into an open "high affinity" state (Takagi, Petre, Walz, & Springer, 2002). Integrin signaling is bidirectional and integrin activation occurs by both "inside-out" and "outside-in" signaling mechanisms. Talin binding to integrin NPxY motif in the short β cytoplasmic tail initiates inside-out signaling (Patil et al., 1999). Overexpression of talin can induce integrin activation (Calderwood et al., 1999) because talin binding releases the inhibitory α β subunit interaction breaking the salt bridge by changing integrin conformation (Tadokoro et al., 2003). Although talin can induce integrin activation, talin alone is not sufficient, and knockdown of kindlin results in a disruption in the ability of talin to activate integrins (Ma, Qin, Wu, & Plow, 2008). Kindlin is a scaffold protein that acts to bridge integrin

with talin to promote integrin clustering (Li et al., 2017). Talin binds to the integrin membrane-proximal NPxY motif, and kindlins bind to the membrane-distal NPxY motif (Wegener et al., 2007). Kindlin is an essential linker of integrins to the actin cytoskeleton (Bledzka et al., 2016) and interaction with talin promotes focal adhesion formation because kindlin can bind to paxillin (Theodosiou et al., 2016). Thus, talin and kindlin interaction with integrin β cytoplasmic tail results in conformational change and ECM ligand binding promoting cell adhesion and cell spreading during inside-out signaling.

Integrins are expressed on cell surfaces in the inactive bent low-affinity state and in this low affinity state are unable to bind ECM (Hynes, 2002). During outside-in signaling, integrins become activated by ECM ligand binding that induces a conformational change in the integrin to a high-affinity state (Takagi et al., 2002). Ligation with ECM causes integrin clustering and the activation of Src family kinases that phosphorylate NPxY motifs to promote binding by talin and kindlin (Arias-Salgado et al. 2003). Talin and kindlin cooperate to lock integrins into a high-affinity state. Integrin phosphorylation must be tightly regulated and phosphorylation by Src family kinases of β_3 tails inhibited $\alpha_v\beta_3$ mediated adhesion to fibronectin (Datta, Huber, & Boettiger, 2002). Divalent cations enhance ECM binding affinity (Bazzoni, Blue, & Hemler, 1998; Gailit & Ruoslahti, 1988). These cations bind integrins at the metal-ion dependent adhesion site (MIDAS; Moser et al., 2009). Stimulation with Mn^{2+} increased the binding affinity of integrin to binding FN at the arginine–glycine–aspartic acid (RGD) site (Gailit & Ruoslahti, 1988). Integrins can also respond to mechanical force and transmit the forces into biochemical signaling. Spatiotemporal regulation of integrin activation and integrin affinity for ECM within a group collectively migrating cells

permits front–back polarity to drive cell migration forward (Lauffenburger & Horwitz, 1996). Integrin activation upregulates biochemical signaling events and creates signaling plaques, allowing for synergy with other membrane receptors.

1.6.2 Integrin Synergy With PDGFr

Integrin receptors provide a physical link to the surrounding ECM. Integrin engagement activates signal transduction cascades up-regulating Pi3k-Akt to activate growth factor signaling. Because integrin receptors and growth factor receptors both enhance Pi3k-Akt, transactivation of receptors can occur in both directions (Fig. 1.4). Integrins can bind to growth factor receptors at the cell surface forming signaling plaques and enhancing transactivation. Indirect activation of growth factor receptors can occur in a nonligand-dependent manner when integrin signaling upregulates downstream signal transduction cascades (Fig. 1.4 A).

β1 integrin engagement induces the activation of Pi3k, resulting in the phosphorylation of Akt (Fig. 1.4 A). Similarly, PDGFr activation results in the activation of Pi3k signaling and the phosphorylation of Akt (Fig. 1.4 B). Together integrin and PDGF signaling synergize to up-regulate Pi3k–Akt signals necessary for cell adhesion and migration. Integrin activation results in the activation of kinases, such as focal adhesion kinase (FAK), that can phosphorylate and activate the PDGFr in a ligand independent manner (Fig. 1.4 A). The significance of converging integrin and PDGF signaling pathways has yet to be evaluated in a complex event such as directional *Xenopus* mesendoderm migration that occurs during gastrulation. This dissertation

addresses the importance of convergent signaling on directional mesendoderm migration.

1.7 *Xenopus* Mesendoderm Migration

1.7.1 Influences of cell-cell adhesion on directional mesendoderm migration

Directional *Xenopus* mesendoderm migration requires cell–cell cohesion. Single mesendoderm cells are unable to migrate directionally along the blastocoel roof (BCR; Winklbauer et al., 1996). However, aggregates of mesendoderm cells migrate on a coverslip conditioned with the BCR (Nagel et al., 2004; Winklbauer, 1990). Importantly, the BCR-derived ECM contains soluble cues that enhance migration in the direction of the animal pole (Nagel et al., 2004; Winklbauer, 1990). The requirement of tissue cohesion and maintenance of the geometry of the mesendoderm tissue has been well described in the literature (Davidson, Marsden, Keller, & DeSimone, 2006). However, the importance of guidance cues embedded or secreted from the BCR remains unclear, particularly because mesendoderm migrates directionally on a planar FN substratum without BCR conditioning or addition of PDGF-A ligand or any other guidance cues (Davidson et al., 2002). In *Xenopus* mesendoderm migration, PDGF-A ligand is a guidance cue that is effective only when there is tissue cohesion and if PDGF-A ligand is knocked down mesoderm is unable t directionally migrate (Nagel et al., 2004; Smith, Mitsi, Nugent, & Symes, 2009; Winklbauer & Nagel, 1991). I hypothesized that the integrin-FN adhesions would be sufficient to activate PDGFr signaling in a ligand independent manner required for directional migration. To better understand the dynamics of mesendoderm migration, the dorsal marginal zone explant (DMZ) was

developed (Davidson et al., 2002). The DMZ explant provides a simple way to evaluate individual cell behaviors during directional mesendoderm migration. Mesendoderm migrates directionally on a nonfibrillar FN substratum without BCR conditioning and without PDGF-A ligand (Davidson et al., 2002). I used mesendoderm explants as a tool to evaluate the contribution of PDGF signaling and integrin adhesion during directional mesendoderm migration.

1.7.2 Influences of cell-ECM adhesion on directional mesendoderm migration

Integrin adhesion to the ECM is required for *Xenopus* mesendoderm migration. Mesendoderm migration is dependent on integrin α5β1 (Davidson et al., 2002), which binds to FN in at the Arg-Gly-Asp (RGD) site (Takagi et al., 2002). When a FN function-blocking antibody is used to block the RGD site (mAb 4B12) on an FN substrate, mesendoderm explants detach from the FN and retract (Davidson et al., 2002). In addition to integrin binding to RGD, integrin also binds to the FN "synergy site" sequence Pro-Pro-Ser-Arg-Asn (PPSRN), and this interaction promotes cell spreading. If a function-blocking antibody recognizing the FN "synergy site" (mAb 1F7) is used on mesendoderm explants on FN, mantle extension stops, but the tissue does not detach because the integrin can still bind to the FN RGD sequence, which is sufficient for cell attachment (Davidson et al., 2002). If integrin α5β1 adhesion to FN is blocked using mAb P8D4, mesendoderm tissue retracts and detaches (Davidson et al., 2002). Similar results are seen using FN fusion proteins (9.11 and 9.11a) containing three FN Type-III repeats, specifically repeats 9, 10, and 11. Cells on 9.11 can attach to RGD and the "synergy site" sequence allowing the cell to spread and migrate (Fig. 1.5 A). Both the binding to the

RGD and “synergy site” sequence promotes integrin activation and the activation of downstream signaling that leads to the phosphorylation of Akt (Fig. 1.5 A). However, the “synergy site” sequence is mutated in the 9.11a construct, and the mutation results in an inability for integrin to bind to the PPSRN sequence. Therefore, the cells attach to RGD but are unable to spread and migrate (Fig. 1.5 B). The inability of the integrins to bind to the “synergy site” results in reduced p-Akt (Fig. 1.5 B). These experimental results demonstrate that integrin α5β1function and binding to the FN RGD and “synergy site” promote mesendoderm migration.

In other mesenchymal cell types, integrin α5β1 can activate the PDGFr to promote cell attachment (Veevers-Lowe, Ball, Shuttleworth, & Kielty, 2011). However, whether integrin α5β1 adhesion to FN promotes complex cellular movements such as mesendoderm migration and whether PDGF signaling can be regulated by integrin adhesion remain unclear. My research helped uncover a model whereby integrin engagement with FN results in ligand independent PDGF signals that result in enhanced cells signaling, specifically p-Akt and pFak-397, which causes the formation of lamellipodia protrusions, assembly of focal adhesions, and directional collective cell migration (Fig. 1.6).

1.7.3 Influences of mechanical forces on directional mesendoderm migration

The gastrulating *Xenopus* embryo is a force-generating machine. Mesoderm undergoes convergence and extension (CE) movements (Keller & Davidson, 2004). The mesoderm cells that involute undergo stiffening along the marginal zone on the

anteroposterior axis (Moore et al., 1995). Attached to and ahead of mesoderm is mesendoderm, which migrates directionally on the FN matrix of the BCR, extending lamellipodial protrusions (Davidson et al., 2002). Mesendoderm cells adhere to and exert tractive forces on the FN matrix and tension at cell-cell junctions (Sonavane et al. 2017). If cell-FN attachments are disrupted, then the tissue "snaps-back" because of the tension within the tissue (Davidson et al., 2002). FN matrix is also necessary for CE and blocking integrin-FN adhesions results in shortened embryos (Marsden & DeSimone, 2003). Additionally, there is integrin–cadherin crosstalk and integrin function is required for cell sorting behaviors (Marsden & DeSimone, 2003). The intersecting functions of cadherin and integrin adhesive networks are essential for gastrulation. The balance of cell-cell and cell-ECM forces regulates *Xenopus* mesendoderm migration as tractive forces mediated by cell-ECM adhesions are counterbalanced by tension at cell-cell junctions with highest tractions along the leading edge of the tissue (Sonavane et al. 2017). Mesendoderm migrates on BCR cells that are also re-arranging. The ectodermal cells that comprise the BCR undergo thinning and spreading in a process known as epiboly (Keller & Davidson, 2004). Each of these force-generating movements must occur simultaneously for gastrulation to proceed.

1.8 Significance and Overview

The purpose of my dissertation was to elucidate the roles of integrin and growth factor signaling during embryonic development. In Chapter 1, I introduce the major regulators of collective cell migration and what is known about integrin signaling and growth factor signaling in directional migration. Mesendoderm migrates directionally on

fibrillar fibronectin with growth factor ligands sequestered in the matrix (Davidson et al., 2002). Previous studies suggested that PDGF dependent chemotaxis was required for directional mesendoderm migration (Nagel et al., 2004). However, mesendoderm explants can migrate directionally without PDGF embedded in the matrix (Davidson et al., 2002). In Chapter 2, I propose that directional mesendoderm migration is governed by the integration of integrin-dependent adhesive signals in cooperation with PDGFr. Talins and kindlins are scaffolding proteins that bind to integrin β tails acts as activators for integrins (Goult et al., 2009). In Chapter 3, I identify a function for kindlin in the assembly of FN and fibrillin (FB) during neurulation. Although it is clear the integrin-ECM adhesion contributes to ECM assembly (Wu, Keivens, O'Toole, McDonald, & Ginsberg, 1995), this is the first demonstration of the role for kindlin functions in matrix assembly during embryonic development. Chapter 4 provides a summary of both projects highlighting major conclusions, significance, and future directions. In conclusion, my dissertation discusses the how integrin-dependent adhesive signals can cooperate with growth factor signals for directional mesendoderm migration and how integrin activation by kindlin can regulate the assembly of the FN and FB matrix.

Figure 1.1

Single cell migration versus collective cell migration. (A) Diagram of single cell migration. A cell migrates on ECM, extending actin-rich lamellipodia or filopodia protrusions in the direction of migration. The cell forms adhesions with the ECM that become mature focal adhesions. These focal adhesions are localized at the front of the cell. This occurs simultaneously with the disassembly of rear cell adhesions. Because of the front localization of focal adhesions, actomyosin contraction results in the translocation of the cell in the forward direction. (B) Diagram of collective cell migration. Cell–cell junctions, represented here by green ovals, connect cells. Cells maintain cell–cell junctions while migrating on ECM. Coordinated actomyosin contraction allows for the group of cells to translocate in the direction of migration. Cells turnover focal contacts in the follower cells and make focal adhesions in the leader cells. (A–B) The orange arrow in each panel indicates the direction of migration. Black lines represent ECM. The yellow shaded area represents lamellipodia or filopodia cellular protrusions. Red ovals represent cell–ECM adhesions that mature into focal adhesions at the front of the cells.

A Single Cell Migration

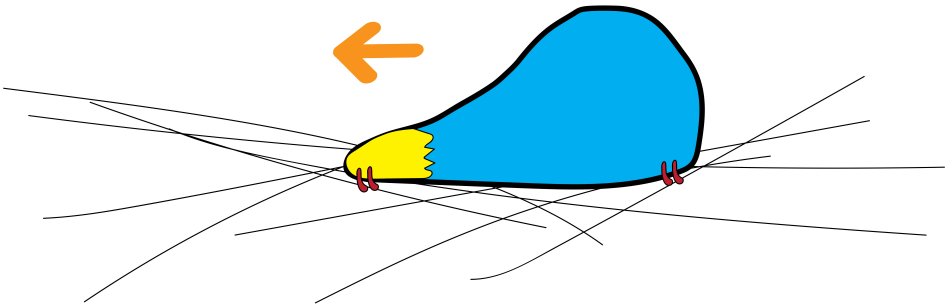

B Collective Cell Migration

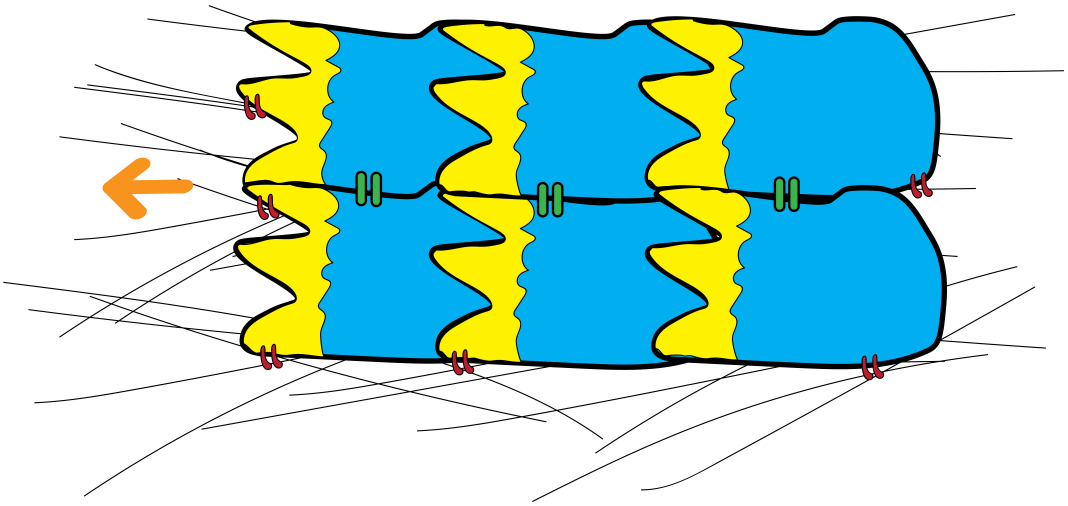

Figure 1.2

Geometry of collective cell migration establishes leader cells. (A) Diagram of cells collectively migrating as a sheet. During sheet migration, there are multiple leader cells. (B) Diagram of cells collectively migrating as a cluster with one leader cell. (C) Diagram of cells collectively migrating as a cord with one leader cell. (A–C) Magenta-colored cell(s) at the front of the group represent the leader cells.

A

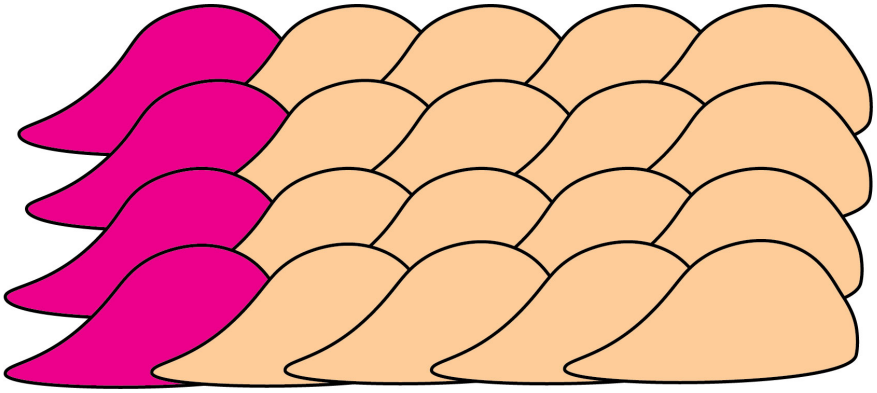

B

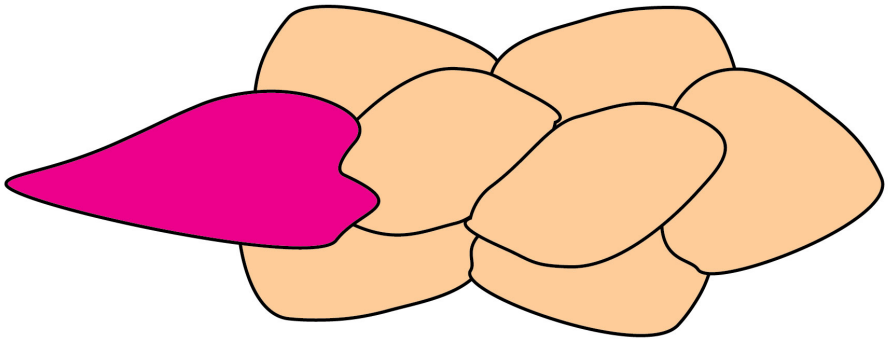

C

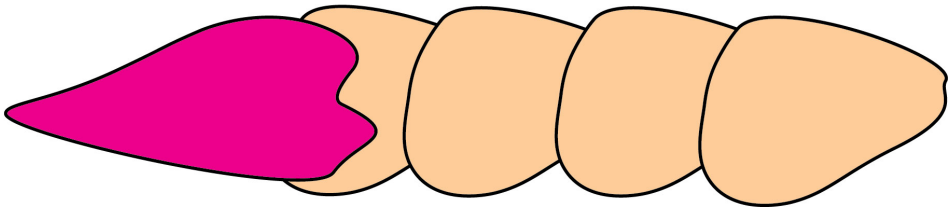

Figure 1.3

Structures of PDGF ligand and PDGFr. Activation of the PDGFr can occur when the PDGF ligand binds to the extracellular domain. The PDGFr is a dimer represented in green, and the PDGF ligand is also a dimer represented by two orange circles. The black line that goes through the cell membrane represents the transmembrane domain of the PDGFr. Dimerization of the PDGFr results in the creation of docking sites for SH2 domain-containing proteins, such as Src, Fak, Pi3k, and PLC, which are then activated by phosphorylation by the PDGFr. Each phosphorylation event is represented by yellow stars.

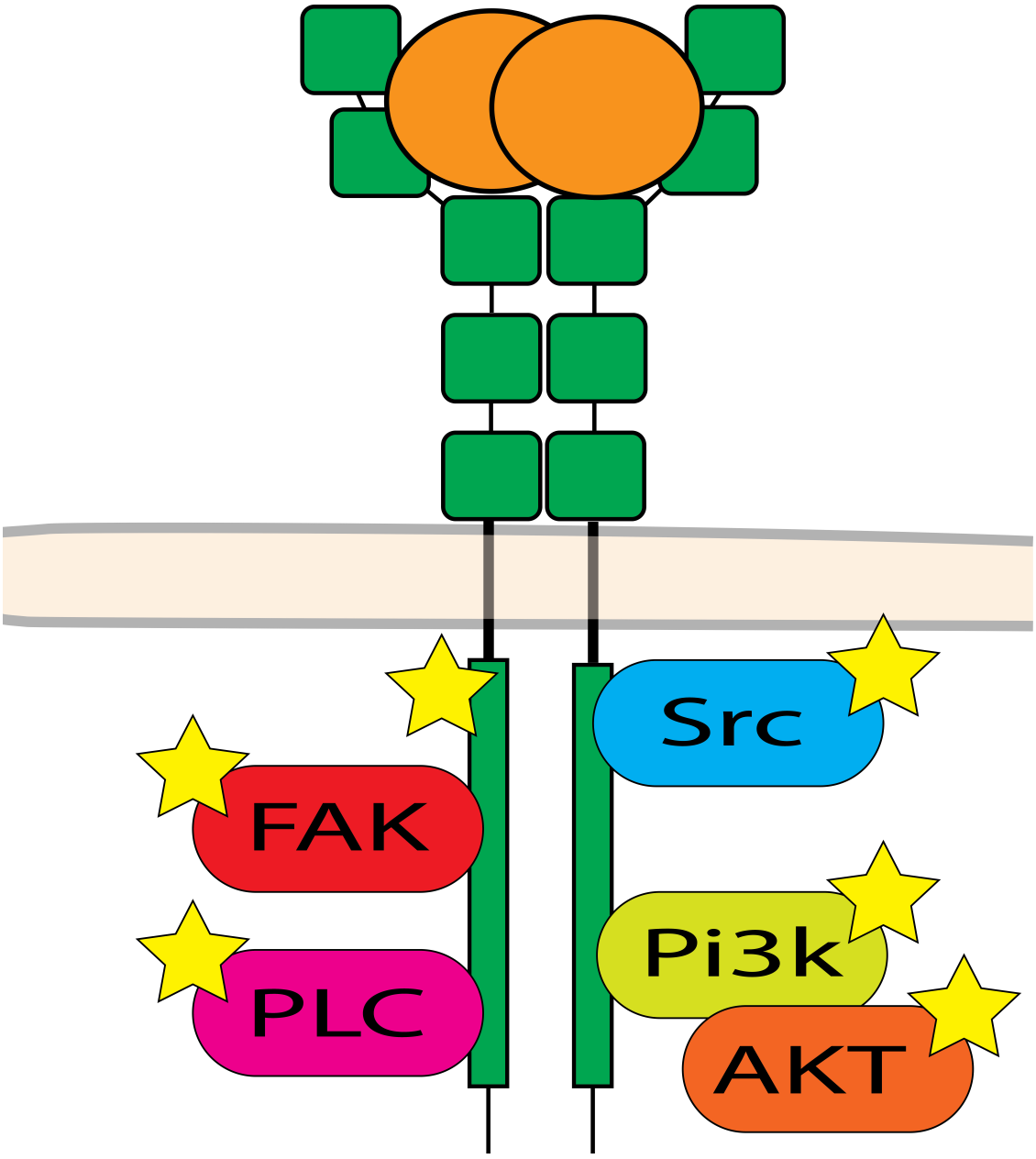
Src
FAK
Pi3k
PLC
AKT

Figure 1.4

Ligand independent and ligand dependent growth factor signaling. (A) Diagram of ligand independent growth factor signaling. Integrin adhesion to ECM results in a conformational change that causes integrin activation and the recruitment of Fak. Fak can phosphorylate and activate the PDGFr, which causes enhanced downstream Pi3k-Akt signaling. (B) Diagram of ligand dependent growth factor signaling. PDGF ligand binding to the PDGFr results in the dimerization and activation of PDGFr. This results in the recruitment and activation of Pi3k, which phosphorylates Akt. Pi3k-Akt signaling results in the activation of Fak, which causes inside-out signaling that results in the activation of integrins.

A. Ligand independent Growth Factor Signaling

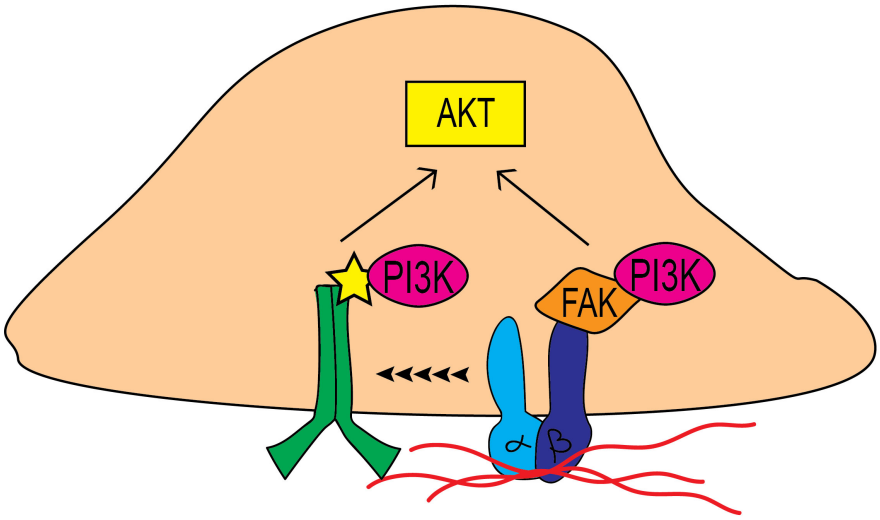

B. Ligand dependent Growth Factor Signaling

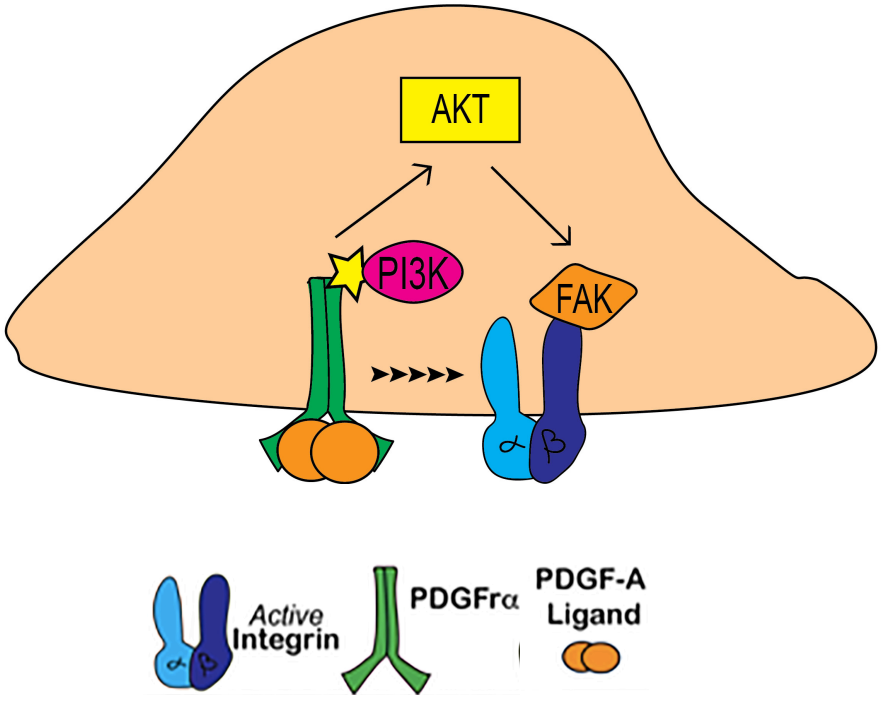

Figure 1.5

Pi3k–Akt signaling when cells adhere to 9.11 or 9.11a. (A) Diagram of a mesendoderm cell on purified FN fusion protein 9.11. On 9.11, integrins can attach to the Arg-Gly-Asp (RGD) and "synergy site" Pro-Pro-Ser-Arg-Asn (PPSRN) sequences, resulting in a conformational change and integrin activation. This enhances downstream Pi3k-Akt signaling, which results in the activation of Fak via Src. Fak phosphorylation of the PDGFr results in nonligand dependent PDGF signaling. 9.11 can promote cell adhesion, spreading, and migration. (B) Diagram of cell attachment to purified FN fusion protein 9.11a. On 9.11a integrins can attach to RGD but not to the "synergy site" sequence PPSRN because of a point mutation. Cells can attach, but they appear rounded because cells are unable to spread. This rounding results in decreased Pi3k-Akt signaling.

A

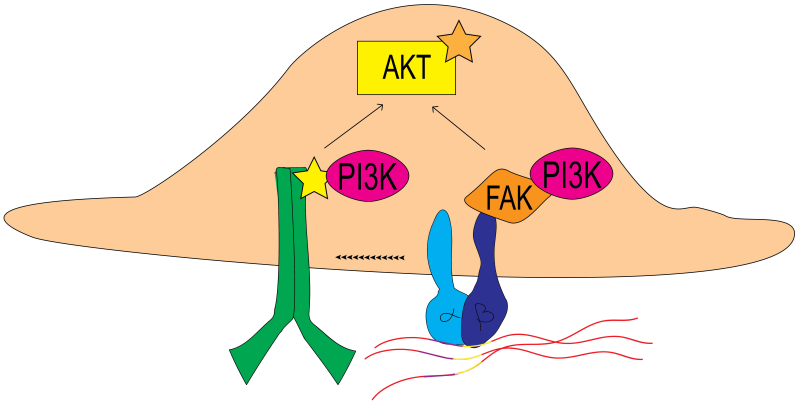

GST-9.11

B

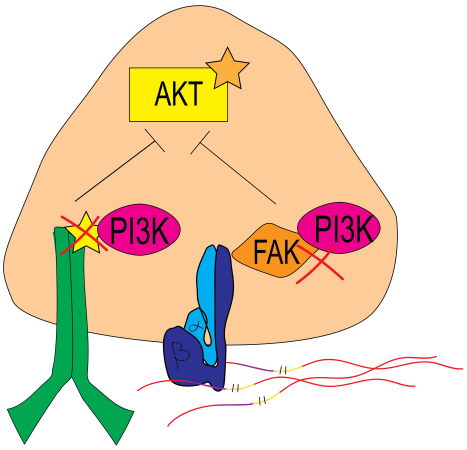

GST-9.11A

Figure 1.6

Model for the role of PDGFr in mesendoderm migration. (A) Diagram of mesendoderm migration. Mesendoderm expresses integrin α5β1, which binds to FN in at the RGD and "synergy site" PPSRN sequence resulting in a conformational change and activation of the integrin. Integrin activation can result in downstream signaling, including the activation of Fak that can activate the PDGFr in a nonligand dependent manner. (B) Inset diagram of a cell within the migrating mesendoderm tissue. Signaling from the PDGFr organizes the actin cytoskeleton and regulates the assembly of focal adhesions for directional mesendoderm migration.

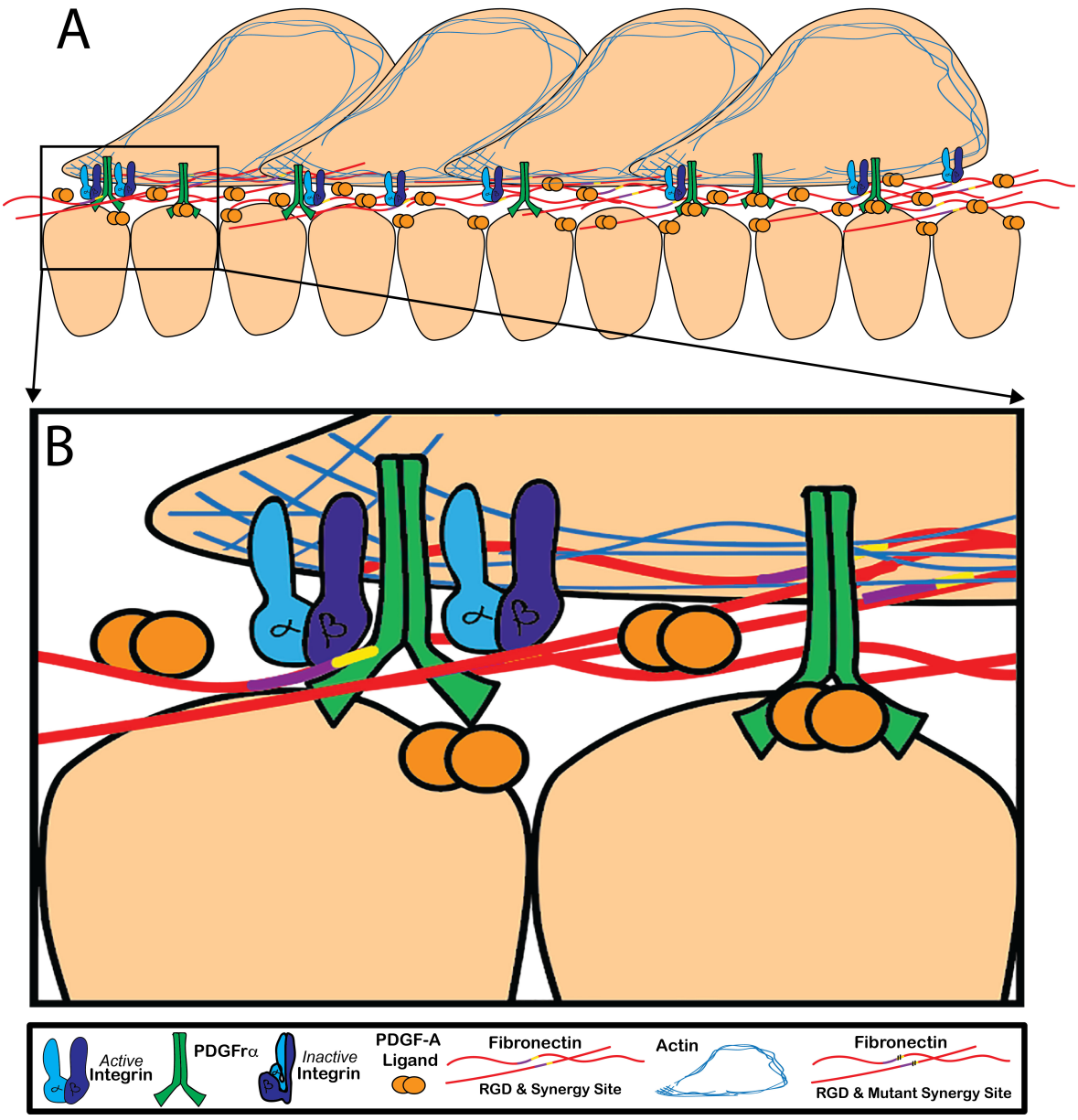
A
B
Active Integrin
PDGFrα
Inactive Integrin
PDGF-A Ligand
Fibronectin
RGD & Synergy Site
Actin
Fibronectin
RGD & Mutant Synergy Site

Chapter 2

PDGFr-α and integrin-fibronectin adhesive signaling enhance directional *Xenopus* mesendoderm migration*

*Manuscript in preparation for submission to *Mechanisms of Development*

2.1 Abstract

Both PDGF signaling and integrin adhesion to FN matrix have been implicated in directional migration of *Xenopus* mesendoderm. The relative importance of each remains unclear. Integrin-FN adhesive signaling is reported to up-regulate signaling by the PDGFr in a ligand independent manner. To address whether this mechanism stimulates PDGFr signaling in the absence of PDGF-A ligand, mesendoderm explants were cultured on Type-III repeats of FN (9.11), which contained the RGD and "synergy" sites required for integrin α5β1 adhesion to FN but that did not contain the PDGF-A ligand-binding site. Reduced levels of p-Akt were noted after PDGFr-α morpholino knockdown in mesendoderm cells on 9.11, suggesting that PDGFr-α functions independently of PDGF-A ligand. Furthermore, a reduction in p-Akt occurred when either the PDGFr-α was knocked down or when integrin activation was disrupted by plating cells on 9.11a that contained a point mutation in the FN "synergy site". Knocking down the PDGFr-α in conjunction with disrupting integrin adhesion to FN did not cause a further decrease in the p-Akt levels, suggesting that PDGFr-α signals and integrin-FN adhesions are converging on the same downstream pathway. Consistent with decreased p-Akt levels, knockdown of the PDGFr-α also caused a reduction in the p-Fak at Tyr-397. When the PDGFr-α was knocked down, defects in tissue migration, cytoskeletal organization, cell protrusion polarity, and focal adhesion size were noted. Mesendoderm cells became rounded, and the actin and cytokeratin filaments appeared collapsed and colocalized at the center of cells. Taken together, these findings suggest that integrin adhesion to FN is responsible for activating Pi3k-Akt signaling in the mesendoderm in the absence of

PDGF-A ligand, and, moreover, that this is sufficient to promote forward-directed protrusions for directional tissue migration.

2.2 Introduction

Embryonic development requires precise coordination of cell and tissue movements. How growth factor and adhesive signaling is integrated during large-scale tissue movements remains unclear. Morphogens, chemokines, and soluble growth factors guide directional movement (Haeger et al., 2015). PDGF is important for single cell chemotaxis and directional collective cell migration in many systems. Cells undergo chemotaxis toward PDGF during wound healing (Lynch, Nixon, Colvin, & Antoniades, 1987; Schneider et al., 2010), cancer invasion (Andrae et al., 2008; Watts et al., 2016; Yeh et al., 2016), *Drosophila* border cell migration (Duchek & Rørth, 2001; Duchek, Somogyi, Jékely, Beccari, & Rørth, 2001; McDonald et al., 2003), *Xenopus* mesoderm cell migration (Nagel et al., 2004; Smith et al., 2009; Symes, Smith, Mitsi, & Nugent, 2010), and zebrafish mesendoderm migration (Montero et al., 2003). PDGFr expression correlates with advanced tumor stages and metastasis in some cancers (Andrae et al., 2008). Integrin-FN adhesive signaling can activate the PDGFr in a ligand independent manner (Ross, 2004; Veevers-Lowe et al., 2011). Although PDGF signaling is important for directional migration (Duchek et al., 2001; Nagel et al., 2004; Yang et al., 2008), whether ligand independent signaling through the PDGFr is important remains unclear.

The migration of *Xenopus* mesendoderm cells at gastrulation is an example of a collective cell movement driving tissue morphogenesis (Winklbauer, 1990). PDGF-A

ligand in this system is reported to act as a directional cue to orient cell protrusions in the direction of the animal pole of the BCR (Nagel et al., 2004; Smith et al., 2009). PDGF-A ligand is expressed by the BCR cells in two alternatively spliced forms: a short form and a long form. Both are secreted at gastrulation. The short form is freely diffusible and acts as a long-range signal for radial intercalation of prechordal mesoderm cells toward the ectoderm (Damm & Winklbauer, 2011). The long form has an ECM-binding domain that allows PDGF-A ligand to attach to the HepII region of FN (Smith et al., 2009). Mesendoderm cells express the corresponding PDGFr-α. As these cells migrate on the BCR, they contact assembled FN matrix with sequestered PDGF-A ligand (Ataliotis, Symes, Chou, Ho, & Mercola, 1995; Damm & Winklbauer, 2011). Leader cells of the mesendoderm are the first to contact this matrix via integrin-based adhesion and send out forward directed protrusions (Nagel et al., 2004). The importance of PDGF as a major guidance cue required for directional mesendoderm migration has been explored using BCR-conditioned substrates (Nagel et al., 2004; Smith et al., 2009; Symes et al., 2010). Knockdown of the PDGF-A ligand results in misdirected protrusions on BCR conditioned substrates, suggesting a role for PDGF-A dependent chemotaxis (Nagel et al., 2004).

However, directional migration of explanted mesendoderm tissue is reported to occur on nonfibrillar FN substrates in the absence of matrix-attached PDGF-A ligand (Davidson et al., 2002), calling into question the importance of PDGF-A ligand in this process. One explanation is that ligand-independent activation of the PDGFr is responsible for directed migration of explanted mesendoderm. Thus, I sought to investigate the relationship between PDGFr dependent signaling and integrin engagement

of FN in directional migration. I found that PDGFr signaling can activate Pi3k-Akt to regulate the organization of cytoskeleton to orient protrusions in the absence of PDGF-A ligand.

Although growth factor receptors typically become activated as a result of direct molecular interactions with their cognate ligands, growth factor receptors can also be activated in a ligand independent manner. For example, the PDGFr is phosphorylated at Tyr-751 and activated after cell adhesion to FN resulting in integrin α5β1 activation and enhanced downstream signaling, leading to the phosphorylation of Fak at Tyr-397 (Veevers-Lowe et al., 2011). This crosstalk between integrin α5β1 and the PDGFr may initiate a positive signaling feedback loop, in which FAK phosphorylates and activates the PDGFr (Veevers-Lowe et al., 2011). Ligand independent activation of EGFr occurs in lung cancer, glioblastoma, and squamous cell carcinoma (Guo et al., 2015; Shen & Kramer, 2004). Integrin β1 and E-cadherin associate with and cause the activation of EGFr in a ligand independent manner (Moro et al., 1998; Shen & Kramer, 2004). In each of these examples, growth factor signaling is up-regulated through cooperation with cell adhesion molecules. However, the interplay between growth factor receptor and integrin signaling during morphogenesis remains unclear. This study explores the relationship between PDGF and integrin signals to promote cell adhesion and directional lamellipodial protrusion formation in the collective cell migration of *Xenopus* mesendoderm.

2.3 Materials and Methods

2.3.1 Collection of Xenopus Eggs and Embryos

Xenopus eggs were obtained from female frogs and were then fertilized. Embryos were allowed to develop, and gastrula stage embryos were staged according to Nieuwkoop and Faber (1994). Embryos were dejellied in 2% cysteine, rinsed with dH2O and cultured in 0.1X modified Barth's saline (MBS: 1X MBS: 88 mM NaCl, 1 mM KCl, 2.5 mM NaHCO3, 0.35 mM CaCl2, 0.5 mM MgSO4, 5 mM HEPES pH 7.8).

2.3.2. Dorsal Marginal Zone Explant Preparation and Single Mesendoderm Cell Dissection

Glass coverslips were treated with 10N NaOH; rinsed successively in deionized water, 70% ethanol, and 100% ethanol; and then flamed. Washed coverslips were coated with 10 μg of bovine plasma FN (Calbiochem, San Diego, CA), or equimolar amounts of 9.11 (0.5 μM), 9.11a (0.5 μM) prepared in 1X Modified Barth's saline (MBS) and left overnight at 4°C in a humidified chamber. FN coated coverslips were blocked with 0.45 μM sterile filtered 5% bovine serum albumin (BSA) then rinsed with 1X MBS.

Mesendoderm cells were dissected and dissociated in Ca2+ and Mg2+ Modified Barth's saline (CMF-MBS). Single mesendoderm cells were plated on bovine plasma FN (Calbiochem, San Diego, CA), or equimolar amounts of 9.11 (0.5 μM), 9.11a (0.5 μM) in 1X MBS and blindly scored as round or spread (defined as one or more protrusion; Ramos & DeSimone, 1996). No serum or PDGF-A ligand containing media was added to explant preparations.

Mesendoderm explants were prepared as described (Davidson et al., 2002; Davidson et al., 2004; Weber et al., 2012). Briefly, the dorsal marginal zone of the *Xenopus* embryo was dissected at Stage 10–, secured with glass coverslips using silicon grease, and allowed to adhere for 1 hour to bovine plasma FN (Calbiochem, San Diego, CA)- coated glass coverslips.

2.3.3 Morpholino Knockdown

Antisense morpholino oligonucleotides obtained from GeneTools (Philomath, OR) were used to knockdown *Xenopus laevis* PDGF-A ligand (PDGF-A) and PDGF Receptor (PDGFr-α). All experiments were done with a total of 60 ng morpholino injected per embryo. Sequences were as follows:

Control Morpholino: 5′- CCTCTTACCTCAGTTACAATTTATA-3′ (stock sequence)

PDGF-A Ligand Morpholino: 5′- AGAATCCAAGCCCAGATCCTCATTG-3′ used previously in Nagel et. al 2004.

PDGFrα Morpholino: 5′-GGCAGGCATCATGGACCGTAACAAC-3′

2.3.4 RNA Transcription

RNA encoding LifeAct-mCherry (pCS2+ LifeAct-mCherry; Pfister et al., 2016), green fluorescent protein (GFP)-XCK1(8) (pCS2+ EGFP-XCK8, V. Allan, University of Manchester; Clarke and Allan, 2003), and enhanced GFP-paxillin (PCS2+ paxillin-EGFP, obtained from Horwitz, University of Virginia, and sub-cloned into pCS2+ as

described in Sonavane et al. 2017) were transcribed *in vitro* from linearized plasmid DNA. Then 5nLs were injected into the two dorsal blastomeres at the four-cell stage for a final concentration of 500pg/embryo.

2.3.5 Western Blot and Immunofluorescence

Xenopus embryos or dissected mesendoderm tissue was solubilized in lysis buffer [100 mM NaCl, 50 mM Tris- HCl pH 7.5, 1% Triton X-100, 2 mM PMSF (phenylmethylsulphonyl fluoride), protease inhibitor cocktail (Sigma, St. Louis, MO), 1 mM EDTA, 1 mM EGTA, 1 mM β-glycerolphosphate, 2.5 mM $Na_4P_2O_7$, 1mM sodium vanadate, 0.2 mM H_2O_2]. Protein extracts were diluted in 2X Laemmli buffer (2% β-mercaptoethanol) and run on a 10% SDS-PAGE gel and transferred to nitrocellulose. Nitrocellulose was stained with Ponceau [5% acetic acid, 0.2 g Ponceau] and blocked with 10% BSA, and then probed using antibodies to Rb mAb-p Akt Tyr 308 (1:1000 in 3% BSA, Cell Signaling #2965, Danvers, MA), Rb mAb Total Akt (1:1000 in 5% milk, Cell Signaling #3C67E7, Danvers, MA), Rb pAb pFak Tyr 397 (1:1000 in 3% BSA, Upstate) and β-actin (1:10,000 in 5% milk, Sigma #A3854).

2.3.6 Immunofluorescence Microscopy

Mesendoderm explants were fixed overnight with ice-cold 100% methanol at 4°C, rehydrated into TBS (75% methanol, 50% methanol, 25% methanol), washed with TBS-T, and stained overnight at 4°C with pan-cytokeratin C11 antibody (1:200, Sigma, St. Louis, MO). After three washes with TBS-T, goat anti-mouse IgG conjugated to

AlexaFluor488 was used to visualize cytokeratin. Actin was visualized using AlexaFluor488-actistain after mesendoderm explant fixation in 0.25% Glutaraldehyde, 3.7% Formaldehyde, and 0.1% Tween for 10 minutes at room temperature. Immunofluorescence imaging was performed on a Nikon C1 confocal microscope with a Nikon PlanApo/60×/1.40 objective. Confocal z-stack images were taken at 0.5-1 μm intervals. TIRF microscopy was performed on an Olympus 1X70 inverted TIRF microscope with an Olympus 60X/1.45 TIRF objective and images were collected 15 seconds apart for 5 minutes. Focal adhesion size was measured using Image J. Images were threshold and pixel density was measured as described previously (Sonavane et al. 2017).

2.3.7 Tracking DMZs Migration Rate Using ImageJ

Images were collected (1 per minute) using a Zeiss Axiovert 35 with OpenLab software (Improvision/Perkin Elmer, Waltham, MA). Image analysis was performed using Volocity and ImageJ (http://rsb.info.nih.gov; National Institutes of Health, Bethesda, MD). Using ImageJ, each image was divided into left (0–341 pixels), middle (341–683 pixels), and right pixel (683–1024 pixels) sections. Tracing was done by placing three fiduciary marks (one per section) along the leading edge of the mesendoderm explant using a 25-μm diameter paintbrush. In each case, the x-coordinate was recorded, and the average of the three dots was recorded as one data point. Explant retractions were defined as any movement opposite the direction of migration and was recorded as negative values in distance traveled.

2.3.8 Statistical Analysis

Graphs and statistical analysis were performed using PRISM V5 software. A Wilcoxon match-paired signed rank test was performed for a pairwise comparison when experiments had two treatment conditions with matched clutches of embryos. Differences between Control MO cells or PDGFr -α MO cells plated on 9.11 and 9.11a substrates were analyzed using a one-way ANOVA followed by Tukey's *post hoc* test. Significance was reported with ns = not significant, *$p \leq 0.05$, **$p \leq 0.01$, ***$p \leq 0.001$.

2.4 Results

2.4.1 PDGFr-α and Integrin-FN Adhesions Contribute to Akt Phosphorylation

Mesendoderm cells express integrin α5β1, which binds to FN RGD in cooperation with the "synergy site" sequence (Ramos & DeSimone, 1996) resulting in integrin activation and transition to a high affinity state (Li, Redick, Erickson, & Moy, 2003). Integrin α5β1 binding to RGD containing Type III_{10} repeat alone is sufficient for integrin adhesion to FN, although the integrins remain in a low-affinity state (García, Schwarzbauer, & Boettiger, 2002). Cells can attach to RGD-containing fragments of FN but are unable to spread when the "synergy site" in Type III_9 is mutated (Ramos & DeSimone, 1996). Integrin binding to FN can lead to the activation of the PDGFr in a PDGF ligand independent manner, and this upregulation of signaling can further stimulate integrin conformational change and activation (Sundberg & Rubin, 1996; Veevers-Lowe et al., 2011). Inputs from both integrin-FN adhesions and PDGF signaling mediate cell attachment and cell spreading (Ramos & DeSimone, 1996; Symes &

Mercola, 1996). Although PDGF signaling and integrin adhesive signaling act cooperatively, the relative contribution of PDGFr-α dependent signaling and integrin signaling remains unclear.

To investigate whether PDGFr-α regulates integrin-dependent adhesive signaling in directional *Xenopus* mesendoderm migration, an antisense morpholino oligodeoxynucleotide [PDGFr-α morpholino (MO)] was designed to block the translation of *Xenopus* PDGFr-α mRNA. PDGFr-α MO mesendoderm cells were plated on purified FN fusion proteins (Fig. 2.1 A). Bacterially purified FN fusion proteins were used instead of purified plasma FN to eliminate the possibility of pFN contamination with PDGF ligand. Moreover, using FN fusion proteins allowed for the evaluation of the contribution of the FN RGD and "synergy" sites to cell adhesion and cell signaling (Li et al., 2003; Ramos, Whittaker, & DeSimone, 1996). The FN fragments used in these experiments corresponded to Type-III repeats 9 through 11 of *Xenopus* FN containing the RGD and the "synergy" sites, which are the key adhesion sites for full integrin α5β1 engagement on FN (Fig. 2.1 A). To assess the contribution of integrin engagement with FN "synergy site" to signaling, the 9.11 fragment, which has a point mutation in the "synergy site", 9.11a, was used (Fig. 2.1 A). As previously demonstrated, Control Morphant (Control MO) mesendoderm cells on 9.11 attach and spread, whereas cells on 9.11a attach but are unable to spread (Fig. 2.1 B; Ramos et al., 1996). Decreased cell spreading was also noted in PDGFr-α MO-treated cells on 9.11 compared with Control MO cells (Fig. 2.1 B, 24% decrease). These data were consistent with a role for both integrin engagement with FN and PDGFr-α functioning in mesendoderm cell spreading on FN.

It is well established that both α5β1 integrin-FN dependent adhesive signaling (King, Mattaliano, Chan, TTsichlis, & Brugge, 1997) and PDGF activate Pi3k-Akt signals (Franke et al., 1995). However, it has only recently been demonstrated that α5β1 integrin-FN dependent adhesive signaling and PDGFr can act synergistically to enhance Pi3k-Akt signals (Veevers-Lowe et al., 2011). To evaluate the relative contribution of integrins and PDGFr-α to the phosphorylation of Akt (p-Akt), Western blot analysis was performed comparing Control MO, PDGF-A ligand MO, and PDGFr-α MO-treated embryos. When the PDGF-A ligand was knocked down, the levels of p-Akt were not significantly different from Control MO (Fig. 2.1 C), whereas PDGFrα knockdown resulted in a significant reduction of p-Akt levels (Fig. 2.1 D). Because there was a decrease in p-Akt levels when the PDGFr-α was knocked down, but not when the PDGF-A ligand was knocked down, the role of ligand independent PDGFr-α signaling in the phosphorylation of Akt was further evaluated using FN fusion proteins lacking the PDGF-A ligand binding site.

A 50% decrease in p-Akt levels was noted in Control MO-treated cells on 9.11a compared with cells on 9.11 (Fig 2.1 E). Knocking down the PDGFr-α also caused a 50% decrease in p-Akt levels, similar to decreased p-Akt levels of Control MO cells on 9.11a (Fig. 2.1 E). When PDGFr-α was knocked down in conjunction with disrupting integrin adhesive signals by plating cells on 9.11a, there was no additive effect, and no additional decrease in p-Akt was noted (Fig. 2.1 E). Thus, reduced cell spreading correlated with decreased p-Akt levels. To maintain full p-Akt levels and cell spreading, both the FN "synergy site" and the PDGFr-α were required. These data were consistent with crosstalk

between PDGFr-α and integrin-FN adhesive signals leading to cell spreading and the phosphorylation of Akt.

Because PDGFr dependent signaling activates Pi3k-Akt leading to the phosphorylation of Fak, and Fak is important for cell adhesion to FN, whether PDGFr-α dependent signals were important for the phosphorylation of FAK at Tyr 397 was investigated next (Fig. 2.1 F). A 50% decrease in levels of p-Fak at Tyr 397 in PDGFr-α MO embryos was noted (Fig. 2.1 F). This decrease correlated with the decrease in p-Akt levels (Fig. 2.1 B). Taken together, these data were consistent with PDGFr-α functioning in cooperation with integrin adhesive signaling to activate downstream signaling pathways that lead to the phosphorylation of Akt and Fak at Tyr 397 to regulate cell spreading on FN.

2.4.2 PDGFr-α Stabilizes Mesendoderm Cell Adhesions With FN

Because mesendoderm explants migrate directionally along nonfibrillar FN without added PDGF-A (Davidson et al., 2002), the functional importance of PDGFr dependent signaling in directional mesendoderm migration is unclear. To test the role of PDGFr signals in mesendoderm migration, the leading edge of the mesendoderm was tracked over time. Migration of Control MO, PDGF-A ligand MO, and PDGFr-α MO treated mesendoderm explants were compared. Mesendoderm is not known to express PDGF-A ligand (Ataliotis et al., 1995; Damm & Winklbauer, 2011), and PDGF was not added to explant culture. However, to reduce the possibility that the mesendoderm was exposed to PDGF-A *in vivo* before explantation, explants were prepared from PDGF-A

MO injected embryos. The PDGF-A MO construct was used previously and caused disruption of directional mesoderm migration on BCR conditioned substrates that contain FN bound PDGF-A ligand (Nagel et al., 2004). The importance of the PDGFr-α during mesendoderm migration on FN without PDGF has not yet been evaluated.

When the leading edge of the mesendoderm tissue was tracked over 30 minutes, a significant increase in retractions in PDGFr-α MO explants was noted compared with Control MO explants (Fig. 2.2 A). Retractions were defined as any rearward movement opposite the direction of migration (Fig. 2.2 A). A significant decrease in the distance traveled was observed in PDGFr-α MO mesendoderm explants compared with Control MO explants at all timepoints after 20 minutes (Fig. 2.2 B). However, there was no significant difference in distance traveled between PDGF-A ligand MO explants and Control MO explants noted at any timepoint (Fig. 2.2 B).

Because PDGF acted as a chemoattractant, I next investigated whether PDGF signaling enhanced the migration rate of mesendoderm. The instantaneous velocity was measured in Control MO, PDGF-A ligand MO, and PDGFr-α MO mesendoderm explants. No significant change was noted in the instantaneous velocity of mesendoderm explants when either the PDGFr-α or the PDGF-A ligand was knocked down compared with controls (Fig. 2.2 C). These data were consistent with increased retractions resulting in a decrease in the distance of the mesendoderm tissue migration overtime but not a reduction in migration speed *per se*. The data supported a possible role for PDGFr-α independent of the PDGF-A ligand.

2.4.3 PDGFr-α Knockdown Disrupts Monopolar Protrusive Cell Behavior

Because integrin-dependent adhesive signaling was required for cell protrusion formation and PDGF was implicated in orienting cell protrusions during migration, I next evaluated the contribution of PDGF signaling in the regulation of polarized protrusive cell behavior during mesendoderm migration. To test whether PDGFr-α was necessary for forward-directed lamellipodial formation, protrusion angles were quantified relative to a line parallel to the direction of explant travel through the center of the cell body. Measured protrusion angles were binned in 30° increments and the percentage of protrusions in each bin was plotted in rose diagrams; 180° represents the protrusions in the direction of travel (Fig. 2.3). The protrusion angles provide a measure of protrusive behaviors characteristic of migrating mesendoderm (Bjerke et al., 2014; Davidson et al., 2002). A 34% decrease in forward-directed protrusions along the leading edge was noted in PDGFr-α MO explants compared with Control MO explants (Fig. 2.3 A–F). The percentage of forward-directed protrusions in PDGF-A ligand MO explants was not significantly different from Control MO explants (Fig. 2.3 D–E). These results indicated a role for the PDGFr-α in maintaining forward-directed protrusions during mesendoderm migration.

Migrating mesendoderm cells displayed monopolar protrusive behavior in which cells typically extend 1 to 2 protrusions in the direction of travel (Bjerke et al., 2014; Davidson et al., 2002). To determine whether PDGFr-α was important for this monopolar protrusive behavior, the number of protrusions per cell was counted in migrating mesendoderm explants. An increase in the average number of protrusions per cell was noted when PDGFr-α was knocked down, whereas the average protrusion number in

PDGF-A ligand MO cells was not significantly different from Control MO cells (Fig. 2.3 G). One mechanism by which knockdown of PDGFr-α could be affecting lamellipodial protrusion number and directionality is through the underlying cytoskeletal architecture.

2.4.4 PDGFr-α Functions in Lamellipodial Protrusion Formation of the Actin Cytoskeleton

PDGF signaling has been shown to regulate actin crosslinking during the formation of lamellipodial protrusions in both epithelial and mesenchymal cell types (Herman & Pledger, 1985; Nagano et al., 2006). Because the data from this study showed that mesendoderm lamellipodial protrusion directionality and number were dependent on the PDGFr-α (Fig. 2.3), I decided to test whether PDGFr-dependent signaling affected actin organization in mesendoderm using phalloidin to label the actin cytoskeleton. Thick actin-filled lamellipodial protrusions oriented in the direction of migration were observed in Control MO and PDGF-A ligand MO explants (Fig. 2.4 A, red arrowheads). However, the actin cytoskeleton was disorganized in PDGFr-α MO mesendoderm compared with controls (Fig. 2.4 A-C). Protrusions were more filopodia-like in appearance with reduced size and misdirected in PDGFr-α MO mesendoderm explants (Fig. 2.4 C). A fine actin filament network extended throughout the cell in Control MO explants (Fig. 2.4 A). Actin structures appeared collapsed, and cells had a decrease in fine actin filaments that extended throughout the cell in PDGFr-α MO explants (Fig. 2.4 C). Traces of actin-based protrusions were observed in front of the mesendoderm tissue when PDGFr-α was knocked down (Fig. 2.4 C, blue arrowheads). A possible explanation is that the cell membrane and actin were left on the FN glass coverslip after tissue retraction. These data

were consistent with decreased integrin adhesive signaling and reduced p-Akt (Fig. 2.1) leading to mesendoderm tissue retraction and cells rounding up in PDGFr-α MO mesendoderm explants (Fig 2.3 C).

2.4.5 Cytokeratin Intermediate Filament Network Collapses in PDGFr-α MO Mesendoderm Explants

Mesendoderm monopolar protrusive behavior is dependent on the organization of the keratin intermediate filament cytoskeleton (Weber et al., 2012) Because the orientation and number of mesendoderm cell protrusions was disrupted in PDGFr-α MO explants, cytokeratin cytoskeletal organization was investigated next. Cytokeratin networks extended throughout the cells in Control MO (Fig. 2.5 A, D, G) and PDGF-A ligand MO (Fig. 2.5 B, E, H) explants; however, cytokeratin appeared to collapse to the center of the mesendoderm cells in PDGFr-α MO explants (Fig. 2.5 C, F, I). The mis-localization of cytokeratin toward the center of the cells correlated with mesendoderm tissue retraction (Fig. 2.2 A). Collapses in the cytokeratin network overlapped with actin foci in PDGFr-α MO explants (Fig. 2.5 F, I, L, blue arrows).

2.2.6 PDGFr-α MO Mesendoderm Cells Have Larger Focal Adhesions

The increase in tissue retractions (Fig. 2.2) and decrease in pFak at Tyr 397 in PDGFr-α MO explants, led me to ask whether focal adhesion size was altered in PDGFr-α MO explants. To visualize focal adhesions, paxillin-GFP was expressed and imaged in migrating mesendoderm explants using total internal reflection fluorescence microscopy

(Fig. 2.6 A–L). A significant increase in the size of focal adhesions was noted upon disruption of PDGF signaling with the largest focal adhesions in PDGFrα MO-treated explants (Fig. 2.6 L-M). The data is consistent with the current understanding of Fak regulation of focal adhesion size and increased focal adhesion size occurs in mouse embryonic mesodermal Fak (–/–) cells (Llić et al., 1995).

2.5 Discussion

2.5.1 Integrin and PDGF Signals Are Required for Directional Xenopus Mesendoderm Migration

Integrins are important mediators of cell signaling and are required for cell adhesion to the surrounding extracellular matrix. Integrin receptors can function in conjunction with other receptors, such as growth factor receptors, to enhance downstream cell signaling pathways (Ross, 2004; Veevers-Lowe et al., 2011). This study provides insight into the interplay between integrin and growth factor signaling during embryonic development. A role for integrin signaling in cooperation with PDGF signaling was identified to regulate cytoskeletal dynamics and focal adhesion assembly and to orient cell protrusions during directional migration of *Xenopus* mesendoderm. This model builds on previous studies that suggested PDGF-A ligand acts as a chemoattractant to enhance directional migration (Ataliotis et al., 1995; Nagel et al., 2004; Smith et al., 2009; Symes & Mercola, 1996). I concluded that PDGFr-α can synergize with integrin-fibronectin adhesive signaling to direct mesendoderm migration.

Although integrins and growth factors converge to activate the Pi3k-Akt signaling pathway (Ross, 2004), how integrins synergize with growth factors remains unclear. The current study identified functions for the PDGFr-α in the absence of PDGF-A ligand. The PDGFr-α MO phenotype has features in common with disruption of integrin-FN adhesions using function blocking antibodies (Davidson et al., 2002; Ramos & DeSimone, 1996; Winklbauer & Nagel, 1991) or knocking down Fak (Bjerke et al., 2014). Inhibiting the interactions of α5β1integrin with the RGD site results in mesendoderm tissue explants detaching and "snapping-back" (Davidson et al., 2002). Fak MO cells are less spread on FN, but explants do not detach (Bjerke et al., 2014). This phenotype is comparable to cells on 9.11a that are unable to attach to the FN "synergy site" (Bjerke et al., 2014; Davidson et al., 2002; Ramos et al., 1996). Similar to Fak MO and cells on 9.11a, PDGFr-α MO cells are less well spread on FN. Although PDGFr-α MO mesendoderm explants are able to migrate on nonfibrillar FN substrates, there is an increase in the number of retractions compared with Control MO explants consistent with a defect in integrin-fibronectin adhesions or a defect in the cytoskeleton. The study also demonstrated a role for integrin adhesive signaling in cooperation with PDGFr-α dependent signaling in the phosphorylation of Akt at Tyr 308. Taken together, these findings increase understanding of how integrin and PDGF signals enhance Pi3k-Akt signals to produce collective cell migration of *Xenopus* mesendoderm tissue.

2.5.2 Ligand Independent Signaling of the PDGFr

The PDGF ligand is a well-established chemoattractant that promotes the orientation of cell protrusions to direct cell migration (Lynch et al., 1987; McDonald et

al., 2003; Montero et al., 2003). *Xenopus* mesoderm can respond to PDGF-A ligand embedded in the FN of blastocoel conditioned substrates by orienting protrusions in the direction of the animal pole (Nagel et al., 2004). An alternatively spliced form of the PDGF-A ligand that lacks the C-terminal matrix-binding domain is freely diffusible and unable to bind FN or promote directional mesendoderm migration (Nagel et al., 2004). Although it remains unclear whether a protein gradient of the PDGF-A ligand forms in the developing embryo, the FN-bound form of PDGF-A ligand can function as a chemoattractant to enhance directional mesendoderm migration (Nagel et al., 2004).

Directional mesendoderm migration can also occur *in vitro* on unmodified nonfibrillar FN without attached PDGF-A ligand (Davidson et al., 2002). This finding calls into question the role of PDGF as a FN-attached chemotactic cue in mesendoderm migration. If mesendoderm migration is directional in the absence of PDGF-A ligand, then is PDGF signaling required for directional migration? Integrin-FN adhesive signaling can activate the PDGFr (Ross, 2004; Veevers-Lowe et al., 2011). Does ligand independent PDGFr signaling enhance directional *Xenopus* mesendoderm migration? If so, how do PDGFr dependent signals act in synergy with other cues to direct migration?

This study was undertaken to address these questions using a morpholino approach to knock down PDGFr-α. I demonstrated that PDGFr-α functions to promote directional migration during mesendoderm migration on FN. Interestingly, PDGFr-α functions in the absence of a gradient of sequestered PDGF-A ligand. These data support a role for integrin–fibronectin adhesive signals acting in cooperation with the PDGFr-α. In the developing embryo, integrin cooperation with PDGFr-α may provide another way to enhance directional migration. One possibility is that maintaining a ligand gradient

over long-range migration can be difficult to control spatiotemporally. Highest traction stresses and focal adhesions are localized to the front of the migrating mesendoderm explants (Sonavane et al., 2017), supporting a model in which integrins are in the highest activation state in the front of the tissue where they spatially enhance PDGFr dependent signaling.

2.5.3 PDGFr Functions to Maintain the Organization of the Underlying Cytoskeleton and Normal Focal Adhesion Size

Actin-filled lamellipodial protrusions are a prominent feature of directional *Xenopus* mesendoderm migration (Bjerke et al., 2014; Davidson et al., 2002). PDGF signaling enhances actin crosslinking, causing the formation of membrane ruffles (Herman & Pledger, 1985; Nagano et al., 2006). Ligand independent signaling by the PDGFr-α is necessary to maintain actin-filled lamellipodial protrusions. In the absence of the PDGFr-α, protrusions become more filopodial-like and become misdirected. The normal arrangement of the cortical actin cytoskeleton, including fine actin filaments found throughout the cell body, is dependent on PDGFr-α. The collapse in the actin cytoskeletal network observed in PDGFr-α MO mesendoderm explants likely contributes to the aberrant migratory behavior.

The organization of both the actin and cytokeratin intermediate filament cytoskeleton is dependent on the PDGFr-α. Recruitment of keratin intermediate filaments to C-cadherin junctions is a result of asymmetric tissue tension, and keratin is required for directional protrusion formation (Weber et al., 2012). Knockdown of either

plakoglobin or Fak results in a disruption in the cytokeratin intermediate filament network without significantly altering cell cohesion within the mesendoderm tissue (Bjerke et al., 2014; Weber et al., 2012). Similarly, knockdown of the PDGFr-α failed to disrupt cell–cell contacts, but recruitment of keratin intermediate filaments to cell contacts was disrupted. Keratin intermediate filaments become collapsed toward the center of the cell where they co-localize with collapsed actin structures. The mislocalization of keratin is interpreted as a result of the cells rounding up within the tissue because of a disruption in integrin-FN adhesive signaling.

The disruption in PDGFr-α dependent signaling leads to a decrease in pFak at Tyr-397 and mesendoderm explants has larger focal adhesions. Larger focal adhesions are comparable with increased focal adhesion size found in FAK (–/–) mouse embryonic mesodermal cells (Llić et al., 1995) or where Fak is knocked down in fibroblasts (Kim & Wirtz, 2013). Knocking down components required for integrin activation such as kindlin 2 or integrin β1 also resulted in an increase in focal adhesion size (Bandyopadhyay, Rothschild, Kim, Calderwood, & Raghavan, 2012) similar to PDGFr-α knockdown. Taken together, these findings are consistent with integrin and PDGFr dependent signals acting cooperatively to modulate Fak phosphorylation at Tyr-397 and adhesion to FN necessary for focal adhesion assembly, directional protrusion formation, and cytoskeletal organization.

Figure 2.1

Decreased levels of p-Akt in PDGFr-α MO mesendoderm cells on FN fusion proteins. (A) Diagram of full-length *Xenopus* fibronectin (FN) and FN bacterial fusion proteins 9.11 and 9.11a. 9.11 and 9.11a contain FN Type III repeats 9-11 including the RGD site in Type III_{10} and the PPSRN "synergy site" in Type III_9; 9.11a has a point mutation that changes the sequence to PPSAN and prevents integrin binding to "synergy site". Type I repeats are light blue, Type II repeats are purple, and Type III repeats are dark blue. (B) Representative images of Control MO and PDGFr-α MO mesendoderm cells on 9.11 and 9.11a with corresponding quantification of percentage of spread cells. Number of cells analyzed: 9.11 Control MO = 571 cells, 9.11A Control MO = 393 cells, 9.11 PDGFr-α MO = 586 cells, and 9.11A PDGFr-α MO = 402 cells across 3 separate experiments. (C) Western blot of p-Akt levels in PDGFr-α MO gastrula Stage 11 embryos. Graph is (N = 8). (D) Western blot of p-Akt levels in PDGF-A ligand MO gastrula Stage 11 embryos. Graph is (N = 3). (E) Western blot of p-Akt levels of Control MO or PDGFr-α MO mesendoderm cells on 9.11 or 911a. Graph is (N = 3). (F) Representative Western blot of p-Fak 397 for Control MO and PDGFr-α MO gastrula Stage 11 embryos. Graph is (N = 3). (B-F) Data are mean + standard error of the mean. A single asterisk (*) indicates p <.05, a double asterisk (**) indicates p <.005, a triple asterisk (***) indicates p <.001, and n.s. indicates no statistically significant difference.

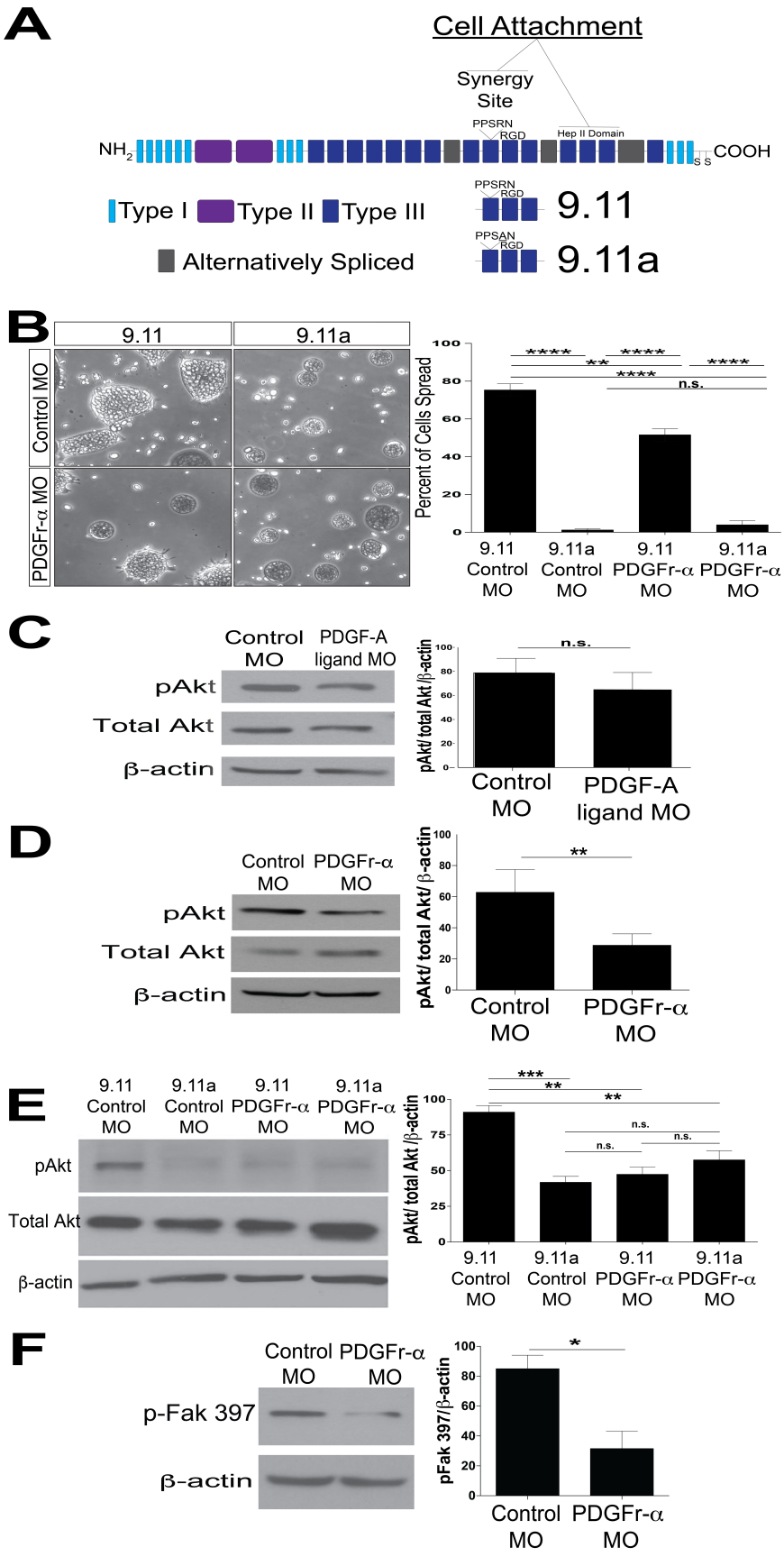
A
Cell Attachment
Synergy Site
PPSRN
RGD
Hep II Domain
NH2
COOH
S S
Type I
Type II
Type III
Alternatively Spliced
PPSRN
RGD
9.11
PPSAN
RGD
9.11a
B
9.11
9.11a
Control MO
PDGFr-α MO
Percent of Cells Spread
****
****
**
****
****
n.s.
9.11 Control MO
9.11a Control MO
9.11 PDGFr-α MO
9.11a PDGFr-α MO
C
Control MO
PDGF-A ligand MO
pAkt
Total Akt
β-actin
pAkt/ total Akt/β-actin
n.s.
Control MO
PDGF-A ligand MO
D
Control MO
PDGFr-α MO
pAkt
Total Akt
β-actin
pAkt/ total Akt/ β-actin
**
Control MO
PDGFr-α MO
E
9.11 Control MO
9.11a Control MO
9.11 PDGFr-α MO
9.11a PDGFr-α MO
pAkt
Total Akt
β-actin
pAkt/ total Akt /β-actin
***
**
**
n.s.
n.s.
n.s.
9.11 Control MO
9.11a Control MO
9.11 PDGFr-α MO
9.11a PDGFr-α MO
F
Control MO
PDGFr-α MO
p-Fak 397
β-actin
pFak 397/β-actin
*
Control MO
PDGFr-α MO

Figure 2.2

Retraction number increased in PDGFr-α MO mesendoderm explants. (A) Quantification of the number of times mesendoderm explants retracted over a 30-minute time period. Data represent the percentage of explants with high (8–10, orange bar), medium (4–7, yellow bar), and low (0–3, pink bar) numbers of retractions. (B) Quantification of the average distance mesendoderm explants traveled over a 30-minute time period. (A–B) A single asterisk (*) indicates $p < .05$ and a double asterisk (**) indicates $p < .005$. (B) No statistically significant differences were noted between Control MO and PDGF-A ligand MO explants at any timepoint. (C) Quantification of the average instantaneous velocity calculated in the forward direction, excluding retractions. n.s. indicates no statistically significant difference for comparison between all conditions. (B-C) Data are represented as mean + standard error of the mean. (A–C) 11 individual explants analyzed per treatment across 3 separate experiments.

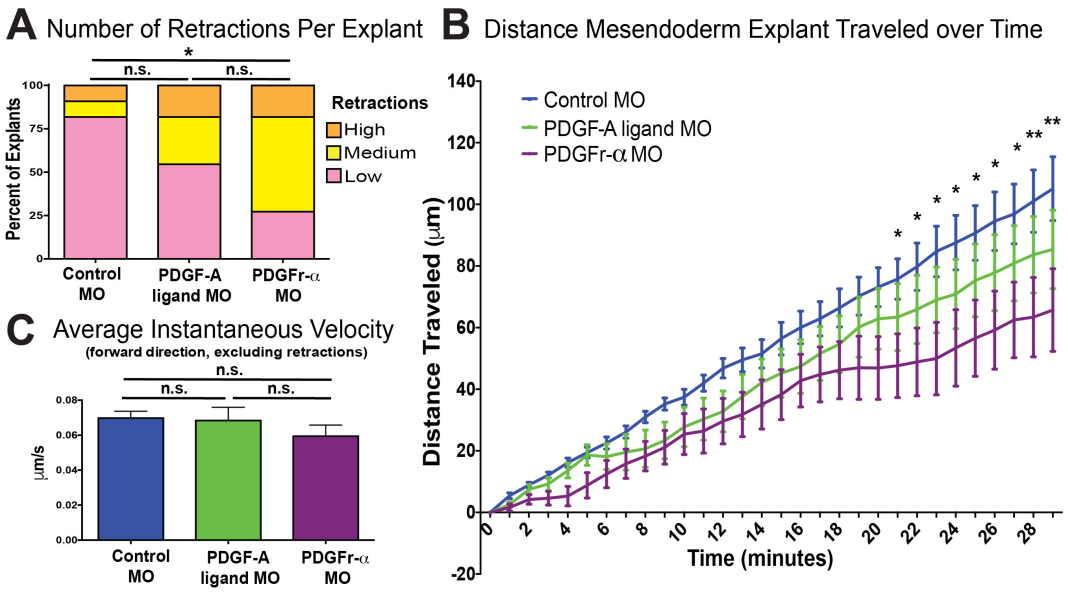
A Number of Retractions Per Explant
*
n.s.
n.s.
Percent of Explants
100
75
50
25
0
Retractions
High
Medium
Low
Control MO
PDGF-A ligand MO
PDGFr-α MO
B Distance Mesendoderm Explant Traveled over Time
Control MO
PDGF-A ligand MO
PDGFr-α MO
Distance Traveled (μm)
140
120
100
80
60
40
20
0
-20
0
2
4
6
8
10
12
14
16
18
20
22
24
26
28
Time (minutes)
C Average Instantaneous Velocity
(forward direction, excluding retractions)
n.s.
n.s.
n.s.
μm/s
0.08
0.06
0.04
0.02
0.00
Control MO
PDGF-A ligand MO
PDGFr-α MO

Figure 2.3

PDGFr-α is required for directional monopolar protrusive activity. (A–C) Representative confocal images of live Control MO, PDGF-A ligand MO, and PDGFr-α MO mesendoderm explants migrating on FN and expressing membrane-EGFP. Collapsed z-stacks with slices taken at the plane of the coverslip (pseudocolored green) and 5μm above (pseudocolored red) to simultaneously visualize the cell body at 5-μm above substrate and cell protrusions at the substrate. (D–F) Rose diagrams representing cell protrusion angles. Protrusion angles are measured relative to the cell centroid and plotted with the center of the rose diagram representing the cell centroid. An angle of 180° represents the direction of migration, and angles within 150°–210° are defined as normally oriented protrusions. Angles outside 150°–210° are defined as misdirected and are pseudocolored red in the rose diagram. (G) Quantification of the average number of protrusions per cell. Data are mean + standard error of the mean. A single asterisk (*) indicates $p < .05$ and n.s. indicates no statistically significant difference. (H) Quantification of the number of protrusions for each cell within the explant. The distribution of the number of protrusions is plotted as a percentage of protrusions per cell binned at 1, 2, 3, and 4–5 protrusions per cell. (D–H) Number of protrusions analyzed: Control MO = 84, PDGF-A ligand MO = 34, and PDGFr-α MO = 61 from 7 experiments.

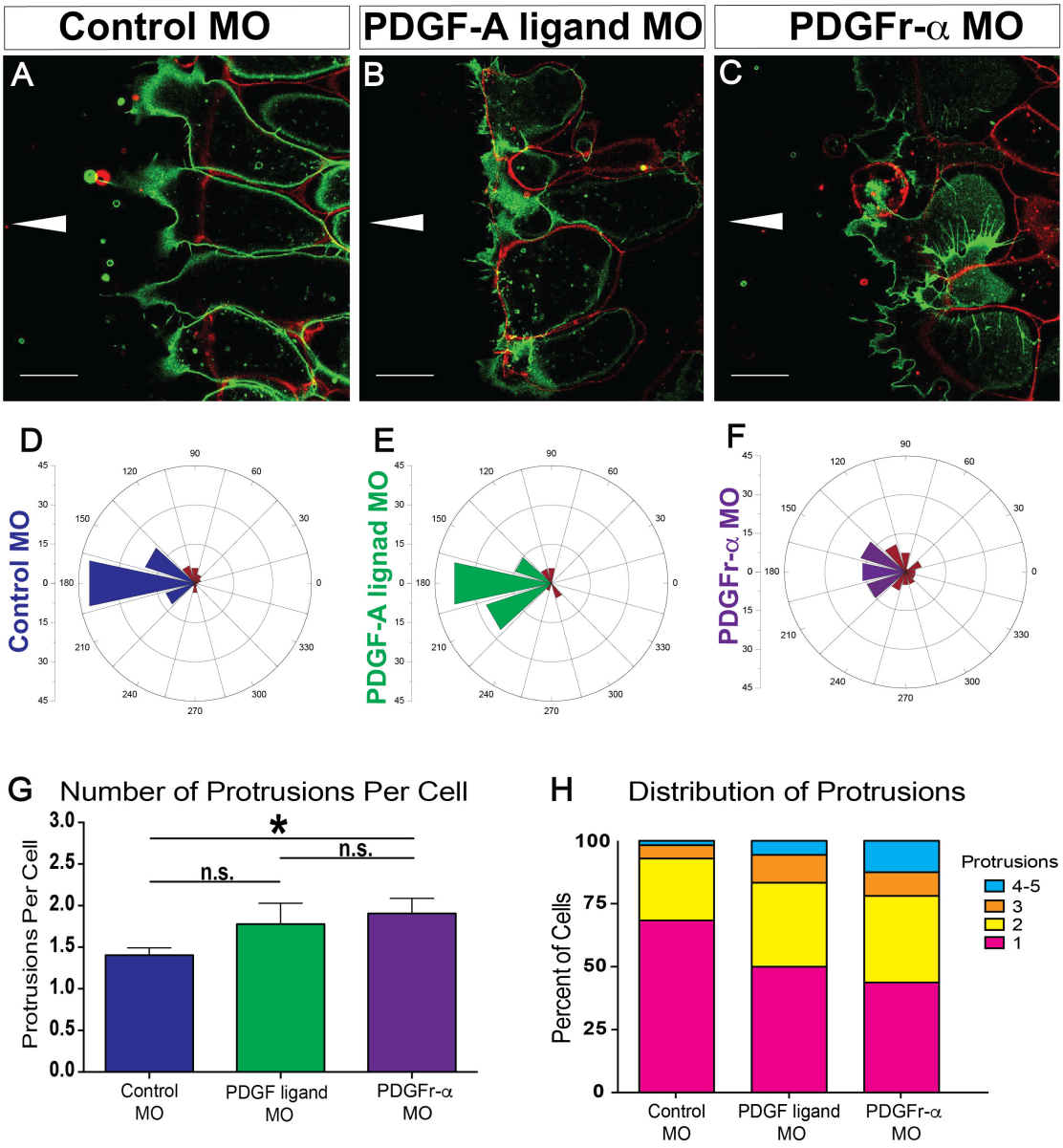
Control MO
PDGF-A ligand MO
PDGFr-α MO
A
B
C
D
E
F
Control MO
PDGF-A lignad MO
PDGFr-α MO
G Number of Protrusions Per Cell
Protrusions Per Cell
3.0
2.5
2.0
1.5
1.0
0.5
0.0
*
n.s.
n.s.
Control MO
PDGF ligand MO
PDGFr-α MO
H Distribution of Protrusions
Percent of Cells
100
75
50
25
0
Protrusions
4-5
3
2
1
Control MO
PDGF ligand MO
PDGFr-α MO

Figure 2.4

Actin organization is altered in PDGFr-α MO explants. (A–C) Representative collapsed 20 μm z-stack confocal images of fixed mesendoderm explants stained with phalloidin to visualize F-actin cytoskeleton. (A–B) Broad actin-rich lamellipodial protrusions at the leading edge of Control MO and PDGF-A ligand MO explants (red arrowheads). Fine F-actin filaments that extend to the edges of the mesendoderm cells (orange arrows). (C) Fragments of membrane containing F-actin found in the front of the PDGFr-α MO mesendoderm explant (blue arrowheads). "Filopodia-like" enrichment of F-actin based protrusions (yellow arrowheads) and collapsed F-actin in PDGFr-α MO explants (green arrows). (A–C) Number of explants: Control MO = 11, PDGF-A ligand MO = 13, and PDGFr-α MO = 11 from 4 experiments. Scale bars are each 20 μm.

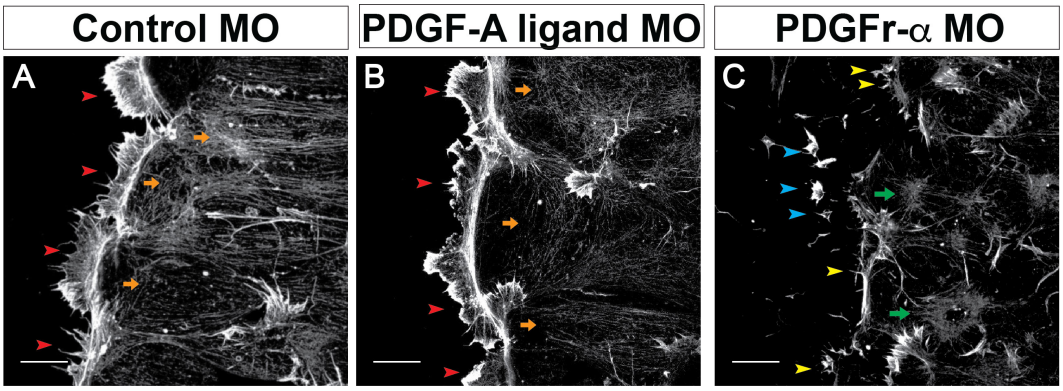
Control MO
PDGF-A ligand MO
PDGFr-α MO
A
B
C

Figure 2.5

Actin disorganization is accompanied by disruptions in the cytokeratin intermediate filament network in PDGFr-α MO explants. (A–C) Representative collapsed z-stack confocal images of fixed mesendoderm explants stained with pan-cytokeratin antibody (C11) to visualize cytokeratin intermediate filament network. Number of explants: Control MO = 24, PDGF-A ligand MO = 12, and PDGFr-α MO = 10 from 7 experiments. (D–L) Representative collapsed z-stack confocal images of mesendoderm explants expressing EGFP-*Xenopus* cytokeratin (EGFP-XCK) and LifeAct-mCherry. EGFP-XCK is pseudocolored green, and LifeAct-mCherry is pseudocolored red. Number of explants: Control MO = 8, PDGF-A ligand MO = 4, and PDGFr-α MO = 9 from 3 experiments. Blue arrowheads indicate cytokeratin filaments that are collapsed in (C, F, I, L). Single-channel images separated of EGFP-XCK (A-I) and LifeAct-mCherry (J–L). Scale bars are each 20 μm.

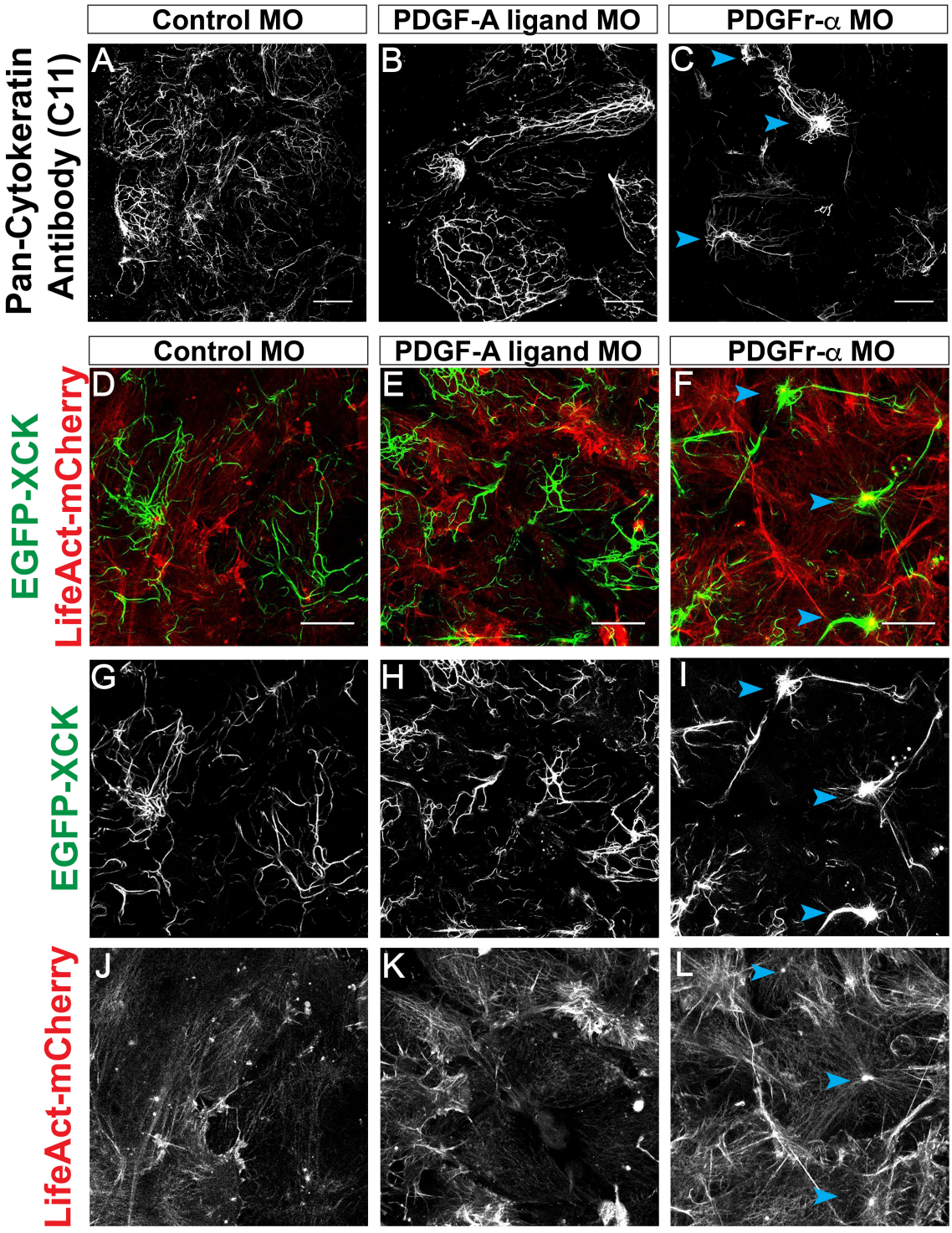
Control MO
PDGF-A ligand MO
PDGFr-α MO
Pan-Cytokeratin Antibody (C11)
A
B
C
Control MO
PDGF-A ligand MO
PDGFr-α MO
EGFP-XCK
LifeAct-mCherry
D
E
F
G
H
I
EGFP-XCK
LifeAct-mCherry
J
K
L

Figure 2.6

Focal adhesion area is increased in PDGFr-α MO explants. Mesendoderm explants expressing LifeAct-mCherry, pseudocolored red, and Paxillin-GFP, pseudocolored green. Live mesendoderm explants were imaged using TIRF microscopy to visualize paxillin-rich focal adhesions on the fibronectin substrate. (A, E, I) White box indicates region enlarged in panels (B–D, F–H, J–L). (A–D) Control MO explants. (E–H) PDGF-A ligand MO explants. (I–L) PDGFr-α MO explants. (M) Quantification of focal adhesion area. Data are mean + standard error of the mean. $p < .001$ for each comparison made. Control MO ($N = 5$, n=14 explants), PDGF-A ligand MO ($N = 3$, n=7 explants), PDGFr-α MO ($N = 5$, n=16 explants). TIRF imaging courtesy of Pooja Sonavane.

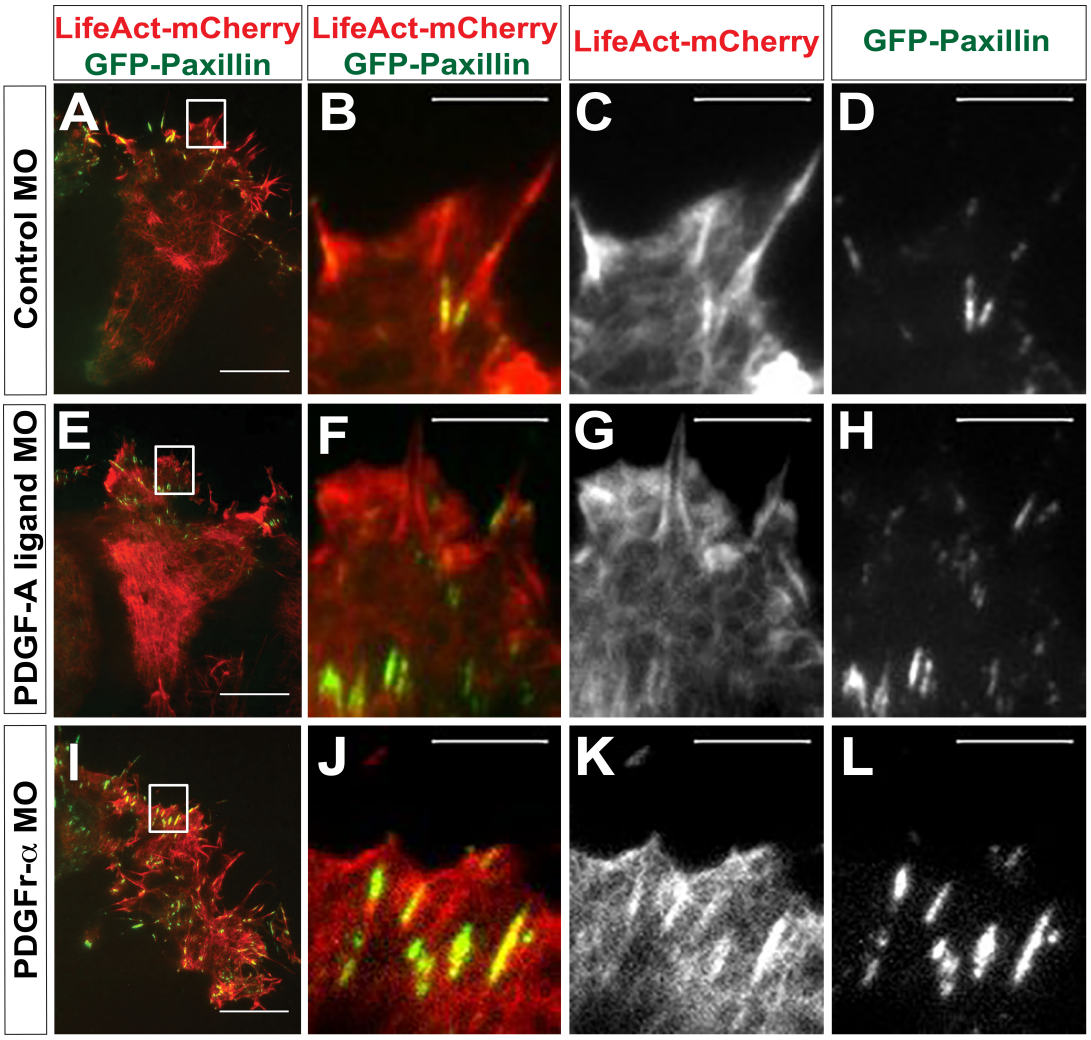
LifeAct-mCherry
GFP-Paxillin
LifeAct-mCherry
GFP-Paxillin
LifeAct-mCherry
GFP-Paxillin
Control MO
PDGF-A ligand MO
PDGFr-α MO
A
B
C
D
E
F
G
H
I
J
K
L

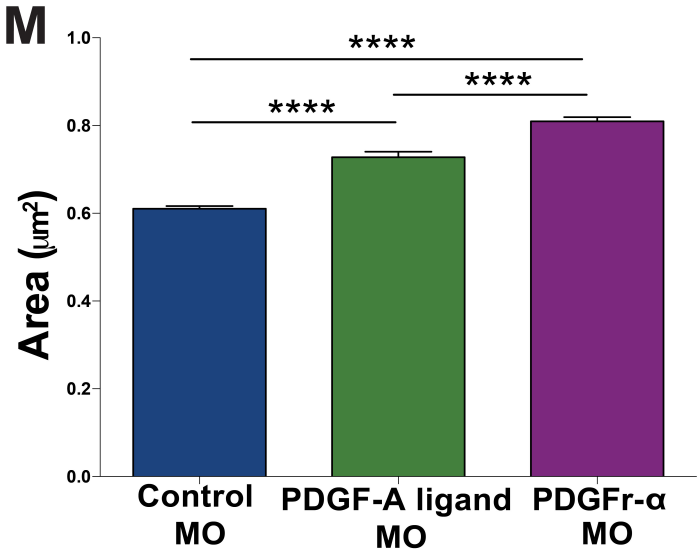
M
Area (μm²)
1.0
0.8
0.6
0.4
0.2
0.0
****
****
****
Control MO
PDGF-A ligand MO
PDGFr-α MO

Chapter 3

Kindlin function in ECM assembly during neurulation in *Xenopus*

3.1 Abstract

Kindlins cooperate with talins to activate integrins to enhance inside-out signaling. Integrin activation by talins and kindlins results in the integrin to undergo a conformational change to a high affinity state, which permits cell adhesion to ECM and fibrillar matrix assembly. Although integrins can assemble matrix, the role of integrin activators in fibrillar matrix assembly remains understudied. My research established a role for integrin activators, specifically kindlin 1, 2, and 3, in the deposition of FN and FB matrix at the notochord–somite boundary during *Xenopus* neurulation. Although all three kindlin family members are expressed during neurulation, kindlin 3 expression is restricted to the notochord–somite boundary. My study found that kindlin 3 is most important for FB assembly and that knockdown of kindlin 3, but not kindlin 1 or 2, resulted in undetectable levels of FB matrix. This kindlin-dependent matrix assembly is specific to FN and FB, and kindlins are not required for every matrix protein enriched at the notochord–somite boundary. I found that FB matrix assembled at the notochord–somite boundary is not dependent on the presence of FN matrix, suggesting that some portion of FB fibrils do not associate with FN. My study enhances understanding of integrin activator kindlin in the deposition of FN and FB matrix during neurulation at the notochord-somite boundary.

3.2 Introduction

Integrin binding to ECM is essential for embryonic development, wound healing, and cancer metastasis (Hynes, 1992). Integrins initiate the assembly of fibrillar networks

of ECM (Wu et al., 1995). When integrin α4β1 was stimulated with Mn^{2+} or β1-activating antibody TS2/16, assembly of the FN matrix occurred in CHO(B2) cells (Sechler, Cumiskey, Gazzola, & Schwarzbaue, 2000). Thus, integrin activation and clustering induced the assembly of a fibrillar FN matrix. Integrin binding to FN at specific sites is also necessary for matrix assembly. Integrin α5β1 binding to the RGD and "synergy site" sequences promote FN assembly (Dzamba et al., 1994; Sechler et al., 1997). Conversely, integrin α4β1 assembly of FN is not dependent on RGD or "synergy site" binding, but rather is dependent on α4β1 binding to the alternatively spliced V-region of FN (Sechler et al., 2000). Because matrix assembly is dependent on integrin activation, it regulation is likely to be subject to inside-out activation mediated by talin (Calderwood et al., 1999) and kindlin (Ma et al., 2008).

Kindlins are scaffolding proteins that enhance binding of talins to integrin β tails for integrin activation (Goult et al., 2009; Kammerer, Aretz, & Fässler, 2017; Li et al., 2017). Integrin activation occurs upon talin binding, which induces integrins to undergo a conformational change to break the salt bridge and transform from an inactive "low-affinity" state to an active "high-affinity" state with increased affinity for ECM (Hynes, 2002). Kindlins bridge talin-activated integrins to promote clustering (Li et al., 2017). Kindlin-2 recruits migfilin and filamin during focal adhesion maturation (Tu, Wu, Shi, Chen, & Wu, 2003), and kindlins interact with actin and paxillin linking integrin adhesions to the cytoskeleton (Bledzka et al., 2016; Theodosiou et al., 2016). Because of the ability to cooperate with talin during integrin activation and link focal adhesion complexes to the cytoskeleton, kindlins have important roles in cell adhesion and spreading.

Kindlins and talins are four-point-one-protein, ezrin, radixin, moesin (FERM) domain containing proteins (Chishti et al., 1998). The kindlin family of proteins consists of three members in vertebrates including kindlin 1, kindlin 2, and kindlin 3. Kindlin 1 is expressed in epithelial tissues, and mutations in kindlin 1 cause Kindler syndrome, a rare congenital skin-blistering disease (Siegel et al., 2003). Kindlin 2 is ubiquitously expressed (Khan, Shimokawa, Strömblad, & Zhang, 2011), and loss of kindlin 2 results in peri-implantation lethality in mice (Montanez et al., 2008). Kindlin 3 is expressed in the hematopoietic system, and mutations to kindlin 3 result in leukocyte-adhesion deficiency type III (LADIII). All three kindlin family members are found in *Xenopus,* with kindlin 1 expression starting at neurulation in nonneural ectoderm, kindlin 2 expression starting broadly at stage 8 and later found around the notochord during neurulation, and kindlin 3 expressed in the neural ectoderm and at the notochord boundaries (Rozario, Mead, & DeSimone, 2014).

FN is assembled on the surface of the BCR where it has important roles in mesendoderm migration (Winklbauer & Keller, 1996), convergence and extension (Davidson et al., 2006), and radial intercalation (Marsden & DeSimone, 2001). A dense network of fibrillar FN is localized at the notochord–somite boundary at the surface of the neural tube, and small puncta of FN are found within the somitic mesoderm during neurulation (Davidson, Keller, & DeSimone, 2004). FB matrix is assembled at the notochord–somite boundary (Skoglund, Dzamba, Coffman, Harris, & Keller, 2006) where it is colocalized with FN and required for convergence and extension (Skoglund & Keller, 2007). Although kindlins have essential roles in integrin activation and adhesion, whether kindlins are important for FN or FB matrix assembly has not yet been

investigated. Furthermore, it remains unclear if kindlin 1, 2, and 3 functions are necessary for talin-induced activation of integrins in fibrillar FN matrix assembly. Chapter 3 provides evidence that kindlins have a role in the deposition of FN and FB matrix during neurulation.

3.3 Materials and Methods

3.3.1 Fertilization of Xenopus Eggs

Xenopus eggs were collected from female frogs and fertilized *ex vivo.* Embryos were allowed to develop to gastrula, and neurula stage embryos were staged according to Nieuwkoop and Faber (1994). Eggs were dejellied in 2% cysteine, rinsed with dH_2O, and cultured in 0.1X MBS (MBS: 1X MBS: 88 mM NaCl, 1 mM KCl, 2.5 mM $NaHCO_3$, 0.35 mM $CaCl_2$, 0.5 mM $MgSO_4$, 5 mM HEPES pH 7.8).

3.3.2 Morpholino Knockdown of Kindlin 1, Kindlin 2, or Kindlin 3

To assess the role of kindlins in matrix deposition, antisense morpholino oligonucleotides were used to knockdown *Xenopus laevis* kindlin 1, kindlin 2, and kindlin 3 (sequences below). All morpholinos were purchased from GeneTools (Philomath, OR). All experiments were done with 20 ng to 40 ng morpholino injected into each embryo (1 blastomere or whole embryo). Efficacy of each morpholino was reported (Rozario et al., 2014), and the morpholinos can knockdown kindlin. Each morpholino sequence is as follows:

- Control Morpholino: 5′- CCTCTTACCTCAGTTACAATTTATA-3′ (stock sequence)
- K1MO: 5′-GCCTACTGCCGCTGTATGGGTCATT-3′
- K2MO-1: 5′-TTCCTTTCCTTGCCCTCCCCTCTTC-3′
- K2MO-2: 5′-CACGAGTAAAGGCGCAAGAAGCCCT-3′
- K2MO-3: 5′-GCATCCGTATACCATCCAAAGCCAT-3′
- K3MO: 5′-GATGTCTTGATTCCAGCCATCCTTA-3′

3.3.3 Immunofluorescence

For visualization of FN and FB matrix, whole embryos were fixed at Stage 14 or Stage 17 using 3.7% formaldehyde in TBS for 1 hour at room temperature, blocked in 1% BSA in TBS-T, and stained with anti-FN antibody (4H2, 3:1000, 1ug/mL), anti-FB antibody (JB3, 1:2000), or anti-LN antibody. After three washes with TBS-T, goat anti-mouse IgG conjugated to AlexaFluor555 was used to visualize FN and goat anti-rabbit IgG conjugated to AlexaFluor647 was used to visualize FB. Bisected embryos were dehydrated into methanol (25%, 50%, 100%) and treated with 2 BB:BA and mounted onto slides. Animal caps were dissected at Stage 11 and then fixed using 3.7% formaldehyde in TBS-T for 1 hour at room temperature and stained with anti-FN antibody (4H2, 3:1000, 1ug/mL). After three washes with TBS-T, goat anti-mouse IgG conjugated to AlexaFluor555 was used to visualize FN. Immunofluorescence imaging was performed on a Nikon C1 confocal microscope with a Nikon with a Nikon

PlanApo/10×/1.40 objective.

3.4 Results

3.4.1 FN and FB Matrix Reduced Following Kindlin Knockdown

To test the function of kindlins in matrix assembly, an antisense morpholino approach was taken to knockdown each kindlin family member; then FN and FB were visualized using antibodies. Each kindlin family member was knocked down using morpholinos: K1MO, K2MO, and K3MO, and morpholinos were co-injected with dextran in one of two blastomeres at 2-cell stage. Injection of one blastomere was done leaving one blastomere uninjected to serve as an internal control. In each instance, defects in matrix deposition were noted only on the side of the embryo that had kindlin morpholino with dextran injection. This is because the morpholino is unable to diffuse past the blastomere where it was injected. Injection of control morpholino (COMO) with dextran had similar FN and FB matrix deposition compared with the uninjected half of the embryo or completely uninjected whole embryos (Fig. 3.1). In controls, FN and FB matrices were assembled at the notochord somite boundary and FN extended around the surface of the neural tube (Fig. 3.1). Thus, morpholino injection did not cause significant defects in the localization of FB and FN.

Kindlin 1 expression is first detected during neurulation in *Xenopus* embryos (Rozario et al., 2014). FN and FB matrix deposition is reduced at the notochord–somite boundary in K1MO-treated embryos at Stage 14 during neurulation (Fig. 3.2). Kindlin 2 is more ubiquitously expressed compared with kindlin 1(Rozario et al., 2014), but morpholino knockdown of kindlin 2 resulted in similar phenotype to kindlin 1

knockdown where FN and FB matrix deposition was reduced but not absent (Fig. 3.2 and Fig. 3.3 A–D). FN and FB matrix was reduced in K2MO-treated embryos at Stage 14 during neurulation at the notochord–somite boundary (Fig. 3.3 A–D). However, there was no reduction in matrix noted in the uninjected blastomere at the notochord–somite boundary (Fig. 3.3 A–D). Furthermore, no reduction in FN was noted at Stage 11 on the BCR (Fig. 3.3 E–G). Although each kindlin family member was expressed at neurulation, kindlin 3 had highest expression at the notochord–somite boundary (Rozario et al., 2014). FN was reduced in K3MO-injected embryos at the notochord–somite boundary and around the surface of the neural tube (Fig.3. 4 A–B, D). FB matrix was reduced to the point where antibody detection was minimal for FB at the notochord–somite boundary in K3MO-treated embryos (Fig. 3.4 A, C–D). In each kindlin MO injected embryo, FN remained detectable even in instances where FB was not detectable (Fig. 3.2–4). Reductions in FN and FB matrix deposition colocalized with dextran in kindlin morpholino-injected blastomeres at neurulation (Fig. 3.2–4). These data indicated a role for kindlin in the deposition of FN and FB matrix during neurulation.

3.4.2 FB Deposition Is Not Dependent on the Presence of the FN Matrix

FN and FB are co-localized around the notochord–somite boundary and enriched for during neurulation (Davidson et al., 2004; Skoglund et al., 2006). A reduction in FN and FB was noted after knockdown of kindlin 1, kindlin 2, or kindlin 3 at the notochord–somite boundary during neurulation at stage 14. In fibroblasts, FB deposition is dependent on FN matrix assembly (Sabatier et al., 2009). To test whether the reduction in FN matrix deposition caused decreased levels of FB, FN and FB were stained for

following morpholino knockdown. There was no reduction in the deposition of FB matrix after FN morpholino knockdown (Fig. 3.5). However, FB was disorganized after FN knockdown, suggesting that FB uses FN as a scaffold (Fig. 3.5). These data suggest that FN is not required for the deposition of FB matrix at neurulation.

3.4.3 Laminin Matrix Assembled Following Kindlin Knockdown

Similar to FN and FB deposition, LN is also expressed during neurulation around the notochord and somites (Fey & Hausen, 1990). Because both FN and FB deposition were reduced after kindlin morpholino knockdown, I next investigated whether knockdown of kindlin affected the deposition of LN matrix. LN remained assembled at the notochord–somite boundary after kindlin 3 morpholino knockdown, despite a significant reduction in the deposition of FN matrix (Fig. 3.6). This suggests that kindlin is required for FN and FB matrix deposition but not LN deposition. It is likely that kindlins activation of LN is not required because LN can assemble independent of integrins (Tsiper & Yurchenco, 2002). This further supports a role for kindlin mediated activation of integrins in the assembly of the FN and FB matrix.

3.4.4 Deposition in FN and FB Matrix Similar to Controls During Later Stages of Neurulation

FN and FB continue to be assembled around the notochord throughout neurulation. To test whether kindlin had a role in the deposition of matrix at later stages of neurulation, FB and FN were stained at Stage 19 following kindlin knock down. FN

and FB deposition was not detectably reduced at Stage 19 of neurulation (Fig. 3.7). This finding suggests that the defects in FB and FN matrix deposition after kindlin knockdown were time-specific and recovered at later stages of neurulation.

3.5 Discussion

These findings demonstrate that kindlins have a role in FN and FB matrix deposition during Stage 14 of *Xenopus* neurulation. There was a reduction in FN and FB after the knockdown of all three kindlin family members, but the most severe reduction in FB deposition occurred after kindlin 3 morpholino knockdown. This finding is likely because kindlin 3 is most highly expressed at the notochord–somite boundary where FN and FB are most assembled (Davidson et al., 2004; Rozario et al., 2014; Skoglund et al., 2006). Although kindlin 2 has been reported to be required for FN matrix deposition in podocytes (Qu et al., 2011), my study reports the first finding of a role for kindlin family members in FB matrix assembly.

3.5.1 Kindlins in Integrin Dependent Matrix Assembly

Previous studies reported that FB matrix assembly is dependent on FN assembly (Sabatier et al., 2009). My study reports that loss of FN did not significantly decrease the amount of FB matrix deposition but did cause disorganization in FB matrix assembly. This suggests that FB deposition is organized at least in part by FN, but that the accumulation of FB is not entirely dependent on the presence FN. FB was not detectable after kindlin 3 knockdown, even though FN remained detectable. This finding suggests that assembly of FB cannot occur without kindlin 3 and that it is not dependent on FN

deposition. These findings also suggest that kindlin dependent matrix assembly is important for FN and FB but not LN, because kindlin knockdown did not detectably reduce the amount of LN matrix deposited at the notochord–somite boundary. LN can assemble into the basement membrane independent of integrin (Tsiper & Yurchenco, 2002). In conclusion, these findings suggest that kindlin-mediated activation of integrins modulates the assembly of FN and FB matrix.

Kindlin 3 could potentially mediate the activation of integrin α5β1 in the assembly of FN and FB matrix around the notochord and somites during Stage 14 of neurulation. Integrin α5β1 is enriched for around the notochord during neurulation in *Xenopus* (Gawantka, Joos, & Hausen, 1994) and has been demonstrated to function in the assembly of FN matrix (Wu et al., 1993). A decrease in the deposition of FN matrix at neurulation occurred after morpholino knockdown of α5 (Kragtorp & Miller, 2007) similar to the decrease in FN matrix deposition when kindlin family members were knocked down. This finding further supports a role for kindlin in regulating α5β1 activation for matrix assembly. Because of the differences in kindlin mediated matrix assembly, one possibility is that spatial restriction of kindlins during neurulation contributes to activation of specific integrins in separate tissues. Although prediction can be made about which integrins are activated by which kindlins based on the integrins expressed during *Xenopus* neurulation, more studies are needed to determine which kindlin-activated integrins modulate the deposition of FN and FB during *Xenopus* neurulation.

Figure 3.1

Uninjected embryos and Control MO embryos have similar FN and FB matrix. (A-H) Representative collapsed z-stack confocal images of fixed and transverse bisected *Xenopus* embryos at Stage 14 of neurulation. Scale bars are 100μm. (A, C, E, and G) Uninjected embryos. (B, D, F, and H) Control MO-injected embryos. (A-B) 488 channel to visualize autofluorescence from yolk and dextran (Dex) injection. (B) Asterisk shows the half of the embryo injected with Control MO and Dex. (C-D) Embryos stained with anti-FN antibody (4H2) to visualize FN matrix deposition around the notochord and somites. (E-F) Embryos stained with anti-FB antibody to visualize FB matrix deposition at the notochord-somite boundary. (G) Merged image of (A, C, and E) with 488 in green, FN in red and FB in blue. (H) Merged image of (B, D, and F) with Dex in green, FN in red, and FB in blue.

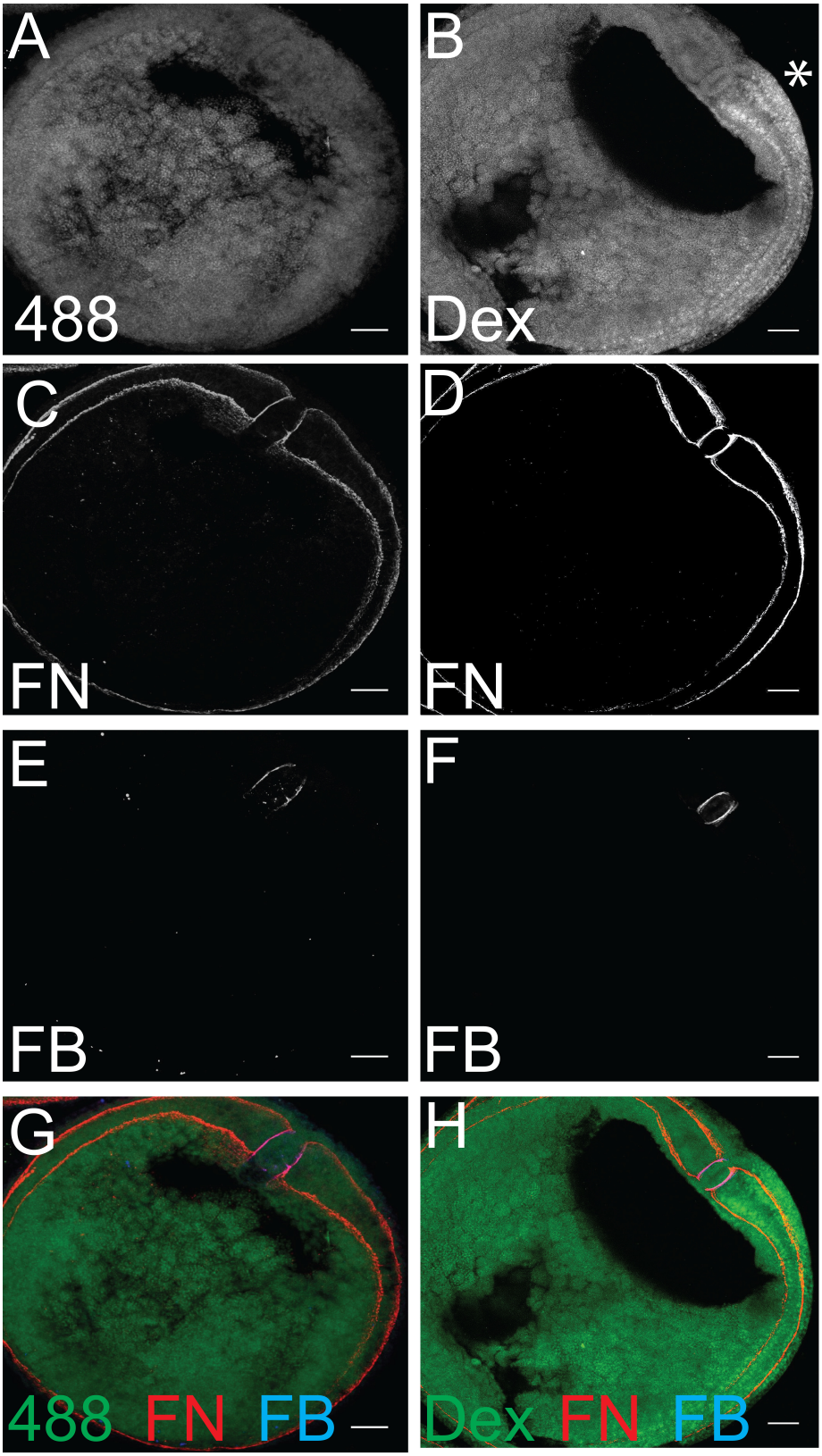
A
488
B
Dex
*
C
FN
D
FN
E
FB
F
FB
G
488 FN FB
H
Dex FN FB

Figure 3.2

Decrease in FN and FB matrix deposition following K1MO knockdown. (A-D) Representative collapsed z-stack confocal images of fixed and transverse bisected *Xenopus* embryos at Stage 14 of neurulation injected with K1MO. Scale bars are 100µm. (A) 488 channel to visualize yolk autofluorescence and dextran (Dex) injection. Asterisk shows the half of the embryo injected with K1MO and Dex. (B) Embryos stained with anti-FN antibody (4H2) to visualize FN matrix deposition around the notochord and somites. Disruption in the organization and deposition of FN in the half the embryo injected with K1MO and Dex. (C) Embryos stained with anti-FB antibody to visualize FB matrix deposition at the notochord-somite boundary. Reduced FB deposition in the half of the embryo injected with K1MO and Dex. (D) Merge of images (A-C) with Dex in green, FN in red, and FB in blue.

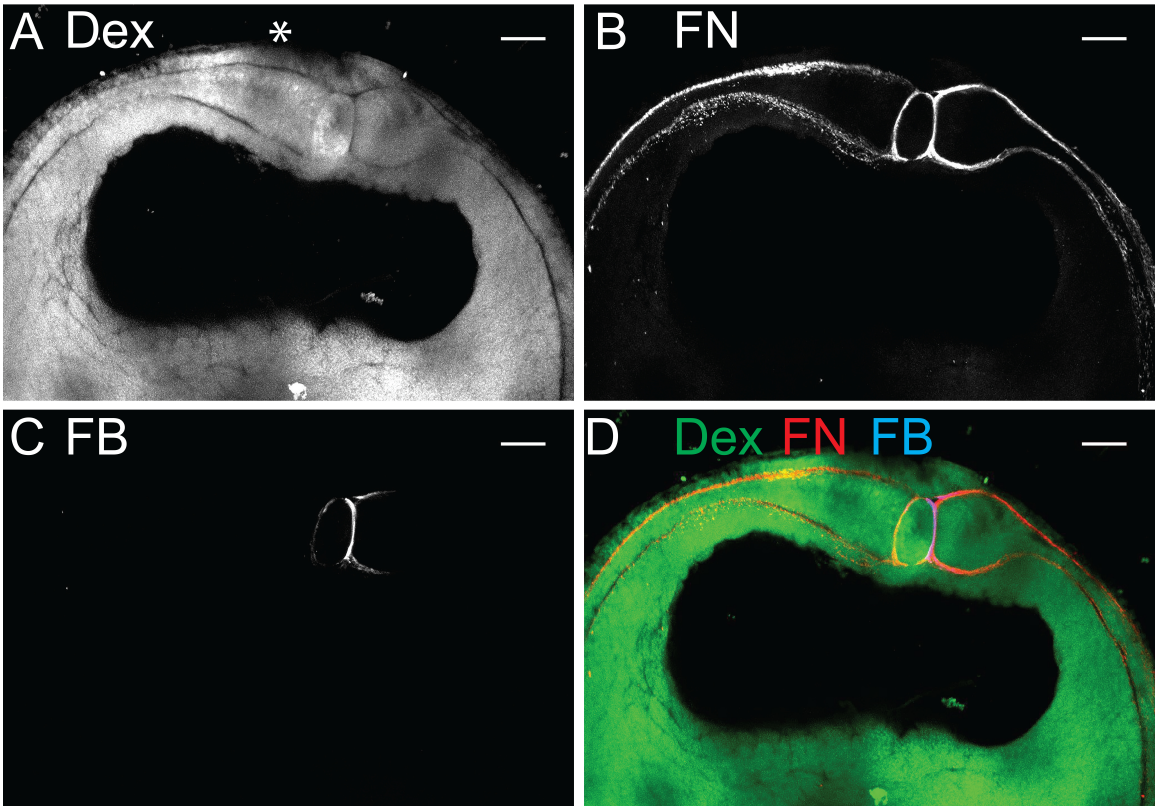
A Dex
*
B FN
C FB
D Dex FN FB

Figure 3.3

FN and FB matrix deposition reduced at neurulation but not at gastrulation following K2MO knockdown. (A-D) Representative collapsed z-stack confocal images of fixed and transverse bisected *Xenopus* embryos at Stage 14 of neurulation injected with K2MO. Scale bars are 100μm. (E-G) Representative collapsed z-stack confocal images of fixed animal caps of embryos at Stage 11 of gastrulation injected with K2MO. Scale bars are 20μm. (A and E) 488 channel to visualize yolk autofluorescence and dextran (Dex) injection. (A) Asterisk shows the half of the embryo injected with K2MO and Dex (B) Embryos stained with anti-FN antibody (4H2) to visualize FN matrix deposition around the notochord and somites. Disruption in the organization and deposition of FN in the half the embryo injected with K2MO and Dex. (C) Embryos stained with anti-FB antibody to visualize FB matrix deposition at the notochord-somite boundary. Reduced FB deposition in the half of the embryo injected with K2MO and Dex. (D) Merge of images (A-C) with Dex in green, FN in red, and FB in blue. (F) Animal caps stained with anti-FN antibody (4H2) to visualize FN matrix deposition on the BCR. No reduction in FN matrix deposition seen in K2MO and Dex injected portion of the animal cap. (G) Merge of images (E-F) with Dex in green and FN in red.

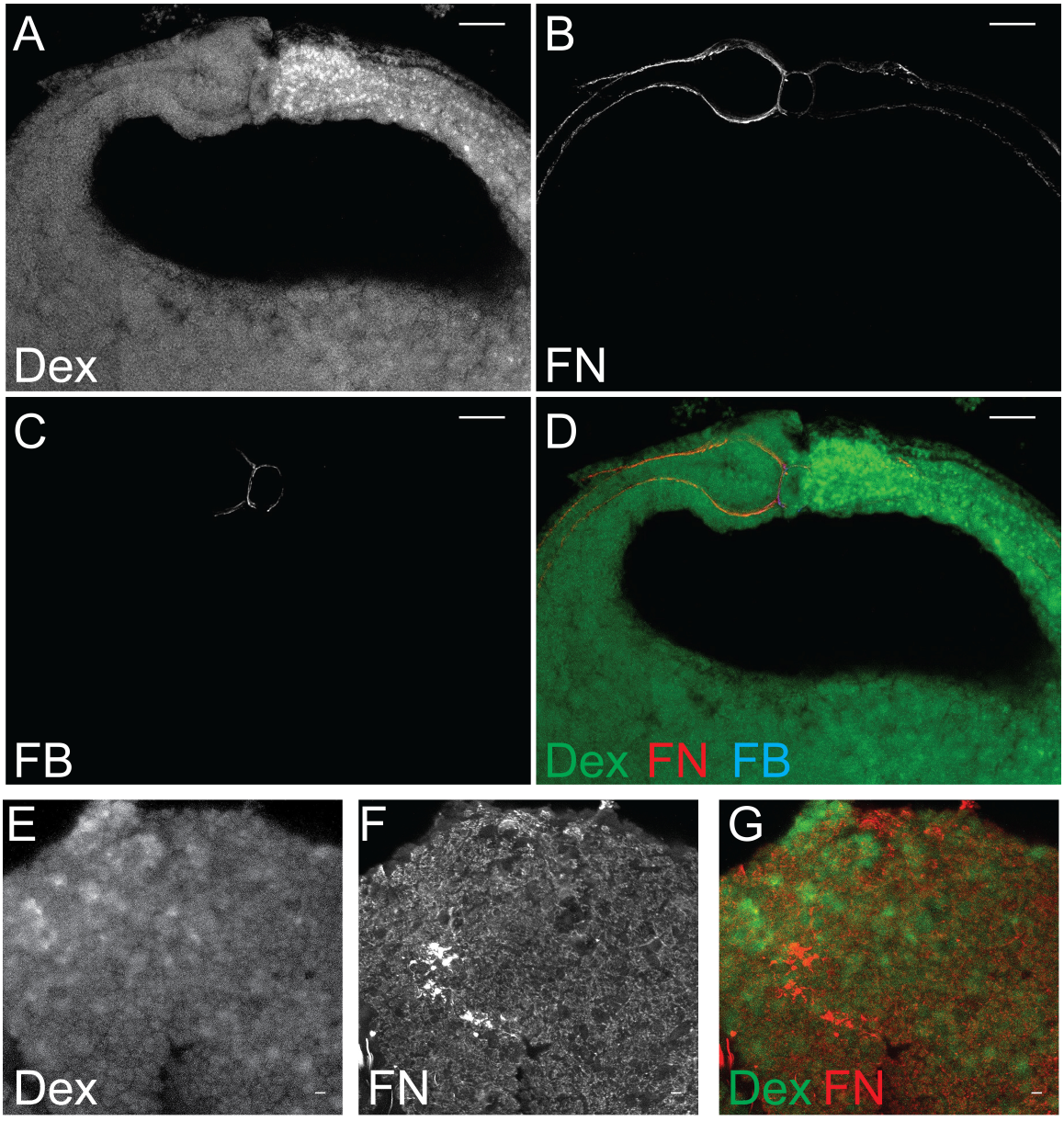
A
Dex
B
FN
C
FB
D
Dex FN FB
E
Dex
F
FN
G
Dex FN

Figure 3.4

FN matrix deposition reduced and FB matrix deposition undetectable at neurulation following K3MO knockdown. (A-D) Representative collapsed z-stack confocal images of fixed and transverse bisected *Xenopus* embryos at Stage 14 of neurulation injected with K3MO. Scale bars are 100μm. (E-G) Representative collapsed z-stack confocal images of fixed animal caps of embryos at Stage 11 of gastrulation injected with K3MO. Scale bars are 20μm. (A and E) 488 channel to visualize yolk autofluorescence and dextran (Dex) injection. (A) Asterisk shows the half of the embryo injected with K3MO and Dex (B) Embryos stained with anti-FN antibody (4H2) to visualize FN matrix deposition around the notochord and somites. Disruption in the organization and deposition of FN in the half the embryo injected with K3MO and Dex. (C) Embryos stained with anti-FB antibody to visualize FB matrix deposition at the notochord-somite boundary. FB deposition is undetectable in the half of the embryo injected with K3MO and Dex. (D) Merge of images (A-C) with Dex in green, FN in red, and FB in blue. (F) Animal caps stained with anti-FN antibody (4H2) to visualize FN matrix deposition on the BCR. No reduction in FN matrix deposition seen in K3MO and Dex injected portion of the animal cap. (G) Merge of images (E-F) with Dex in green and FN in red.

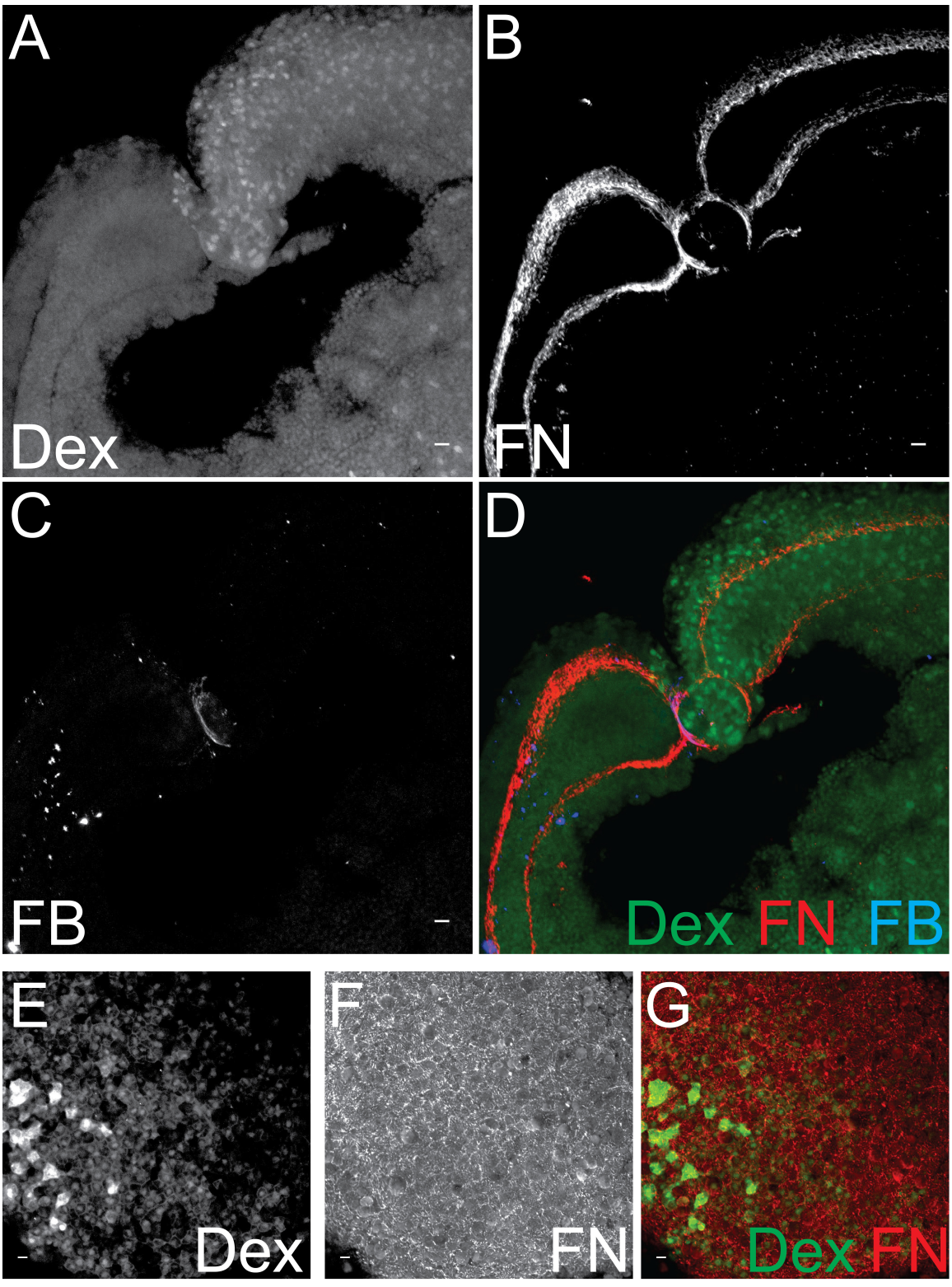
A
Dex
B
FN
C
FB
D
Dex FN FB
E
Dex
F
FN
G
Dex FN

Figure 3.5

FB matrix disorganized following FN knockdown. (A-D) Representative collapsed z-stack confocal images of fixed and transverse bisected *Xenopus* embryos at Stage 14 of neurulation injected with FN MO in the whole embryo. (A) 488 channel to visualize yolk autofluorescence and dextran (Dex) injection. Asterisk shows the half of the embryo injected with FN MO and Dex (B) Embryos stained with anti-FN antibody (4H2) to visualize FN matrix deposition decreased around the notochord and somites. (C) Embryos stained with anti-FB antibody to visualize FB matrix deposition at the notochord-somite boundary. FB deposition is disorganized in the whole embryo following FN MO and Dex injection. (D) Merge of images (A-C) with Dex in green, FN in red, and FB in blue.

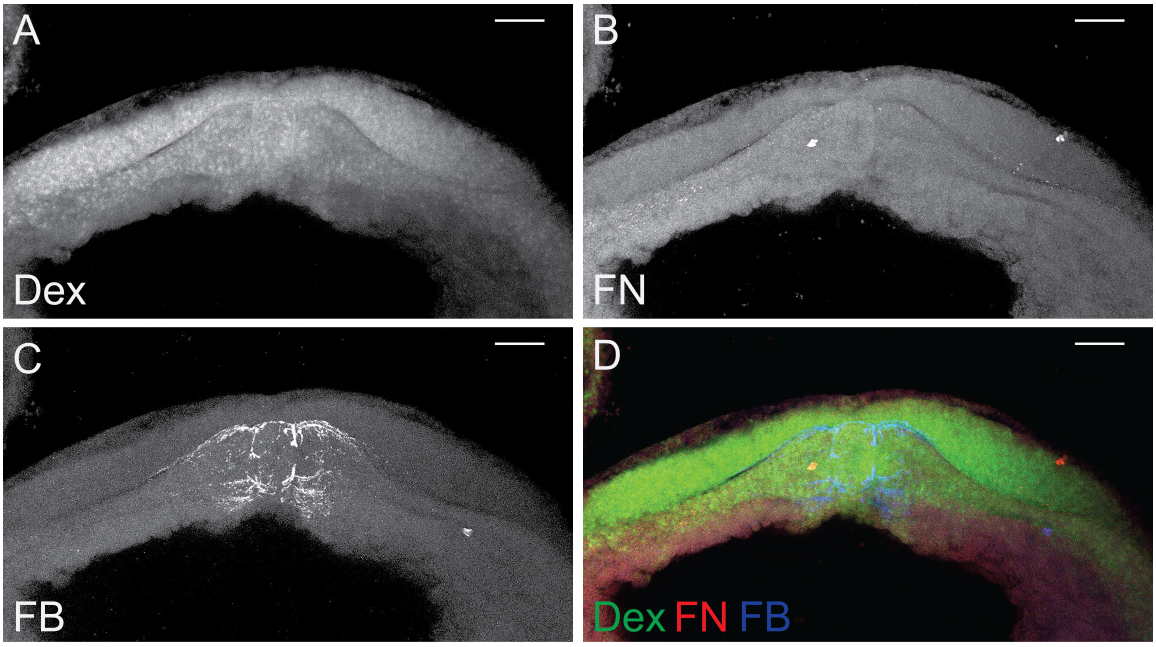
A
Dex
B
FN
C
FB
D
Dex FN FB

Figure 3.6

LN matrix assembled following kindlin knockdown. (A-D) Representative collapsed z-stack confocal images of fixed and transverse bisected *Xenopus* embryos at Stage 14 of neurulation injected with K3MO. Scale bars are 100μm. (A) 488 channel to visualize yolk autofluorescence and dextran (Dex) injection. Asterisk shows the half of the embryo injected with K3MO and Dex (B) Embryos stained with anti-FN antibody (4H2) to visualize FN matrix deposition around the notochord and somites. Disruption in the organization and deposition of FN in the half the embryo injected with K3MO and Dex. (C) Embryos stained with anti-LN antibody to visualize LN matrix deposition at the notochord-somite boundary and around the somites. LN is assembled in the half of the embryo injected with K3MO and Dex. (D) Merge of images (A-C) with Dex in green, FN in red, and FB in blue.

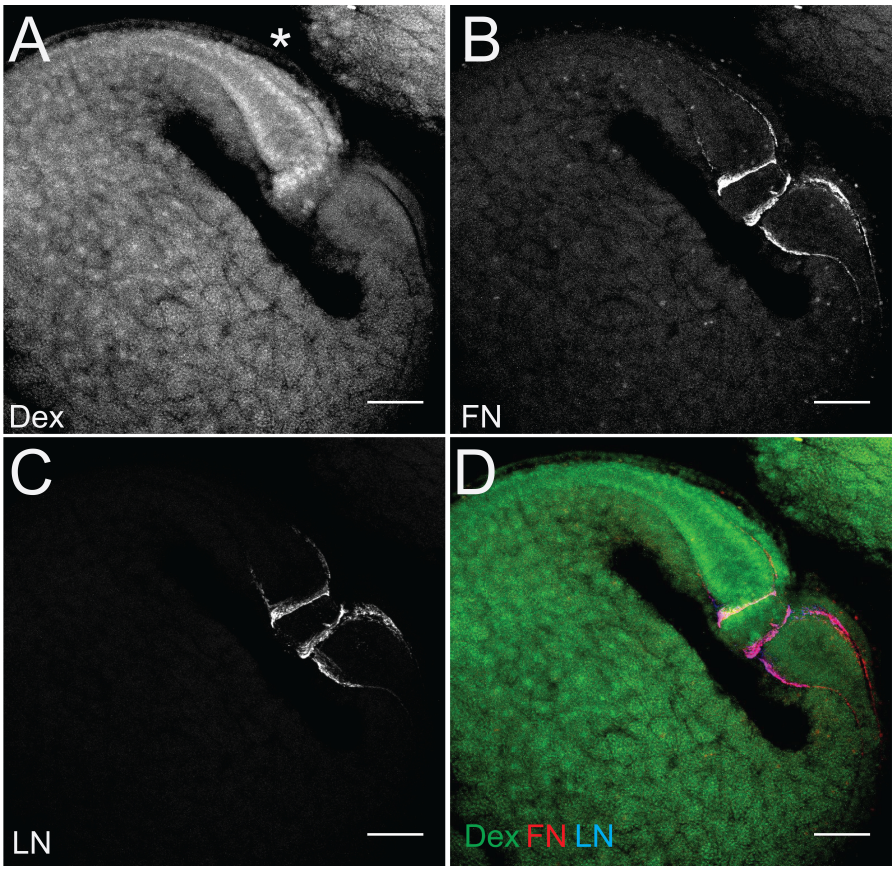
A
*
Dex
B
FN
C
LN
D
Dex FN LN

Figure 3.7

FN and FB matrix deposition defect caused by kindlin knockdown recovered by Stage 17 of neurulation. (A-D) Representative 20X collapsed z-stack confocal images of fixed and transverse bisected *Xenopus* embryos at Stage 17 of neurulation injected with K3MO. Scale bars are 20μm. (E-H) Representative collapsed z-stack 10X confocal images of fixed and transverse bisected *Xenopus* embryos at Stage 17 of neurulation injected with K3MO. Scale bars are 100μm. (A and E) 488 channel to visualize yolk autofluorescence and dextran (Dex) injection. Asterisk shows the half of the embryo injected with K3MO and Dex (B and F) Embryos stained with anti-FN antibody (4H2) to visualize FN matrix deposition around the notochord and somites. FN is assembled in the half of the embryo injected with K3MO and Dex. (C and G) Embryos stained with anti-FB antibody to visualize FB matrix deposition at the notochord-somite boundary and around the somites. FB is assembled in the half of the embryo injected with K3MO and Dex. (D) Merge of images (A-C) with Dex in green, FN in red, and FB in blue. (H) Merge of images (E-G) with Dex in green, FN in red, and FB in blue.

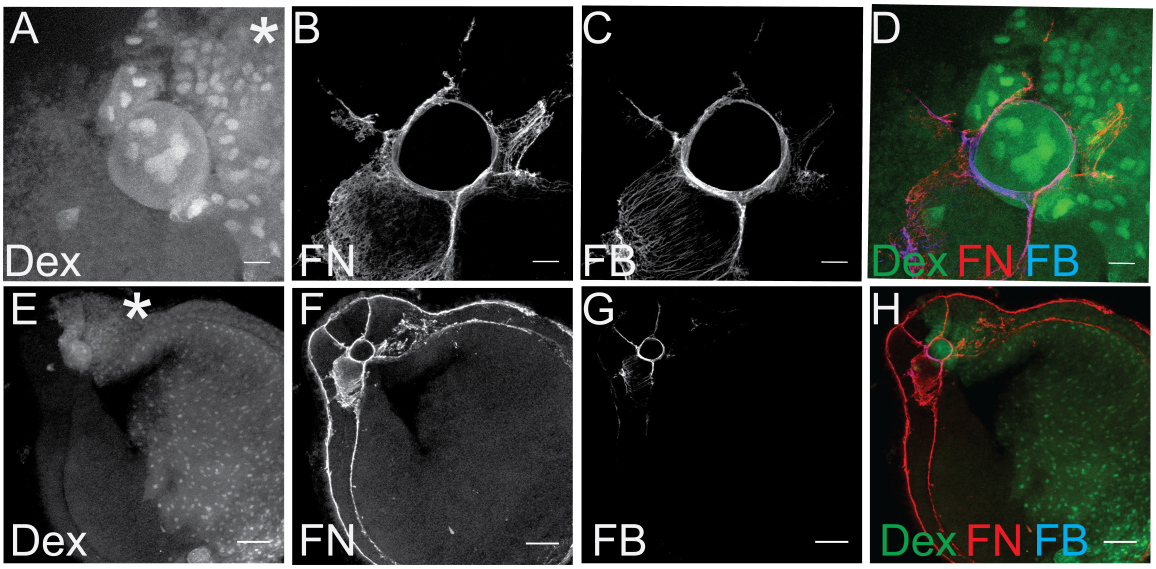
A
*
Dex
B
FN
C
FB
D
Dex FN FB
E
*
Dex
F
FN
G
FB
H
Dex FN FB

Chapter 4

Perspectives

4.1 Summary of Dissertation and Findings

My dissertation focuses on understanding the dramatic movements that take place during morphogenesis. Cells travel long distances at high speeds during embryonic development. These movements are necessary for the development of tissues and organs. Coordinating cell movement while maintaining cell adhesion is essential for both embryonic development and disease progression. The research project in this dissertation identified PDGFr-α as a key signaling molecule necessary for directional mesendoderm migration in a PDGF-A ligand independent manner. I found that PDGFr-α dependent Pi3k-Akt signaling promotes directional lamellipodial protrusions, actin organization, and integrin-mediated cell adhesion to FN.

Disrupting the fibrillar state of the FN matrix has severe consequences on the movements that occur during morphogenesis (Rozario, T. et al., 2009). Integrin activation regulates the assembly of fibrillar matrix, but how the fibrillar matrix is assembled during morphogenesis has yet to be elucidated. I established a role for the integrin activator kindlin in the assembly of the FN and FB matrix during neurulation. Together, these findings help researchers better understand how directional migration is coordinated and how the matrix is assembled during morphogenesis.

4.2 Evaluating PDGF-A Ligand and PDGFr-α in Directional Mesendoderm Migration

Previous studies have identified PDGF-A ligand as a chemoattractant necessary for directional mesendoderm migration (Nagel et al., 2004). These data suggest that

PDGF-A is embedded in the fibrillar FN matrix in a gradient with the highest concentration of the PDGF-A at the animal pole. This is why migrating mesendoderm moves directionally toward the animal pole on BCR-conditioned substrates. Although PDGF-A RNA is localized within the BCR as detected by *in situ* (Ataliotis et al., 1995) and disrupting the PDGF-A results in aberrant movements by mesendoderm slugs (Nagel et al., 2004; slug experiments recapitulated in Fig. A.1), a gradient of PDGF-A has not been established. These previous studies reported that PDGF-A must be embedded in the FN matrix to confer directional cues and that disruption of the non-ECM bound mRNA splice variant of the PDGF-A ligand had no effect on slug displacement toward the animal pole on BCR conditioned substrates (Nagel et al., 2004; Smith at al., 2009). I have demonstrated that slugs can respond to non-ECM bound PDGF-A causing enhanced cell spreading on FN and that larger mesendoderm explants (DMZs) can migrate directionally on *Bovine* plasma FN that does not have a gradient of PDGF-A ligand embedded in the matrix. Furthermore, mesendoderm explants migrate directionally on FN fusion proteins that do not have the PDGF-A ligand-binding site. These findings led me to question the importance of matrix-bound PDGF-A ligand in directional mesendoderm migration.

The geometry of the tissue can dictate mesendoderm protrusive and migratory behaviors (Davidson et al., 2002). DMZs contain both migrating mesendoderm and mesoderm tissue undergoing CE (Davidson et al., 2002). Mesendoderm slugs spread in all directions on FN, but when attached to follower mesoderm, the mesendoderm spreads and extends directional protrusions away from the mesoderm (Winklbauer, 1990). Tugging forces on C-cadherin junctions also regulate directional lamellipodial protrusive behavior of mesendoderm (Weber et al., 2012). Disrupting cadherin junctions results in

aberrant protrusions and randomized migratory behaviors on FN substrates (Weber et al., 2012) and on BCR-conditioned substrates (Winklbauer, 1996). Thus, the inherent tissue polarity and asymmetric tissue tension is required for conferring the directionality of mesendoderm lamellipodial protrusions both with PDGF-A ligand and even in the absence of a PDGF-A ligand chemoattractant. Furthermore, because only groups of mesendoderm cells can respond to BCR-embedded cues on conditioned substrates, the major mechanism for migration does not rely solely on a gradient of PDGF-A ligand. This finding begs the question of whether PDGF signaling is important for directional migration. Although PDGF-A ligand can be removed and mesendoderm can still migrate directionally, this does not necessarily mean that PDGF signaling does not occur through the PDGFr-α in a ligand independent manner. In fact, it is well established that the PDGFr can function independently of the PDGF ligand in a mechanism that is dependent on FN adhesions (Veevers-Lowe et al., 2011). But is this occurring during *Xenopus* mesendoderm migration? My dissertation provides evidence for ligand-independent PDGFr-α signaling in directional mesendoderm migration.

4.3 PDGFr-α in Cooperation With Integrin-FN Adhesive Signaling

The crosstalk between integrins and growth factor receptors has been well described in the literature (Ross, 2004). Integrin α5β1 adhesion to FN promotes the phosphorylation and activation of the PDGFr, and stimulation of PDGF signaling can cause the conformation change and activation of integrins (Veevers-Lowe et al., 2011). Together, the activation of the PDGFr and integrins enhance downstream signals that lead to the phosphorylation of Akt. PDGFr, and integrin signals promote cell adhesion,

spreading, and migration. Previous studies that identified the crosstalk between PDGFr and integrins have been done only in tissue culture. Thus, the biological significance of this crosstalk has yet to be fully evaluated. My dissertation provides the first evidence for growth factor crosstalk with integrins during morphogenesis. These studies demonstrate that PDGFr-α is important for integrin α5β1 mediated cell adhesion to FN and that disrupting the PDGFr-α causes mesendoderm cells to round up and detach from FN substrates (Fig. 2.1 B). Until these studies, whether the PDGFr-α could function independent of the PDGF-A ligand in mesendoderm migration remained unclear. This dissertation reports that the PDGFr-α functions independent of PDGF-A ligand and that knocking down the PDGFr-α in the absence of the PDGF-A ligand caused a reduction in the levels of p-Akt (Fig. 2.1 E). Morpholino knockdown of the PDGFr-α results in severe defects, including aberrant protrusion formation, altered focal adhesion size, and a collapse in the actin and cytokeratin intermediate filament network, further supporting the ligand independent functions of the PDGFr-α. However, just because the PDGFr-α can function independently of the PDGF-A ligand does not necessarily mean that the PDGF-A ligand is not important for migration. In the next section, I describe how PDGF-A ligand-dependent and ligand -independent signals can be integrated to produce efficient mesendoderm migration in the embryo.

4.4 Integration of PDGF-A Ligand and PDGFr-α in Conferring Directional Mesendoderm Migration

In the embryo, mesendoderm migrates directionally along the fibrillar FN matrix of the BCR toward the animal pole. Mesendoderm slugs polarize toward the animal pole

on BCR condition substrates, and slugs cannot repolarize when PDGF-A ligand is disrupted (Nagel et al., 2004; Smith et al., 2009; Fig. A.1). Although DMZ explants can migrate directionally on nonfibrillar FN without PDGF-A ligand (Davidson et al., 2002), DMZ explants have decreased migration distance on BCR-conditioned substrates when PDGF-A ligand is disrupted (Fig. A.2) This finding suggests that the PDGF-A ligand could enhance directional migration of mesendoderm *in vivo*. Further supporting this finding in each experiment performed in Chapter 2, it was reported that PDGF-A ligand knockdown caused an intermediate effect that was often not significantly different from controls but also not significantly different from PDGFr-α MO. The least distance traveled occurred when the PDGF-A ligand on BCR conditioned substrates was disrupted combined with disrupting the PDGFr-α in mesendoderm (Fig. A.2). However, disrupting the PDGFr-α alone was more severe then disrupting the PDGF-A ligand alone, suggesting that ligand independent functions of the PDGFr-α can partially compensate for the lack of PDGF-A ligand in the BCR (Fig. A. 2). Taken together, this supports a model that ligand-independent functions of the PDGFr-α act in conjunction with PDGF-A ligand-dependent signaling to promote directional mesendoderm migration on the fibrillar FN matrix of the BCR.

4.5 PDGFr found in the BCR

The initial in situ evidence supported a spatial restriction of PDGF-A ligand RNA in the BCR and PDGFr-α RNA in the mesoderm and mesendoderm tissues (Ataliotis et al., 1995). However, these studies do not address the localization of PDGF-A ligand and PDGFr-α protein in the gastrulating *Xenopus* embryo. Unfortunately, I was unable to find

an antibody that recognized PDGF-A ligand in *Xenopus*, so it remains unclear where the PDGF-A ligand protein is localized in the embryo. However, we did discover PDGFr-α protein in the BCR (Fig. A.3). PDGFr-α is localized to the cell edges where it outlines the ectoderm cells in the BCR (Fig. A.3 A). Further confirming the protein localization in the BCR, PDGFr-α was detected by Western blot in explanted BCR (Fig. A.3 A). This new finding adds another layer of complexity to the notion of a PDGF-A ligand is expressed only in the BCR to act as a FN-attached chemoattractant for directional mesendoderm migration. Perhaps there is active PDGFr-α dependent signaling within the BCR because both the ligand and the receptor are localized there. Previous reports indicate that PDGF signals are important for radial intercalation of mesendoderm cells (Damm, E. and Winklbauer, R., 2011), perhaps a PDGF signaling enhances intercalation behaviors in the BCR. It remains unclear how these cues are spatially restricted and what exactly the role is in directional mesendoderm migration. There is evidence that PDGFr-α can interact with cadherins to maintain cadherin adhesions (Yang et al., 2008) and perhaps PDGFr-α-PDGF-A ligand signaling in the ectoderm maintains the C-Cadherin cell-cell junctions in the BCR. This evidence would explain why there is a large enrichment for PDGFr-α specifically at the ectodermal cell-cell junctions. In the next section, I will evaluate active PDGFr-α in the BCR, mesendoderm, and mesoderm tissues.

4.6 Specific Patterns of Active PDGFr-α in Varying Tissues

There evidence for a spatial restriction of active PDGFr-α specific to each tissue. In the mesendoderm, active PDGFr-α is enriched for at the leading edge of the cells (Fig. A.4 A). Also at the leading edge, integrins form focal adhesion complexes that exert

higher traction stresses (Sonavane et al., 2017). Integrins and PDGFr can co-localize to form signaling plaques (Veevers-Lowe et al., 2011). The best way to determine the distribution of active integrins is using integrin-activating antibodies (Byron et al., 2009). However, integrin antibodies do not crossreact with *Xenopus,* and I was not able to evaluate specifically where active integrins are in the mesendoderm tissue. Based on previous reports and studies from our lab (Sonavane et al., 2017), I predict that integrins are activated at sites of focal contacts that exert highest tractions and that these active integrins can cause the phosphorylation and activation of PDGFr-α. This is consistent with the active PDGFr-α enrichment at the leading edge of the mesendoderm tissue. Active PDGFr-α is also enriched at the boundary between the ectoderm and mesoderm tissues (Fig. A.4 B). This finding is consistent with PDGF-A ligand from the ectoderm activating PDGFr-α in the mesoderm tissue. Interestingly, the localization of active PDGFr-α changes dramatically from a punctate throughout the mesoderm cells to a become localized and enriched for at the cell boundaries in the ectoderm (Fig. A.4 B). Future studies are needed to determine the exact role of the PDGFr-α in ectodermal tissues.

4.7 Perspectives on Actin and Cytokeratin IF Reorganization Following PDGFr-α Knockdown

4.7.1 Evaluation of Actin Reorganization and Focal Adhesion Size

Mesendoderm cells become rounded and detach from the substrate after PDGFr-α MO knockdown (Fig. 2.1 B). Correspondingly, the actin network collapses toward the

center of the cell and becomes co-localized with cytokeratin IFs (Fig. 2.5). My interpretation is that the reorganization of the actin and cytokeratin intermediate filament (IF) cytoskeleton toward the center of the cell causes the cells to round up. Supporting this mesendoderm cells on poly-L-lysine (PLL) substrates appear rounded, and cytokeratin is localized to the center of the cell (Weber et al., 2012) similar to PDGFr-α MO cells. Thus, altering cell adhesion to the substrate can result in the reorganization of the actin and cytokeratin IFs, causing dramatic changes in the cell shape.

The reorganization of actin at the leading edge may be a direct result of signaling from the PDGFr-α. PDGF signals can enhance the polymerization of actin structures, causing the formation of membrane ruffles, and PDGFr can colocalize with actin structures at focal contacts (Anton, 2003; Campa, Machuy, Klein, & Rudel, 2006; Chen, She, Kim, Woodley, & Li,, 2000; Herman & Pledger, 1985; Moes, Zhou, & Boonstra, 2012). When PDGFr-α is disrupted, actin protrusions at the leading edge become disorganized and change from actin-rich lamellipodial protrusions to filopodial-like protrusions. This change in morphology likely the result of a disruption in PDGFr-α mediated actin polymerization (Nagano, K. et al., 2006). The disruption in focal adhesion structures after disruption in PDGFr-α (Fig. 2.6) may also be a result of aberrant actin polymerization, or perhaps the decrease in p-Fak at Tyr 397 is modulating the size of the focal contacts.

4.7.2 Evaluation of the Reorganization of Cytokeratin IF Network

In addition to the actin network collapsing toward the center of the cell, the

cytokeratin IF network becomes colocalized as it collapses to the center of the cell (Fig. 2.5). This is likely the direct result of cell shape changes and cells rounding up. However, in DMZ explants, the cells do not fully come off the substrate and maintain focal contacts (Fig 2.6). Although no studies directly link PDGF signals to the regulation of the cytokeratin IF cytoskeleton, evidence suggests that PDGF signaling can enhance Rac activation, resulting in a reorganization of the vimentin IF network (Valgeirsdóttir et al., 1998). Rac-GTP enhances lamellipodial protrusion formation in a manner that is antagonistic with vimentin IFs (Helfand et al., 2011). Although it is unclear whether PDGFr-α functions to modulate Rac-GTP for cytokeratin organization, recent studies in our lab suggest an antagonism between cytokeratin IFs and Rac-GTP in mesendoderm (Sonavane et al., 2017). Furthermore, vimentin reorganization can have dramatic effects on the cells' ability to migrate (Helfand et al., 2011) and focal adhesions are essential for IF assembly (Windoffer, Kölsch, Wöll, & Leube, 2006). Perhaps the reorganization in cytokeratin after PDGFr-α knockdown contributes to the misdirected lamellipodial protrusions and focal adhesion formation in migrating mesendoderm.

Another line of evidence supporting a disruption in the cytokeratin IF network is that mesendoderm cells become softer after morpholino knockdown of PDGFr-α (Fig. A.5). I interpret that the increase in cell softness may be a direct result of changes in the IF network. Disruption of Fak also caused a disorganization in the cytokeratin IF network (Bjerke et al., 2014) similar to disrupting the PDGFr-α. Evidence also suggests that vimentin IFs can interact with and modulate the activity of integrins (Kim et al., 2016). Perhaps the disorganization in cytokeratin IFs when the PDGFr-α is disrupted affects integrin mediated cell signals by IFs. Interestingly, these changes did not affect the initial

attachment of cells to either C-cadherin or FN substrates (Fig. A.5). This is likely because PDGFr-α knockdown did not abolish focal adhesions. The mechanism here may include either direct binding of IFs to integrins or indirect signaling by PDGFr-α modulating the phosphorylation of Fak at Tyr 397.

4.8 Assessment of the Decrease FN and FB Matrix following Kindlin Knockdown

My dissertation research identified a role for kindlin 1, kindlin 2, and kindlin 3 in the deposition of the FN and FB matrix during neurulation. The exact mechanism by which kindlin affects FN and FB matrix assembly remains unclear. However, evidence in the literature suggests that the kindlin family members function in cooperation with talin to mediate integrin activation (Ussar, Wang, Linder, Fässler, & Moser, 2006) and that integrin activation promotes matrix assembly (Wu et al., 1995). FN remains detectable after the knockdown of each kindlin family member. Perhaps kindlin function is overlapping for integrin activation that leads to the deposition of the FN matrix because FN matrix a prevalent ECM component. My study also reports that kindlin 3 appears to be most essential for the deposition of the FB matrix around the notochord. This result is consistent with the expression pattern of kindlin 3 and the enrichment of kindlin 3 at the notochord-somite boundary (Rozario et al., 2014). I predict that all the kindlin family members have overlapping functions in the modulation of the assembly of the FN matrix, but kindlin 3 is specifically recruited for the assembly of the FB matrix. Combinatorial knockdowns will need to be performed to assess the overlapping contributions of each kindlin family member. Even if all three kindlin family members were knocked down, I think it is unlikely that FN would be undetectable particularly because kindlin

knockdown did not affect matrix assembly on the cap. Either this is due to maternal deposition of FN or perhaps talin-mediated activation of integrins is sufficient for FN matrix assembly in a manner that is not entirely dependent on kindlin. Evidence suggests that talin can promote at least partial integrin activation in the absence of kindlins (Li et al., 2017). Although the exact integrin activation states are unknown during *Xenopus* neurulation, these studies provide some evidence for kindlin-mediated integrin activation around the somites and notochord for the deposition of the FN and FB matrix.

Appendix

This chapter contains data not included in the manuscript but that is important for the interpretation of data in Chapter 2 and the discussion in Chapter 4

Figure A.1

Mesendoderm slugs on BCR-conditioned substrates require PDGF-A ligand to polarize. (A) Mesendoderm slugs are composed of dorsal mesendoderm tissue that has been dissected from a gastrulating *Xenopus* embryo at Stage 11. The distance that each mesendoderm slug traveled on BCR-conditioned substrate is plotted as an x-y coordinate. Distance on the x-axis and y-axis are both in μm. Each square plotted on the graph represents one slug, and each point indicates the slug's displacement after 1 hour. Animal pole is represented at the top of the graph. Slugs that extend protrusions and polarize toward the animal pole are above the x-axis. Mesendoderm slugs on Control MO BCR-conditioned substrates are in represented by black squares, and mesendoderm slugs on PDGF-A Ligand MO BCR-conditioned substrates are represented by blue squares. Slugs have greater displacement and polarize toward the animal pole on Control MO BCR-conditioned substrates, whereas slugs on PDGF-A Ligand MO BCR-conditioned substrates travel less distance and with a more randomized displacement. (B) Representative image of BCR conditioned substrate stained with anti-FN antibody (4H2) to visualize FN transferred on to tissue culture plastic. FN is pseudocolored red.

A **Control MO** vs. **PDGF-A Ligand MO**
BCR Conditioned Substrates

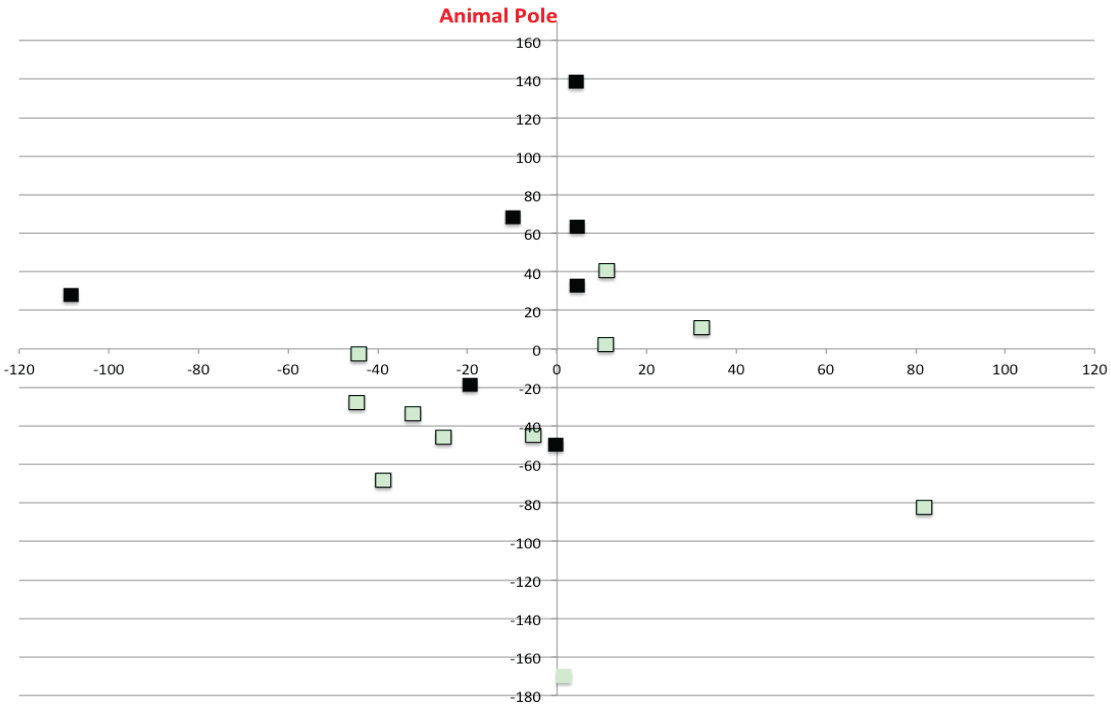

B

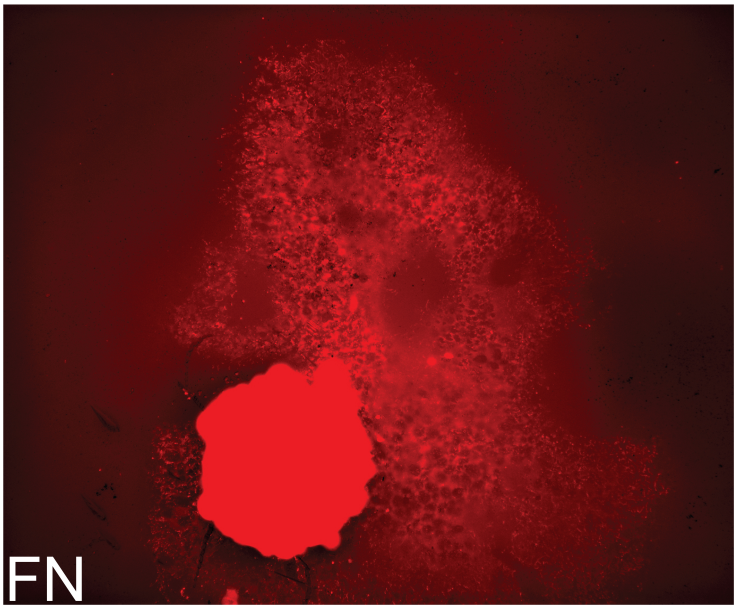

Figure A.2

DMZ explants on *Bovine* plasma FN or on BCR-conditioned substrate (CS). Morpholino knockdowns were performed to both the DMZ and/or to the BCR before conditioning. Each condition is as follows: Untreated DMZ on Control Mo on CS (blue line), Untreated DMZ on *Bovine* plasma FN (green line), Untreated DMZ on PLMO BCR CS (pink line), PDGFr-α Mo DMZ on Control Mo CS (black line), PDGFr-α Mo DMZ on PLMO BCR CS (orange line). Conditioning with the BCR permitted DMZs to travel further distances compared with unconditioned BPFN substrates (blue line compared to green line). Morpholino knockdown of the PDGFr-α caused shortest distance traveled (black line and orange line). The PDGF-A ligand can confer polarity to DMZs. When the PDGF-A was knocked down in the CS the total distance traveled decreased (pink line). The most significant perturbation comes from simultaneously disrupting PDGF-A ligand in CS and knocking down the PDGFr-α in the DMZ (orange line).

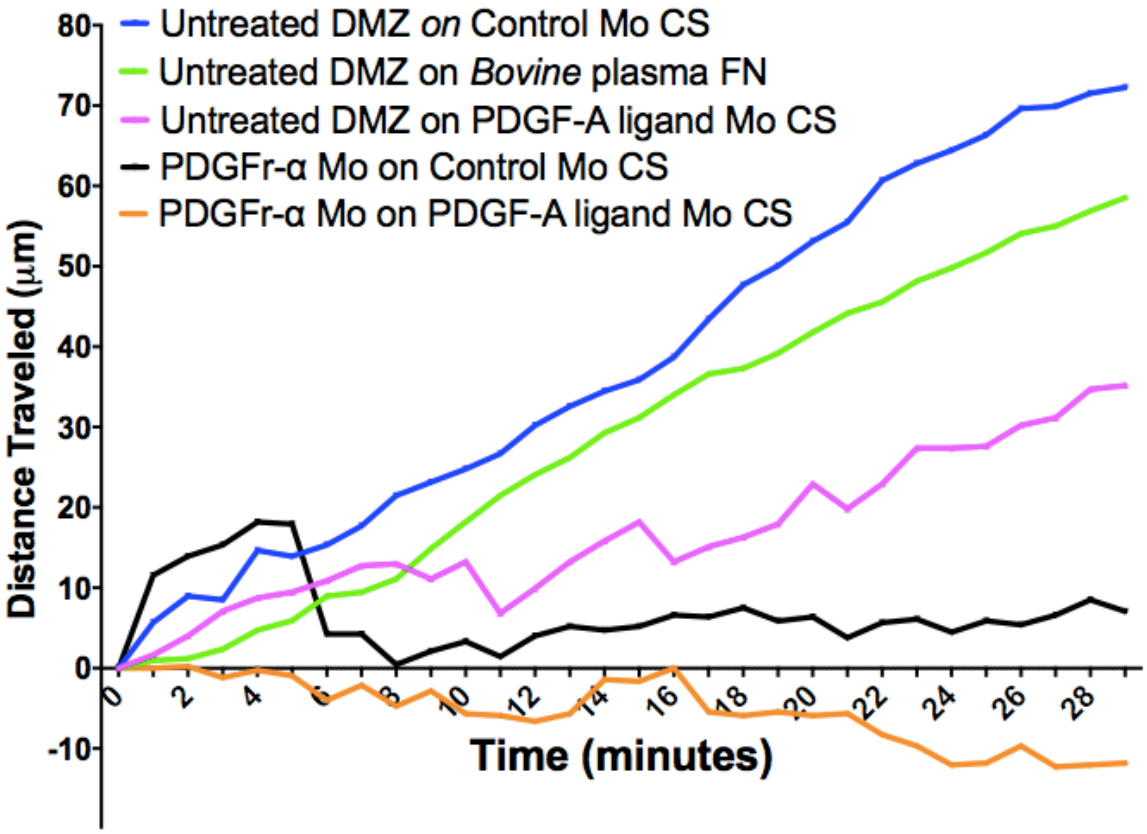
Untreated DMZ *on* Control Mo CS
Untreated DMZ on *Bovine* plasma FN
Untreated DMZ on PDGF-A ligand Mo CS
PDGFr-α Mo on Control Mo CS
PDGFr-α Mo on PDGF-A ligand Mo CS
Distance Traveled (μm)
80
70
60
50
40
30
20
10
0
-10
0
2
4
6
8
10
12
14
16
18
20
22
24
26
28
Time (minutes)

Figure A.3

PDGFr-α found in BCR during gastrulation. (A) Representative collapsed confocal z-stack of BCR explant stained with PDGFr-α antibody. PDGFr-α is found concentrated at cell edges with minimal PDGFr-α inside the cell. Scale bar is 20 μm. (B) Western blot for gastrulating whole embryo and dissected BCR. PDGFr-α was detected in both the whole embryo and the BCR explant. Western blot courtesy of Bette Dzamba.

A

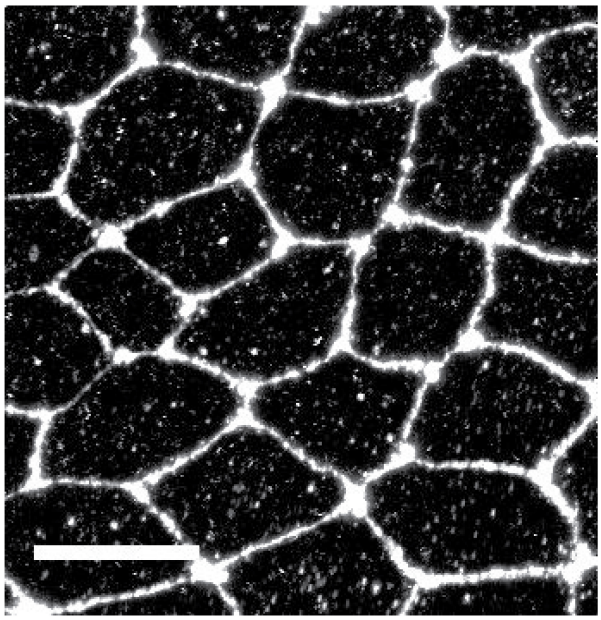

B

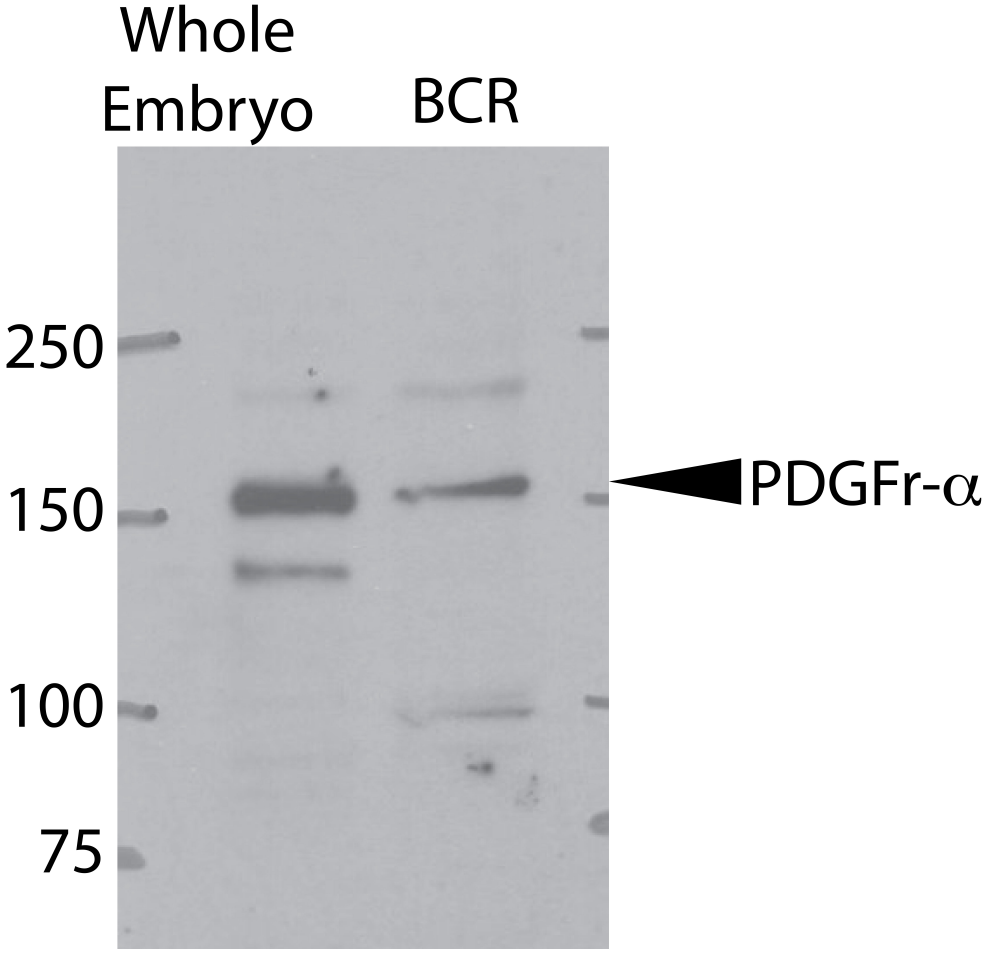

Figure A.4

Active PDGFr-α localized to leading edge of mesendoderm. (A) Representative collapsed confocal z-stack of fixed mesendoderm explant stained with pPDGFr-α to visualize active PDGFr-α. pPDGFr-α is enriched for at the leading edge of the mesendoderm. (B) Representative collapsed confocal z-stack of fixed mesoderm and ectoderm explant stained with pPDGFr-α. Trailing mesoderm tissue does not have localized pPDGFr-α, and ectoderm tissue has pPDGFr-α at cell boundaries.

A

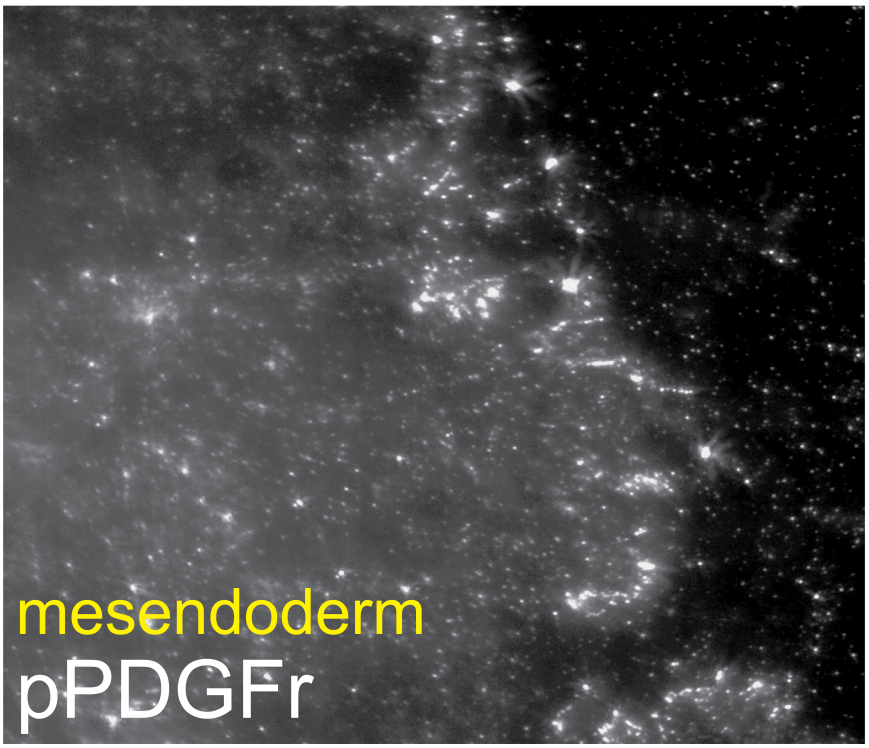

B

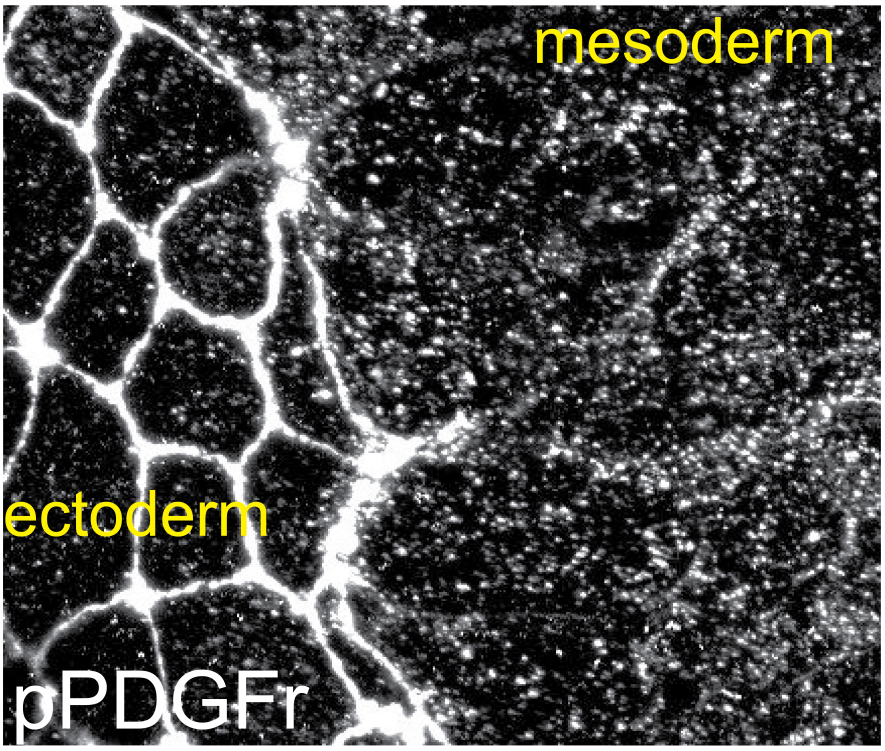

Figure A.5

PDGFr-α MO mesendoderm cells are softer then Control MO cells. (A–B) Adhesive force was measured using AFM. Single mesendoderm cells were attached to a Cell-Tak-coated cantilever for 20 minutes using 5nN of force. Then the cell was attached to substrates (20μg/mL of *Bovine* plasma FN, *Xenopus* C-cadherin, or PLL) by applying 1 nN of force for 5 seconds. Cells were detached from substrates by moving the cantilever off the substrate. The maximum adhesive strength was measured based on the distance the cantilever traveled. (A) Adhesive force of single mesendoderm cell on FN and C-cadherin substrates after PDGFr-α morpholino knockdown. No significant difference in nascent adhesive force was noted between Control MO and PDGFr-α MO mesendoderm cells on either *Bovine* plasma FN or *Xenopus* C-cadherin substrates. (B) Young's modulus was calculated based on the distance the cantilever can deform the mesendoderm cell during attachment to substrate. On all substrates, Young's modulus was significantly lower for PDGFr-α MO cells compared with Control MO, indicating the PDGFr-α MO cells are softer then controls. The Young's modulus on PLL demonstrates that the softness of the cells is not due to attachment of a specific receptor.

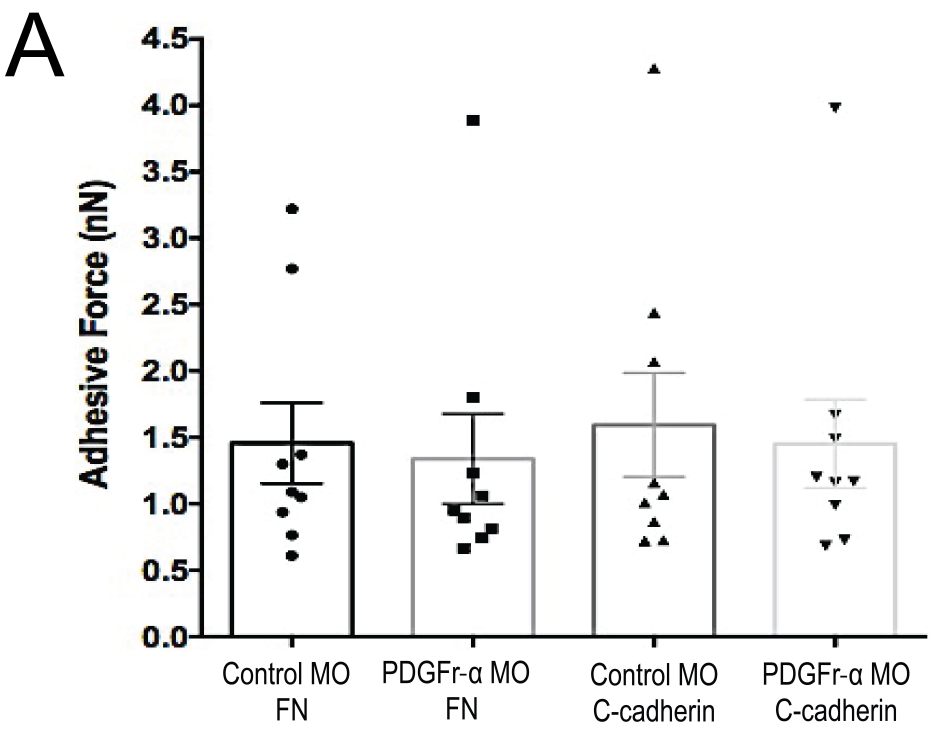
A
Adhesive Force (nN)
4.5
4.0
3.5
3.0
2.5
2.0
1.5
1.0
0.5
0.0
Control MO FN
PDGFr-α MO FN
Control MO C-cadherin
PDGFr-α MO C-cadherin

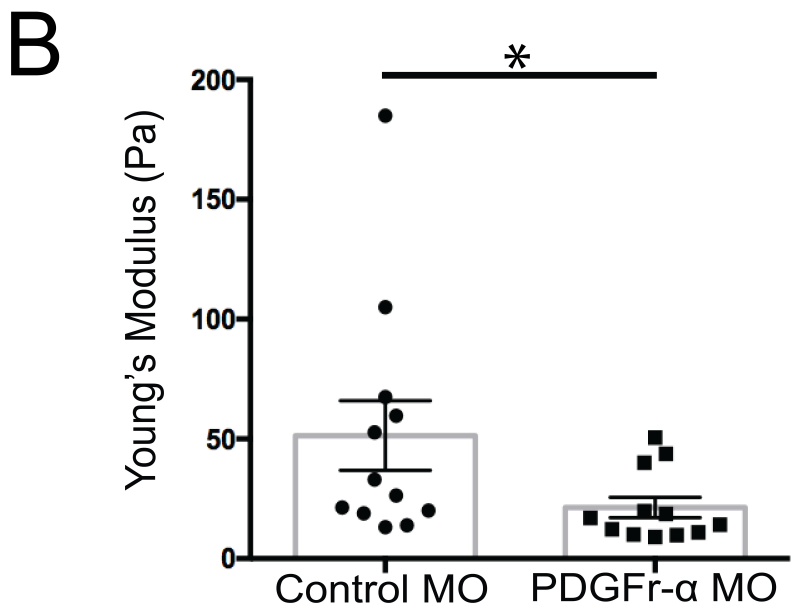
B
Young's Modulus (Pa)
200
150
100
50
0
*
Control MO
PDGFr-α MO

Figure A.6.

PDGFr-α MO is able to knockdown protein levels of *Xenopus* PDGFr-α. (A) PDGFr-α MO sequence are red, and corresponding target *Xenopus* PDGFr-α mRNA and protein sequences are in black. The PDGFr-α MO was obtained from *GeneTools* and wasa designed for translation blocking. (B) Western blot and quantification of PDGFr-α protein levels for Control MO (COMO) and PDGFr-α MO (PDGFRMO) gastrulating embryos. PDGFr-α protein levels decreased approximately 60% after PDGFr-α morpholino knockdown.

PDGFRMO

3′ **C AAC AAT GCC AGG TAC TAC GGA CGG** 5′

GAAAG TTG TTA CGG TCC ATG ATG CCT GCC ATG AGG

L L P S M M P A M R

xPdgfr-alpha

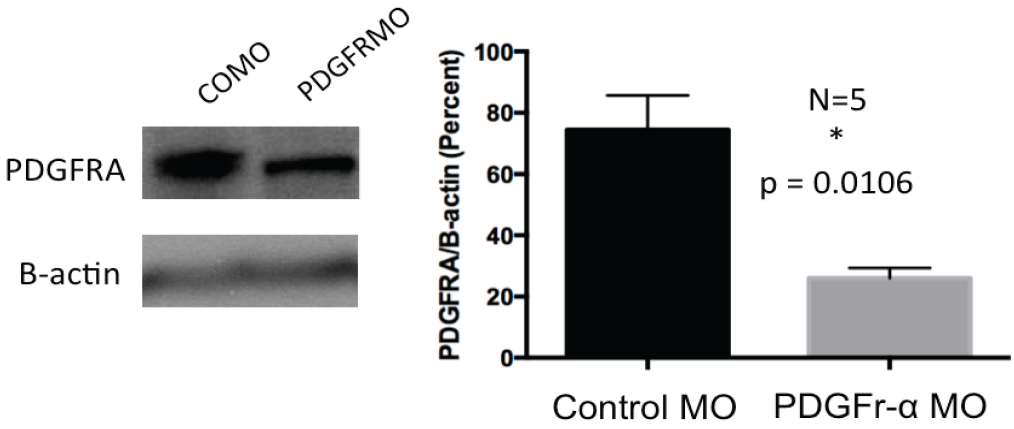

References

Alexander, S., Koehl, G.E., Hirschberg, M., Geissler, E.K., Friedl, P., 2008. Dynamic imaging of cancer growth and invasion: a modified skin-fold chamber model. Histochem. Cell Biol. 130, 1147–1154. doi:10.1007/s00418-008-0529-1

Andrae, J., Gallini, R., Betsholtz, C., 2008. Role of platelet-derived growth factors in physiology and medicine. Genes Dev. 22, 1276–1312. doi:10.1101/gad.1653708

Anon, E. *et al.* Cell crawling mediates collective cell migration to close undamaged epithelial gaps. *Proc. Natl. Acad. Sci. U.S.A.* **109,** 10891–10896 (2012).

Anton, I.M., 2003. WIP participates in actin reorganization and ruffle formation induced by PDGF. J Cell Sci 116, 2443–2451. doi:10.1242/jcs.00433

Arias-Salgado, E. G. *et al.* Src kinase activation by direct interaction with the integrin beta cytoplasmic domain. *PNAS* 100, 13298–13302 (2003).

Assanah, M.C., Bruce, J.N., Suzuki, S.O., Chen, A., Goldman, J.E., Canoll, P., 2009. PDGF stimulates the massive expansion of glial progenitors in the neonatal forebrain. Glia 57, 1835–1847. doi:10.1002/glia.20895

Ataliotis, P., Symes, K., Chou, M.M., Ho, L., Mercola, M., 1995. PDGF signalling is required for gastrulation of Xenopus laevis 121, 3099–3110.

Bandyopadhyay, A., Rothschild, G., Kim, S., Calderwood, D.A., Raghavan, S., 2012. Functional differences between kindlin-1 and kindlin-2 in keratinocytes. J Cell Sci 125, 2172–2184. doi:10.1242/jcs.096214

Bazzoni, G., Ma, L., Blue, M.L., Hemler, M.E., 1998. Divalent cations and ligands induce conformational changes that are highly divergent among beta1 integrins. J. Biol. Chem. 273, 6670–6678. doi:10.1074/jbc.273.12.6670

Bjerke, M.A., Dzamba, B.J., Wang, C., DeSimone, D.W., 2014. FAK is required for tension-dependent organization of collective cell movements in Xenopus mesendoderm. Developmental Biology 394, 340–356. doi:10.1016/j.ydbio.2014.07.023

Bledzka, K., Bialkowska, K., Sossey-Alaoui, K., Vaynberg, J., Pluskota, E., Qin, J., Plow, E.F., 2016. Kindlin-2 directly binds actin and regulates integrin outside-in signaling. J Cell Biol 213, jcb.201501006–108. doi:10.1083/jcb.201501006

Byron, A. *et al.* Anti-integrin monoclonal antibodies. *J Cell Sci* **122,** 4009–4011 (2009).

Cai, D., Chen, S.-C., Prasad, M., He, L., Wang, X., Choesmel-Cadamuro, V., Sawyer, J.K., Danuser, G., Montell, D.J., 2014. Mechanical Feedback through E-Cadherin

Promotes Direction Sensing during Collective Cell Migration. Cell 157, 1146–1159. doi:10.1016/j.cell.2014.03.045

Calderwood, D.A., Zent, R., Grant, R., Rees, D.J.G., Hynes, R.O., Ginsberg, M.H., 1999. The Talin Head Domain Binds to Integrin β Subunit Cytoplasmic Tails and Regulates Integrin Activation. J. Biol. Chem. 274, 28071–28074. doi:10.1074/jbc.274.40.28071

Campa, F., Machuy, N., Klein, A., Rudel, T., 2006. A new interaction between Abi-1 and βPIX involved in PDGF-activated actin cytoskeleton reorganisation. Cell Research 16, 759–770. doi:10.1038/sj.cr.7310091

Carmona-Fontaine, C., Matthews, H.K., Kuriyama, S., Moreno, M., Dunn, G.A., Parsons, M., Stern, C.D., Mayor, R., 2008. Contact inhibition of locomotion in vivo controls neural crest directional migration. Nature 456, 957–961. doi:10.1038/nature07441

Carter, S. B. Haptotaxis and the mechanism of cell motility. *Nature* **213,** 256–260 (1967).

Cattin, A.-L., Burden, J.J., Van Emmenis, L., Mackenzie, F.E., Hoving, J.J.A., Garcia Calavia, N., Guo, Y., McLaughlin, M., Rosenberg, L.H., Quereda, V., Jamecna, D., Napoli, I., Parrinello, S., Enver, T., Ruhrberg, C., Lloyd, A.C., 2015. Macrophage-Induced Blood Vessels Guide Schwann Cell-Mediated Regeneration of Peripheral Nerves. Cell 162, 1127–1139. doi:10.1016/j.cell.2015.07.021

Caussinus, E., Colombelli, J., Affolter, M., 2008. Tip-Cell Migration Controls Stalk-Cell Intercalation during Drosophila Tracheal Tube Elongation. Current Biology 18, 1727–1734. doi:10.1016/j.cub.2008.10.062

Chen, M., She, H., Kim, A., Woodley, D.T., Li, W., 2000. Nckbeta adapter regulates actin polymerization in NIH 3T3 fibroblasts in response to platelet-derived growth factor bb. Mol Cell Biol 20, 7867–7880. doi:10.1016/j.febslet.2010.01.045

Chishti, A.H., Kim, A.C., Marfatia, S.M., Lutchman, M., Hanspal, M., Jindal, H., Liu, S.C., Low, P.S., Rouleau, G.A., Mohandas, N., Chasis, J.A., Conboy, J.G., Gascard, P., Takakuwa, Y., Huang, S.C., Benz, E.J., Bretscher, A., Fehon, R.G., Gusella, A.F., Ramesh, V., Solomon, F., Marchesi, V.T., Tsukita, S., Tsukita, S., Arpin, M., Louvard, D., Tonks, N.K., Anderson, J.M., Fanning, A.S., Bryant, P.J., Woods, D.F., Hoover, K.B., 1998. The FERM domain: a unique module involved in the linkage of cytoplasmic proteins to the membrane. Trends Biochem. Sci. 23, 281–282.

Damm, E.W., Winklbauer, R., 2011. PDGF-A controls mesoderm cell orientation and radial intercalation during Xenopus gastrulation. Development 138, 565–575. doi:10.1242/dev.056903

Datta, A., Huber, F., Boettiger, D., 2002. Phosphorylation of β3 Integrin Controls Ligand Binding Strength. J. Biol. Chem. 277, 3943–3949. doi:10.1074/jbc.M109536200

Davidson, L.A., Hoffstrom, B.G., Keller, R., DeSimone, D.W., 2002. Mesendoderm extension and mantle closure in Xenopus laevis gastrulation: combined roles for integrin alpha(5)beta(1), fibronectin, and tissue geometry. Developmental Biology 242, 109–129. doi:10.1006/dbio.2002.0537

Davidson, L.A., Keller, R., DeSimone, D.W., 2004. Assembly and remodeling of the fibrillar fibronectin extracellular matrix during gastrulation and neurulation in Xenopus laevis. Developmental Dynamics 231, 888–895. doi:10.1002/dvdy.20217

Davidson, L.A., Marsden, M., Keller, R., DeSimone, D.W., 2006. Integrin α5β1 and Fibronectin Regulate Polarized Cell Protrusions Required for Xenopus Convergence and Extension. Current Biology 16, 833–844. doi:10.1016/j.cub.2006.03.038

Deuel, T.F., Senior, R.M., Huang, J.S., Griffin, G.L., 1982. Chemotaxis of monocytes and neutrophils to platelet-derived growth factor. J Clin Invest 69, 1046–1049. doi:10.1172/JCI110509

Duchek, P., Rørth, P., 2001. Guidance of cell migration by EGF receptor signaling during Drosophila oogenesis. Science 291, 131–133. doi:10.1126/science.291.5501.131

Duchek, P., Somogyi, K., Jékely, G., Beccari, S., Rørth, P., 2001. Guidance of cell migration by the Drosophila PDGF/VEGF receptor. Cell 107, 17–26.

Dunn, G. A. & Heath, J. P. A new hypothesis of contact guidance in tissue cells. *Experimental Cell Research* **101,** 1–14 (1976).

Dzamba, B.J., Bultmann, H., Akiyama, S.K., Peters, D.M., 1994. Substrate-specific binding of the amino terminus of fibronectin to an integrin complex in focal adhesions. J. Biol. Chem. 269, 19646–19652.

Ewald, A.J., Brenot, A., Duong, M., Chan, B.S., Werb, Z., 2008. Collective Epithelial Migration and Cell Rearrangements Drive Mammary Branching Morphogenesis. Developmental Cell 14, 570–581. doi:10.1016/j.devcel.2008.03.003

Fey, J., Hausen, P., 1990. Appearance and distribution of laminin during development of Xenopus laevis. Differentiation 42, 144–152.

Franke, T.F., Yang, S.I., Chan, T.O., Datta, K., Kazlauskas, A., Morrison, D.K., Kaplan, D.R., Tsichlis, P.N., 1995. The protein kinase encoded by the Akt proto-oncogene is a target of the PDGF-activated phosphatidylinositol 3-kinase. Cell 81, 727–736.

Friedl, P., 2004. Prespecification and plasticity: shifting mechanisms of cell migration. Current Opinion in Cell Biology 16, 14–23. doi:10.1016/j.ceb.2003.11.001

Friedl, P., Gilmour, D., 2009. Collective cell migration in morphogenesis, regeneration

and cancer. Nat. Rev. Mol. Cell Biol. 10, 445–457. doi:10.1038/nrm2720

Friedl, P., Locker, J., Sahai, E., Segall, J.E., 2012. Classifying collective cancer cell invasion. Nat Cell Biol 14, 777–783. doi:10.1038/ncb2548

Friedl, P., Wolf, K., 2003. Tumour-cell invasion and migration: diversity and escape mechanisms. Nat. Rev. Cancer 3, 362–374. doi:10.1038/nrc1075

Fuchs, E., Dowling, J., Segre, J., Lo, S.H., Yu, Q.-C., 1997. Integrators of epidermal growth and differentiation: distinct functions for β1 and β4 integrins. Curr Opin Genet Dev 7, 672–682. doi:10.1016/S0959-437X(97)80016-0

Gaggioli, C., Hooper, S., Hidalgo-Carcedo, C., Grosse, R., Marshall, J.F., Harrington, K., Sahai, E., 2007. Fibroblast-led collective invasion of carcinoma cells with differing roles for RhoGTPases in leading and following cells. Nat Cell Biol 9, 1392–1400. doi:10.1038/ncb1658

Gailit, J., Ruoslahti, E., 1988. Regulation of the fibronectin receptor affinity by divalent cations. J. Biol. Chem. 263, 12927–12932.

García, A.J., Schwarzbauer, J.E., Boettiger, D., 2002. Distinct Activation States of α5β1 Integrin Show Differential Binding to RGD and Synergy Domains of Fibronectin †. Biochemistry 41, 9063–9069. doi:10.1021/bi025752f

Gawantka, V., Joos, T.O., Hausen, P., 1994. A β1-integrin associated α-chain is differentially expressed during Xenopus embryogenesis. Mechanisms of Development 47, 199–211. doi:10.1016/0925-4773(94)90039-6

Ghabrial, A.S., Krasnow, M.A., 2006. Social interactions among epithelial cells during tracheal branching morphogenesis. Nature 441, 746–749.

Goult, B.T., Bouaouina, M., Harburger, D.S., Bate, N., Patel, B., Anthis, N.J., Campbell, I.D., Calderwood, D.A., Barsukov, I.L., Roberts, G.C., Critchley, D.R., 2009. The Structure of the N-Terminus of Kindlin-1: A Domain Important for αIIbβ3 Integrin Activation. Journal of Molecular Biology 394, 944–956. doi:10.1016/j.jmb.2009.09.061

Grasso, S., Hernandez, J.A., Chifflet, S., 2007. Roles of wound geometry, wound size, and extracellular matrix in the healing response of bovine corneal endothelial cells in culture. Am. J. Physiol., Cell Physiol. 293, C1327–C1337. doi:10.1152/ajpcell.00001.2007

Grotendorst, G.R., Chang, T., Seppä, H.E.J., Kleinman, H.K., Martin, G.R., 1982. Platelet-derived growth factor is a chemoattractant for vascular smooth muscle cells. Journal of Cellular Physiology 113, 261–266. doi:10.1002/jcp.1041130213

Gumbiner, B.M., 2005. Regulation of cadherin-mediated adhesion in morphogenesis. Nat. Rev. Mol. Cell Biol. 6, 622–634. doi:10.1038/nrm1699

Guo, G., Gong, K., Wohlfeld, B., Hatanpaa, K.J., Zhao, D., Habib, A.A., 2015. Ligand-Independent EGFR Signaling. Cancer Res 75, 3436–3441. doi:10.1158/0008-5472.CAN-15-0989

Haas, P., Gilmour, D., 2006. Chemokine Signaling Mediates Self-Organizing Tissue Migration in the Zebrafish Lateral Line. Developmental Cell 10, 673–680. doi:10.1016/j.devcel.2006.02.019

Haeger, A., Wolf, K., Zegers, M.M., Friedl, P., 2015. Collective cell migration: guidance principles and hierarchies. Trends in Cell Biology 25, 556–566. doi:10.1016/j.tcb.2015.06.003

Hegerfeldt, Y., Tusch, M., Bröcker, E.-B., Friedl, P., 2002. Collective Cell Movement in Primary Melanoma Explants. Cancer Res 62, 2125–2130. doi:10.1016/S0092-8674(00)81280-5

Heldin, C.-H., Westermark, B., 1999. Mechanism of Action and In Vivo Role of Platelet-Derived Growth Factor. Physiological Reviews 79, 1283–1316. doi:10.1146/annurev.ph.57.030195.001501

Helfand, B.T., Mendez, M.G., Murthy, S.N.P., Shumaker, D.K., Grin, B., Mahammad, S., Aebi, U., Wedig, T., Wu, Y.I., Hahn, K.M., Inagaki, M., Herrmann, H., Goldman, R.D., 2011. Vimentin organization modulates the formation of lamellipodia. Mol. Biol. Cell 22, 1274–1289. doi:10.1091/mbc.E10-08-0699

Hellström, M., Phng, L.-K., Hofmann, J.J., Wallgard, E., Coultas, L., Lindblom, P., Alva, J., Nilsson, A.-K., Karlsson, L., Gaiano, N., Yoon, K., Rossant, J., Iruela-Arispe, M.L., Kalén, M., Gerhardt, H., Betsholtz, C., 2007. Dll4 signalling through Notch1 regulates formation of tip cells during angiogenesis. Nature 445, 776–780. doi:10.1038/nature05571

Henry, M.D., Satz, J.S., Brakebusch, C., Costell, M., Gustafsson, E., Fässler, R., Campbell, K.P., 2001. Distinct roles for dystroglycan, beta1 integrin and perlecan in cell surface laminin organization. J Cell Sci 114, 1137–1144.

Herman, B., Pledger, W.J., 1985. Platelet-derived growth factor-induced alterations in vinculin and actin distribution in BALB/c-3T3 cells. J Cell Biol 100, 1031–1040. doi:10.1083/jcb.100.4.1031

Hynes, R.O., 2002. Integrins: Bidirectional, Allosteric Signaling Machines. Cell 110, 673–687. doi:10.1016/S0092-8674(02)00971-6

Hynes, R.O., 1992. Integrins: Versatility, modulation, and signaling in cell adhesion. Cell

69, 11–25. doi:10.1016/0092-8674(92)90115-S

Jacinto, A., Wood, W., Balayo, T., Turmaine, M., Martinez-Arias, A., Martin, P., 2000. Dynamic actin-based epithelial adhesion and cell matching during Drosophila dorsal closure. Current Biology 10, 1420–1426. doi:10.1016/S0960-9822(00)00796-X

Kammerer, P., Aretz, J., Fässler, R., 2017. Lucky kindlin: A cloverleaf at the integrin tail. Proc. Natl. Acad. Sci. U.S.A. 114, 9234–9236. doi:10.1073/pnas.1712471114

Kaplan, D.R., Chao, F.C., Stiles, C.D., Antoniades, H.N., Scher, C.D., 1979. Platelet alpha granules contain a growth factor for fibroblasts. Blood 53, 1043–1052.

Keller R, Davidson L: Cell movements of gastrulation. In Gastrulation: from cells to embryos. Edited by Stern C: Cold Spring Harbor Laboratory Press; 2004:291-304.

Khalil, A.A., Friedl, P., 2010. Determinants of leader cells in collective cell migration. Integrative Biology 2, 568–574. doi:10.1039/C0IB00052C

Khan, A., Shimokawa, T., Strömblad, S., Zhang, H., 2011. Functional characterization of human Kindlin-2 core promoter identifies a key role of SP1 in Kindlin-2 transcriptional regulation. Cellular and Molecular Biology Letters 16, 638–651. doi:10.2478/s11658-011-0028-6

Kim, D.-H., Wirtz, D., 2013. Focal adhesion size uniquely predicts cell migration. FASEB J. 27, 1351–1361. doi:10.1096/fj.12-220160

Kim, J., Yang, C., Kim, E.J., Jang, J., Kim, S.-J., Kang, S.M., Kim, M.G., Jung, H., Park, D., Kim, C., 2016. Vimentin filaments regulate integrin-ligand interactions by binding to the cytoplasmic tail of integrin β3. J Cell Sci 129, jcs.180315–2042. doi:10.1242/jcs.180315

Kimmel, A.R., Parent, C.A., 2003. The signal to move: D. discoideum go orienteering. Science 300, 1525–1527. doi:10.1126/science.1085439

King, W.G., Mattaliano, M.D., Chan, T.O., Tsichlis, P.N., Brugge, J.S., 1997. Phosphatidylinositol 3-kinase is required for integrin-stimulated AKT and Raf-1/mitogen-activated protein kinase pathway activation. Mol Cell Biol 17, 4406–4418.

Klotzsch E, Smith ML, Kubow KE, Muntwyler S, Little WC, Beyeler F, Gourdon D, Nelson BJ, Vogel V (2009) Fibronectin forms the most extensible biological fibers displaying switchable force-exposed cryptic binding sites. Proc Natl Acad Sci USA 106:18267–18272

Kolega, J., 1981. The movement of cell clusters in vitro: morphology and directionality. J Cell Sci 49, 15–32.

Kragtorp, K.A., Miller, J.R., 2007. Integrin alpha5 is required for somite rotation and boundary formation in Xenopus. Dev. Dyn. 236, 2713–2720. doi:10.1002/dvdy.21280

Kumar, G., Chen, B., Co, C.C., Ho, C.-C., 2011. Differential migration and proliferation of geometrical ensembles of cell clusters. Experimental Cell Research 317, 1340–1352. doi:10.1016/j.yexcr.2011.02.009

Lauffenburger, D.A., Horwitz, A.F., 1996. Cell migration: a physically integrated molecular process. Cell 84, 359–369.

Lecaudey, V., Gilmour, D., 2006. Organizing moving groups during morphogenesis. Current Opinion in Cell Biology 18, 102–107. doi:10.1016/j.ceb.2005.12.001

Li, F., Redick, S.D., Erickson, H.P., Moy, V.T., 2003. Force Measurements of the α5β1 Integrin–Fibronectin Interaction. Biophys J 84, 1252–1262. doi:10.1016/S0006-3495(03)74940-6

Li, H., Deng, Y., Sun, K., Yang, H., Liu, J., Wang, M., Zhang, Z., Lin, J., Wu, C., Wei, Z., Yu, C., 2017. Structural basis of kindlin-mediated integrin recognition and activation. Proc. Natl. Acad. Sci. U.S.A. 114, 9349–9354. doi:10.1073/pnas.1703064114

Lo, C. M., Wang, H. B., Dembo, M. & Wang, Y. L. Cell movement is guided by the rigidity of the substrate. *Biophys J* **79,** 144–152 (2000).

llić, D., Furuta, Y., Kanazawa, S., Takeda, N., Sobue, K., Nakatsuji, N., Nomura, S., Fujimoto, J., Okada, M., Yamamoto, T., Aizawa, S., 1995. Reduced cell motility and enhanced focal adhesion contact formation in cells from FAK-deficient mice. Nature 377, 539–544. doi:10.1038/377539a0

Janssens, K., Sung, H.-H. & Rørth, P. Direct detection of guidance receptor activity during border cell migration. *Proc. Natl. Acad. Sci. U.S.A.* **107,** 7323–7328 (2010).

Luo, B.-H., Carman, C.V., Springer, T.A., 2007. Structural basis of integrin regulation and signaling. Annu. Rev. Immunol. 25, 619–647. doi:10.1146/annurev.immunol.25.022106.141618

Lynch, S.E., Nixon, J.C., Colvin, R.B., Antoniades, H.N., 1987. Role of platelet-derived growth factor in wound healing: synergistic effects with other growth factors. PNAS 84, 7696–7700. doi:10.1073/pnas.84.21.7696

Ma, Y.-Q., Qin, J., Wu, C., Plow, E.F., 2008. Kindlin-2 (Mig-2): a co-activator of beta3 integrins. J Cell Biol 181, 439–446. doi:10.1083/jcb.200710196

Marsden, M., DeSimone, D.W., 2001. Regulation of cell polarity, radial intercalation and

epiboly in Xenopus: novel roles for integrin and fibronectin 128, 3635–3647.

Matsubayashi, Y., Ebisuya, M., Honjoh, S., Nishida, E., 2004. ERK activation propagates in epithelial cell sheets and regulates their migration during wound healing. Curr. Biol. 14, 731–735. doi:10.1016/j.cub.2004.03.060

Mayor, R., Etienne-Manneville, S., 2016. The front and rear of collective cell migration. Nat. Rev. Mol. Cell Biol. 17, 97–109. doi:10.1038/nrm.2015.14

McDonald, J.A., Pinheiro, E.M., Montell, D.J., 2003. PVF1, a PDGF/VEGF homolog, is sufficient to guide border cells and interacts genetically with Taiman. 130, 3469–3478. doi:10.1242/dev.00574

McMahon, A., Supatto, W., Fraser, S.E., Stathopoulos, A., 2008. Dynamic Analyses of Drosophila Gastrulation Provide Insights into Collective Cell Migration. Science 322, 1546–1550. doi:10.1126/science.1167094

Moes, M.J.A., Zhou, Y., Boonstra, J., 2012. Co-localization of the PDGF Receptor and Actin during PDGF Stimulation in Mouse Fibroblasts. International Scholarly Research Notices 2012, 1–14. doi:10.5402/2012/568104

Montanez, E., Ussar, S., Schifferer, M., Bösl, M., Zent, R., Moser, M., Fässler, R., 2008. Kindlin-2 controls bidirectional signaling of integrins. Genes Dev. 22, 1325–1330. doi:10.1101/gad.469408

Montell, D.J., 2001. Command and control: regulatory pathways controlling invasive behavior of the border cells. Mechanisms of Development 105, 19–25.

Montero, J.-A., Kilian, B., Chan, J., Bayliss, P.E., Heisenberg, C.-P., 2003. Phosphoinositide 3-kinase is required for process outgrowth and cell polarization of gastrulating mesendodermal cells. Curr. Biol. 13, 1279–1289.

Moore SW, Keller RE, Koehl MAR: The dorsal involuting marginal zone stiffens anisotropically during its convergent extension in the gastrula of Xenopus leavis. Development 1995, 121:3131-3140.

Moro, L., Venturino, M., Bozzo, C., Silengo, L., Altruda, F., Beguinot, L., Tarone, G., Defilippi, P., 1998. Integrins induce activation of EGF receptor: role in MAP kinase induction and adhesion‐dependent cell survival. The EMBO Journal 17, 6622–6632. doi:10.1093/emboj/17.22.6622

Moser, M., Legate, K.R., Zent, R., Fässler, R., 2009. The Tail of Integrins, Talin, and Kindlins. Science 324, 895–899. doi:10.1126/science.1163865

Nagano, K., Bornhauser, B.C., Warnasuriya, G., Entwistle, A., Cramer, R., Lindholm, D., Naaby-Hansen, S., 2006. PDGF regulates the actin cytoskeleton through hnRNP-K-

mediated activation of the ubiquitin E3-ligase MIR. The EMBO Journal 25, 1871–1882. doi:10.1038/sj.emboj.7601059

Nagel, M., Tahinci, E., Symes, K., Winklbauer, R., 2004. Guidance of mesoderm cell migration in the Xenopus gastrula requires PDGF signaling. 131, 2727–2736. doi:10.1242/dev.01141

Nieuwkoop, P.D., Faber, J., 1994. Normal table of Xenopus laevis (Daudin): A Systematical and Chronological Survey of the Development from the Fertilized Egg till the end of

Omelchenko, T., Vasiliev, J.M., Gelfand, I.M., Feder, H.H., Bonder, E.M., 2003. Rho-dependent formation of epithelial "leader" cells during wound healing. PNAS 100, 10788–10793. doi:10.1073/pnas.1834401100

Patil, S., Jedsadayanmata, A., Wencel-Drake, J.D., Wang, W., Knezevic, I., Lam, S.C.T., 1999. Identification of a Talin-binding Site in the Integrin β3 Subunit Distinct from the NPLY Regulatory Motif of Post-ligand Binding Functions THE TALIN N-TERMINAL HEAD DOMAIN INTERACTS WITH THE MEMBRANE-PROXIMAL REGION OF THE β3 CYTOPLASMIC TAIL. J. Biol. Chem. 274, 28575–28583. doi:10.1074/jbc.274.40.28575

Poukkula, M., Cliffe, A., Changede, R., Rørth, P., 2011. Cell behaviors regulated by guidance cues in collective migration of border cells. J Cell Biol 192, 513–524. doi:10.1083/jcb.201010003

Prasad, M., Montell, D.J., 2007. Cellular and molecular mechanisms of border cell migration analyzed using time-lapse live-cell imaging. Developmental Cell. doi:10.1016/j.devcel.2007.03.021

Qu, H., Tu, Y., Shi, X., Larjava, H., Saleem, M.A., Shattil, S.J., Fukuda, K., Qin, J., Kretzler, M., Wu, C., 2011. Kindlin-2 regulates podocyte adhesion and fibronectin matrix deposition through interactions with phosphoinositides and integrins. J Cell Sci 124, 879–891. doi:10.1242/jcs.076976

Quillien, A., Moore, J.C., Shin, M., Siekmann, A.F., Smith, T., Pan, L., Moens, C.B., Parsons, M.J., Lawson, N.D., 2014. Distinct Notch signaling outputs pattern the developing arterial system. Development 141, 1544–1552. doi:10.1242/dev.099986

Ramos, J.W., DeSimone, D.W., 1996. Xenopus embryonic cell adhesion to fibronectin: position-specific activation of RGD/synergy site-dependent migratory behavior at gastrulation. J Cell Biol 134, 227–240. doi:10.1083/jcb.134.1.227

Ramos, J.W., Whittaker, C.A., DeSimone, D.W., 1996. Integrin-dependent adhesive activity is spatially controlled by inductive signals at gastrulation 122, 2873–2883.

Ravasio, A., Cheddadi, I., Chen, T., Pereira, T., Ong, H.T., Bertocchi, C., Brugues, A., Jacinto, A., Kabla, A.J., Toyama, Y., Trepat, X., Gov, N., Neves de Almeida, L., Ladoux, B., 2015. Gap geometry dictates epithelial closure efficiency. Nat Commun 6, 7683. doi:10.1038/ncomms8683

Ridley, A.J., Schwartz, M.A., Burridge, K., Firtel, R.A., Ginsberg, M.H., Borisy, G., Parsons, J.T., Horwitz, A.R., 2003. Cell migration: integrating signals from front to back. Science 302, 1704–1709. doi:10.1126/science.1092053

Ross, R.S., 2004. Molecular and mechanical synergy: cross-talk between integrins and growth factor receptors. Cardiovascular Research 63, 381–390. doi:10.1016/j.cardiores.2004.04.027

Rozario, T., Dzamba, B., Weber, G. F., Davidson, L. A. & DeSimone, D. W. The physical state of fibronectin matrix differentially regulates morphogenetic movements in vivo. *Developmental Biology* **327,** 386–398 (2009).

Rozario, T., Mead, P.E., DeSimone, D.W., 2014. Diverse functions of kindlin/fermitin proteins during embryonic development in Xenopus laevis. Mechanisms of Development 133, 203–217. doi:10.1016/j.mod.2014.07.004

Sabatier, L., Chen, D., Fagotto-Kaufmann, C., Hubmacher, D., McKee, M.D., Annis, D.S., Mosher, D.F., Reinhardt, D.P., 2009. Fibrillin assembly requires fibronectin. Mol. Biol. Cell 20, 846–858. doi:10.1091/mbc.E08-08-0830

Sato, M., Kornberg, T.B., 2002. FGF is an essential mitogen and chemoattractant for the air sacs of the Drosophila tracheal system. Developmental Cell 3, 195–207.

Scher, C.D., SHEPARD, R.C., Antoniades, H.N., Stiles, C.D., 1979. Platelet-Derived Growth-Factor and the Regulation of the Mammalian Fibroblast Cell-Cycle. Biochim. Biophys. Acta 560, 217–241.

Schneider, L., Cammer, M., Lehman, J., Nielsen, S., Guerra, C., Veland, I., Stock, C., Hoffmann, E., Yoder, B., Schwab, A., Satir, P., Christensen, S., 2010. Directional Cell Migration and Chemotaxis in Wound Healing Response to PDGF-AA are Coordinated by the Primary Cilium in Fibroblasts. Cellular Physiology and Biochemistry 25, 279–292. doi:10.1159/000276562

Sechler, J.L., Corbett, S.A., Schwarzbauer, J.E., 1997. Modulatory roles for integrin activation and the synergy site of fibronectin during matrix assembly. Molecular Biology of the Cell 8, 2563–2573. doi:10.1091/mbc.8.12.2563

Sechler, J.L., Cumiskey, A.M., Gazzola, D.M., Schwarzbauer, J.E., 2000. A novel RGD-independent fibronectin assembly pathway initiated by alpha4beta1 integrin binding to the alternatively spliced V region. J Cell Sci 113 (Pt 8), 1491–1498.

Seppä, H., Grotendorst, G., Seppä, S., Schiffmann, E., Martin, G.R., 1982. Platelet-derived growth factor in chemotactic for fibroblasts. J Cell Biol 92, 584–588. doi:10.1083/jcb.92.2.584

Sheetz, M.P., Felsenfeld, D., Galbraith, C.G., Choquet, D., 1999. Cell migration as a five-step cycle. Biochem Soc Symp 65, 233–243.

Shen, X., Kramer, R.H., 2004. Adhesion-Mediated Squamous Cell Carcinoma Survival through Ligand-Independent Activation of Epidermal Growth Factor Receptor. The American Journal of Pathology 165, 1315–1329. doi:10.1016/S0002-9440(10)63390-1

Siegel, D.H., Ashton, G.H.S., Penagos, H.G., Lee, J.V., Feiler, H.S., Wilhelmsen, K.C., South, A.P., Smith, F.J.D., Prescott, A.R., Wessagowit, V., Oyama, N., Akiyama, M., Aboud, Al, D., Aboud, Al, K., Githami, Al, A., Hawsawi, Al, K., Ismaily, Al, A., Al-Suwaid, R., Atherton, D.J., Caputo, R., Fine, J.-D., Frieden, I.J., Fuchs, E., Haber, R.M., Harada, T., Kitajima, Y., Mallory, S.B., Ogawa, H., Sahin, S., Shimizu, H., Suga, Y., Tadini, G., Tsuchiya, K., Wiebe, C.B., Wojnarowska, F., Zaghloul, A.B., Hamada, T., Mallipeddi, R., Eady, R.A.J., McLean, W.H.I., McGrath, J.A., Epstein, E.H., Jr., 2003. Loss of Kindlin-1, a Human Homolog of the Caenorhabditis elegans Actin–Extracellular-Matrix Linker Protein UNC-112, Causes Kindler Syndrome. The American Journal of Human Genetics 73, 174–187. doi:10.1086/376609

Skoglund, P., Dzamba, B., Coffman, C.R., Harris, W.A., Keller, R., 2006. Xenopus fibrillin is expressed in the organizer and is the earliest component of matrix at the developing notochord-somite boundary. Dev. Dyn. 235, 1974–1983. doi:10.1002/dvdy.20818

Skoglund, P., Keller, R., 2007. Xenopus fibrillin regulates directed convergence and extension. Developmental Biology 301, 404–416. doi:10.1016/j.ydbio.2006.09.005

Smith, E.M., Mitsi, M., Nugent, M.A., Symes, K., 2009. PDGF-A interactions with fibronectin reveal a critical role for heparan sulfate in directed cell migration during Xenopus gastrulation. Proc. Natl. Acad. Sci. U.S.A. 106, 21683–21688. doi:10.1073/pnas.0902510106

Sonavane, P. R. *et al.* Mechanical and signaling roles for keratin intermediate filaments in the assembly and morphogenesis of mesendoderm tissue at gastrulation. *Development* dev.155200 (2017). doi:10.1242/dev.155200

Sternlicht, M. D. & Werb, Z. How Matrix Metalloproteinases Regulate Cell Behavior. *Annu. Rev. Cell Dev. Biol.* **17,** 463–516 (2001).

Sundberg, C., Rubin, K., 1996. Stimulation of beta1 integrins on fibroblasts induces PDGF independent tyrosine phosphorylation of PDGF beta-receptors. J Cell Biol 132, 741–752.

Sutherland, D., Samakovlis, C., Krasnow, M.A., 1996. branchless encodes a Drosophila FGF homolog that controls tracheal cell migration and the pattern of branching. Cell 87, 1091–1101.

Swaney, K. F., Huang, C.-H. & Devreotes, P. N. Eukaryotic chemotaxis: a network of signaling pathways controls motility, directional sensing, and polarity. *Annu Rev Biophys* **39,** 265–289 (2010).

Symes, K., Mercola, M., 1996. Embryonic mesoderm cells spread in response to platelet-derived growth factor and signaling by phosphatidylinositol 3-kinase. PNAS 93, 9641–9644.

Symes, K., Smith, E.M., Mitsi, M., Nugent, M.A., 2010. Sweet cues. http://dx.doi.org/10.4161/cam.4.4.12427. doi:10.4161/cam.4.4.12427

Tadokoro, S., Shattil, S.J., Eto, K., Tai, V., Liddington, R.C., de Pereda, J.M., Ginsberg, M.H., Calderwood, D.A., 2003. Talin Binding to Integrin ß Tails: A Final Common Step in Integrin Activation. Science 302, 103–106. doi:10.1126/science.1086652

Takagi, J., Petre, B.M., Walz, T., Springer, T.A., 2002. Global Conformational Rearrangements in Integrin Extracellular Domains in Outside-In and Inside-Out Signaling. Cell 110, 599–611. doi:10.1016/S0092-8674(02)00935-2

Takagi, J. *et al.* Structure of integrin α5β1 in complex with fibronectin. **22,** 4607–4615 (2003).

Theodosiou, M., Widmaier, M., Böttcher, R.T., Rognoni, E., 2016. Kindlin-2 cooperates with talin to activate integrins and induces cell spreading by directly binding paxillin. Elife.

Tsiper, M. V. & Yurchenco, P. D. Laminin assembles into separate basement membrane and fibrillar matrices in Schwann cells. *J Cell Sci* **115,** 1005–1015 (2002).

Tu, Y.Z., Wu, S., Shi, X.H., Chen, K., Wu, C.Y., 2003. Migfilin and Mig-2 link focal adhesions to filamin and the actin cytoskeleton and function in cell shape modulation. Cell 113, 37–47.

Ussar, S., Wang, H.-V., Linder, S., Fässler, R., Moser, M., 2006. The Kindlins: Subcellular localization and expression during murine development. Experimental Cell Research 312, 3142–3151. doi:10.1016/j.yexcr.2006.06.030

Valgeirsdóttir, S., Claesson-Welsh, L., Bongcam-Rudloff, E., Hellman, U., Westermark, B., Heldin, C.H., 1998. PDGF induces reorganization of vimentin filaments. J Cell Sci 111 (Pt 14), 1973–1980.

Veevers-Lowe, J., Ball, S.G., Shuttleworth, A., Kielty, C.M., 2011. Mesenchymal stem

cell migration is regulated by fibronectin through α5β1-integrin-mediated activation of PDGFR-β and potentiation of growth factor signals. J Cell Sci 124, 1288–1300. doi:10.1242/jcs.076935

Veracini, L., Franco, M., Boureux, A., Simon, V., Roche, S., Benistant, C., 2006. Two distinct pools of Src family tyrosine kinases regulate PDGF-induced DNA synthesis and actin dorsal ruffles. J Cell Sci 119, 2921–2934. doi:10.1242/jcs.03015

Watts, T.L., Cui, R., Szaniszlo, P., Resto, V.A., Powell, D.W., Pinchuk, I.V., 2016. PDGF-AA mediates mesenchymal stromal cell chemotaxis to the head and neck squamous cell carcinoma tumor microenvironment. J Transl Med 14, 337. doi:10.1186/s12967-016-1091-6

Weavers, H., Skaer, H., 2014. Tip cells: Master regulators of tubulogenesis? Semin. Cell Dev. Biol. 31, 91–99. doi:10.1016/j.semcdb.2014.04.009

Weber, G.F., Bjerke, M.A., DeSimone, D.W., 2012. A mechanoresponsive cadherin-keratin complex directs polarized protrusive behavior and collective cell migration. Developmental Cell 22, 104–115. doi:10.1016/j.devcel.2011.10.013

Wegener, K. L. *et al.* Structural Basis of Integrin Activation by Talin. *Cell* **128,** 171–182 (2007).

Weijer, C.J., 2009. Collective cell migration in development. J Cell Sci 122, 3215–3223. doi:10.1242/jcs.036517

Windoffer, R., Kölsch, A., Wöll, S., Leube, R.E., 2006. Focal adhesions are hotspots for keratin filament precursor formation. J Cell Biol 173, 341–348. doi:10.1083/jcb.200511124

Winklbauer, R., 1990. Mesodermal Cell Migration During Xenopus Gastrulation. Developmental Biology 142, 155–168. doi:10.1016/0012-1606(90)90159-G

Winklbauer, R., Keller, R.E., 1996. Fibronectin, Mesoderm Migration, and Gastrulation inXenopus. Developmental Biology 177, 413–426. doi:10.1006/dbio.1996.0174

Winklbauer, R., Nagel, M., 1991. Directional mesoderm cell migration in the Xenopus gastrula. Developmental Biology 148, 573–589. doi:10.1016/0012-1606(91)90275-8

Winklbauer, R., Nagel, M., Selchow, A., Wacker, S., 1996. Mesoderm migration in the Xenopus gastrula. Int J Dev Biol 40, 305–311.

Wolf, K., Wu, Y.I., Liu, Y., Geiger, J., Tam, E., Overall, C., Stack, M.S., Friedl, P., 2007. Multi-step pericellular proteolysis controls the transition from individual to collective cancer cell invasion. Nat Cell Biol 9, 893–904. doi:10.1038/ncb1616

Wu, C., Bauer, J.S., Juliano, R.L., McDonald, J.A., 1993. The alpha 5 beta 1 integrin fibronectin receptor, but not the alpha 5 cytoplasmic domain, functions in an early and essential step in fibronectin matrix assembly. J. Biol. Chem. 268, 21883–21888.

Wu, C.Y., KEIVENS, V.M., OTOOLE, T.E., McDonald, J.A., GINSBERG, M.H., 1995. Integrin Activation and Cytoskeletal Interaction Are Essential for the Assembly of a Fibronectin Matrix. Cell 83, 715–724. doi:10.1016/0092-8674(95)90184-1

Yamaguchi, N., Mizutani, T., Kawabata, K., Haga, H., 2015. Leader cells regulate collective cell migration via Rac activation in the downstream signaling of integrin β1 and PI3K. Scientific Reports 5, 7656. doi:10.1038/srep07656

Yang, X., Chrisman, H., Weijer, C.J., 2008. PDGF signalling controls the migration of mesoderm cells during chick gastrulation by regulating N-cadherin expression. 135, 3521–3530. doi:10.1242/dev.023416

Yeh, C.-H., Chen, P.-C., Chen, C.-H., Hsu, C.-F., Huang, R.-L., Ding, D.-C., Chu, T.-Y., 2016. Platelet-Derived Growth Factor in the Ovarian Follicle Attracts the Stromal Cells of the Fallopian Tube Fimbriae. PLoS ONE 11. doi:10.1371/journal.pone.0158266